Green Hydrogen from Wind Energy for Long-Duration Energy Storage in Alberta

by

William Donald Noel

A thesis submitted in partial fulfillment of the requirements for the degree of

Master of Science

Department of Mechanical Engineering
University of Alberta

Abstract

With continued growth in global carbon emissions, much of the developed world is curtailing its dependence on fossil fuels. Broad decarbonization will not come from a single source, but rather a combination of policy, technology, and innovation. Wind power has seen significant development in Canada, having over 6,700 operational turbines installed over the last decade. Increased investment into wind energy has lead to improvements in the technology, with wind turbines roughly doubling in height since the early 1990's. In recent years, hydrogen has seen a resurgence in popularity as a low carbon energy carrier. Pairing existing wind farms with energy storage, such as hydrogen, could increase their electricity revenue through price arbitrage, or generate new revenue through selling the hydrogen. This work examines the opportunity to generate green hydrogen in Alberta using a wind-hydrogen hybrid plant. To do so, Alberta's electricity market operations were forecast to 2030 using commercial market simulation software, Aurora, including hourly prices and unit dispatch. To better simulate price spikes, electricity price perturbations, achieved through time series decomposition of historic price signals, are administered as random shocks to the hourly price forecasts. Wind-hydrogen hybrid plant characteristics, capacity and operating schedule, are optimized using linear programming. Results of this work show some potential for wind-generated green hydrogen to be cost competitive with steam-methane reforming in the next decade, with some scenarios achieving levelized cost of green hydrogen below $2/kg. Regardless of market conditions, optimal electrolyser sizing is contingent on achieving a capacity factor between 40% and 60%. At current costs, energy arbitrage through hydrogen fuel cells is not financially viable.

Preface

A portion of the work presented in this thesis comes from a collaboration led by Dr. Andrew Leach and Dr. Tim Weis at the Center for Applied Business Research in Energy & the Environment (CABREE), an independent research facility located located in the Alberta School of Business at the University of Alberta, with funding from Future Energy Systems. Chapter 3 of this thesis is, in part, a result of a contract obtained through Natural Resources Canada (NRCan). The resulting manuscript, *Mapping Canada's Wind Energy Fleet*, has been submitted for publication in Renewable and Sustainable Energy Reviews, an Elsevier journal. Alberta electricity models, forecast in Aurora, are built off of previous work by CABREE alumni, though with significant alterations as discussed in Chapter 4. The remainder of the research, i.e. literature review and hydrogen plant optimization, are my own work, with manuscript edits and debugging support provided by Dr. Andrew Leach, Dr. Tim Weis, and Dr. Brian A. Fleck. Additional assistance was also provided by undergraduate research assistants, Qiulin Yu, Julia Zonneveld, and Faith Nobert.

Table of Contents

List of Tables

List of Figures

Chapter 1

Introduction

With increasing concerns regarding global warming, many countries are looking to renewable energy to lower their carbon emissions while continuing to meet electricity loads. Characterized by near-zero life-cycle emissions, and more recently by low levelized energy costs [1], wind and solar offer an attractive solution in helping to meet this demand; however, the variable nature of these technologies will eventually present a barrier to deep integration in electricity grids, as intermittence will strain reliability [2]. One solution to this problem is pairing renewable generators with energy storage. In general, an energy storage system is one which collects energy for later use, but for the purpose of this work, energy storage refers to the transformation of electrical energy for accumulation and discharge at a utility scale. Renewable power generated during low price, or high availability, hours can be stored for dispatch at higher market prices or, alternatively, energy storage can be used as a sink to reduce, or even eliminate, renewable energy curtailment. Storage makes renewable energy more valuable, while at the same time, the nature of renewable energy sources makes a compelling business case for storage.

Energy can be stored in a number of ways, providing power from a sub-kilowatts to multi-megawatt capacities and for seconds to weeks in duration. Hydrogen-based energy storage is well suited for high power, long duration applications [3, 4] and is of particular interest in Alberta due to the province's already established hydrogen

economy [5]. This work investigates the opportunity for wind-driven hydrogen energy storage in Alberta, providing insight on hydrogen's role in helping Canada achieve its goal of net-zero emissions by 2050 [6].

1.1 Background

1.1.1 Alberta's Electricity Market

Many Canadian provinces, such as Saskatchewan [7] and Manitoba [8], operate under a government-owned vertically-integrated electricity market, whereby the majority of electricity generation, transmission, and distribution infrastructure is owned and operated by crown corporations. Alberta, on the other hand, functions under a much different market design. The Alberta electricity market is deregulated, operating under a wholesale energy-only model, facilitated by the Alberta Electric System Operator (AESO). In an energy-only market, power producers are only paid for the electricity that they actually produce. A separate ancillary services market is also in place, through which generators are paid to help maintain grid reliability [9]. While storage assets may also participate in the ancillary services market, we focus only on energy value in this work.

Every minute, the AESO determines the price of electricity through an economic merit order. Power producers provide AESO an electricity supply offer, which includes up to 7 blocks valued at increasing prices between between \$0/MWh and \$1000/MWh, to indicate the minimum price at which they will provide power [9, 10]. Cumulative supply block offers, excluding imports, must equal the plant installed capacity net of any power diverted to the ancillary services market. Imports and variable renewable generators (solar and wind) must offer their power at \$0/MWh [11], with any variability accounted for by the grid operator. Similarly, consumers submit demand bids, indicating a maximum price they are willing to purchase at. The merit order is built by sorting supply offers and demand bids in ascending order,

with the power price being set at the intersection of supply and demand [9].

Under the current market design, wind and solar generation, especially at high penetration, can have a significant impact on the price of power. Consider the following scenario: at some time, t there is an electricity demand, D being met exclusively by coal and gas plants. The coal and gas plants offer their full capacity, C_1 and C_2, at a prices, P_1 and P_2, respectively. Here, both coal and gas supply are required to meet demand, such that $C_1 < D \leq C_1 + C_2$. As a result, with $P_1 < P_2$, the power price, P is set by the gas plant. Here, the coal plant will be paid for its entire capacity, earning revenue at a rate of $P \cdot C_1$ in units of \$/hr. The gas plant, operating at less than 100% capacity, will only be paid for portion of its capacity, $D - C_1$ that is in merit. The merit order for this hour is shown on the left side of Figure 1.1.
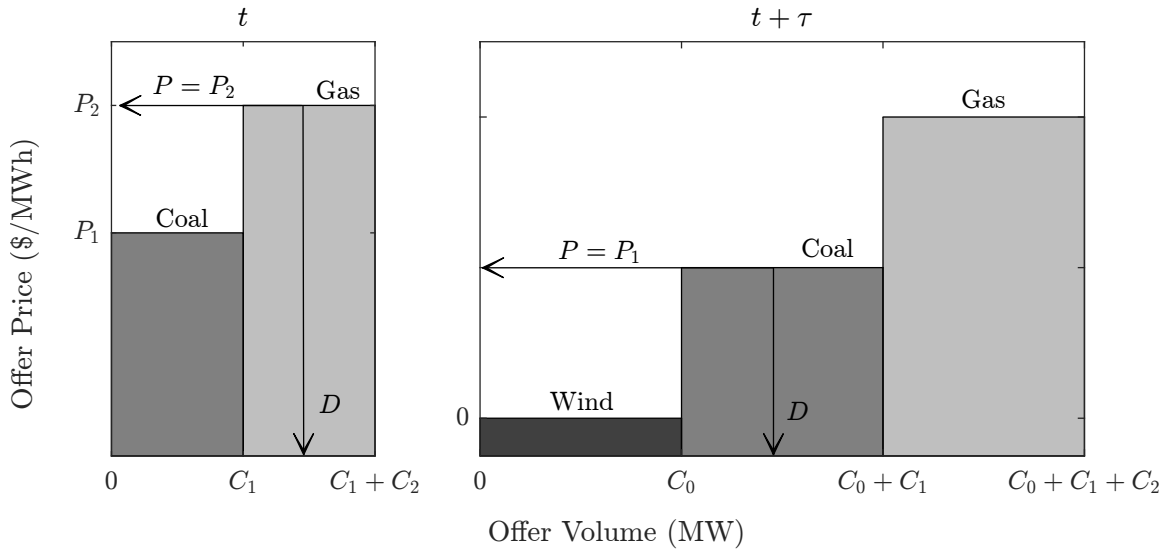
Figure 1.1: Example of an economic merit order with and without wind generation

At some later time, $t+\tau$ demand, D has not changed but a wind plant of capacity, C_0 enters the merit with an offer of \$0/MWh. If wind generation is sufficient, i.e. $C_0 < D \leq C_0 + C_1$, the gas plant is pushed out of merit and forced to shut down, halting its energy revenue. In this case, the price of power, $P = P_1$ is set by the coal plant, as shown on the right side of Figure 1.1. As a result, the coal plant will only be paid for the operational portion of its capacity, $D - C_0$ whereas the wind farm

will generate revenue on its full capability, C_0. The gas plant, having shut down, will not be actively participating in the market at this time. In reality, of course, market operations are more complex than this simple schematic, and plants will face a variety of operating conditions and constraints.

Alberta gets its energy from a variety of sources. In 2018, the majority of electricity production, 81 TWh in total, came from natural gas (49%), coal (43%), wind (6%), and hydro (3%) [12], though, with federal plans to phase out coal [13] and raise the price of carbon to \$170/t [14] by 2030, Alberta's electricity fleet will likely see drastic changes in the next few years. A sizable portion of Alberta's industrial load, around 20% of total demand [15], is served behind the fence through natural gas cogeneration, whereby electricity is the byproduct of oil sands operations. As a result, Alberta's demand profile is atypically involatile when compared to similar power markets, e.g. Texas. Also, due to it's northern climate, Alberta is a historically winter-peaking system, though this recently changed due to high summer temperatures causing a spike in demand [16].

1.1.2 The Wind Discount

A wind farm's operating schedules is contingent on local weather conditions. In Alberta, wind generation has a weak correlation with system demand and, for fleets with low geographic dispersion, any individual wind farm's output is strongly correlated with the rest of the wind fleet. Due to their near-zero fuel costs, wind power tends to decrease the price of electricity as it offers into the merit order at \$0/MWh and displaces more expensive generation from dispatch. On average, wind farms earn a lower price for their power than the rest of the generating fleet, referred to as price cannibalization [17] or wind discount [18]. The wind value factor [19], also known as capture rate, is quantified by the ratio of wind-weighted, $\overline{P_w}$ and volume-weighted,

$\overline{P_v}$ mean pool price, given respectively by

$$\overline{P_w} = \frac{\sum_{t=t_0}^{t_N} (G_{w,t} P_t)}{\sum_{t=t_0}^{t_N} (G_{w,t})}, \text{ and} \qquad (1.1\text{a})$$

$$\overline{P_v} = \frac{\sum_{t=t_0}^{t_N} (G_{v,t} P_t)}{\sum_{t=t_0}^{t_N} (G_{v,t})}, \qquad (1.1\text{b})$$

where $G_{w,t}$ and $G_{v,t}$ are hourly wind and total generation respectively, P_t is the hourly pool price, and $t \in t_N$ spans all hours of available data. A capture rate $(\overline{P_w}/\overline{P_v})$ of 1.0 represents a generator collecting the average market price throughout the time period; capture rates above and below 1.0 suggest a generator is earning more or less than the average market price respectively. Solar power is similar to wind in that it is dependent on environmental conditions and displaces higher cost offers when it generates. Unlike wind, however, solar generation tends to occur during what are generally high demand hours. As a result, solar often starts at a higher market price, resulting in a price premium irregardless of its market depressing effect [15]; note however, that increasing volumes of solar will eventually have the same discount effect as wind [20, 21].

Wind farms in Alberta, the majority of which are located in the southwest corner of the province, are often operational overnight during off-peak hours. Figure 1.2 gives the correlation of individual wind farm generation to the rest of the renewable fleet (*bar*), value factor as defined above (*scatter*), and commissioning date (*bar-color*) of the Alberta wind fleet, labelled using AESO asset IDs[1] [22]. Figure 1.2 shows higher correlations for an individual wind farm often equate to a lower value factor (capture rate).

Figure 1.3 shows the effect different levels of wind generation can have on the price of electricity. Hourly wind output, normalized to total dispatch, is binned using quartiles: denoted by *low* (0 - 25th-percentile), *medium* (25th - 75th-percentile), and *high* (75th-percentile - peak output). The power price at each of level of wind output

---

[1]See Table A.1 in the appendix for a list of wind farms and AESO asset IDs
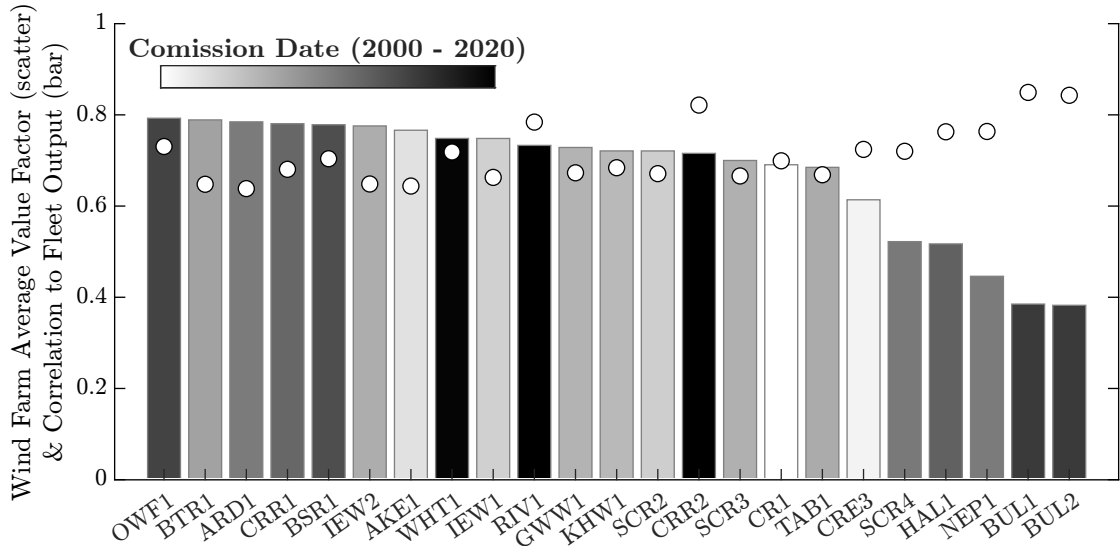
Figure 1.2: Average value factor (capture rate) and correlation of individual wind farm generation with respect to the entire wind fleet, using September 2009 - December 2020 Alberta electricity market data

(*stacked bars*) is plotted relative to actual pool price (*x-axis*), as well as on- and off-peak prices (*solid line* and *dotted line* respectively), all given in terms monthly averages. Both figures 1.2 and 1.3 use publically available data obtained from AESO.

Wind generation is contingent on the environmental conditions in which it operates; as such, it stands to reason that wind farms should be sited in areas characterized by frequent and high wind speeds. However, wind farms which operate in the same wind regime, using similar vintage technology, will often achieve similar capacity factors and, as shown in Figure 1.2, the correlated generation caused by crowding can decrease market value. If this power was to be stored and sold at a higher price, even average market prices, it would see a significant gain in value. As shown in Figure 1.2, Bull Creek Wind Facility (*BUL1* and *BUL2*), Alberta's north-most wind farms, have a value factor 15-20% above the majority of the fleet. Limited generation data for new wind farms, such as Oldman 2 (*OWW1*), Whitla (*WHT1*), Riverview (*RIV1*), and Castle Rock Ridge 2 (*CRR2*), may be a driving factor behind inflated value factors shown above.

In Alberta, wind makes up less than 11% [22] of Alberta's total installed capacity,
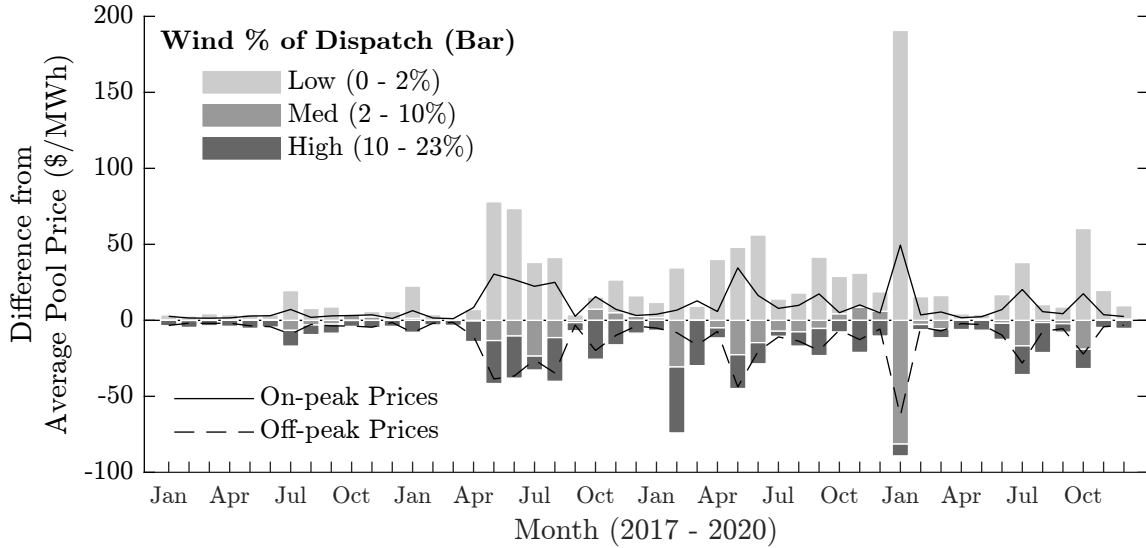
Figure 1.3: Impact of wind generation on Alberta electricity prices, 2017 - 2020

but is capable of serving nearly 25% [15] of hourly market demand. Figure 1.3 shows the significant impact wind can have on electricity price. During low-wind hours (0 - 2% of total market dispatch), the price of electricity is consistently higher than even the on-peak prices, with multiple instances showing increases of $\geq\$40/MWh$ over average. Similarly, during high-wind hours (10 - 23% of dispatch), electricity prices are commonly below off-peak prices, with market price falling nearly \$100/MWh below average in the most extreme cases. Total height of the bars in Figure 1.3 provide a reasonable estimate of historical arbitrage opportunity: the potential price differential between charging a storage asset during high wind hours and discharging it during low wind hours.

Between 2009 and 2020, the levelized cost of new wind farms has decreased, on average, by 71% [1]; that is to say that a wind farm built in 2020 will make a reasonable rate of return on investment at an average revenue 71% lower than one built 11 years prior. Likewise, it is safe to assume, based on the data presented in Figure 1.3, that if Alberta's wind fleet continues to grow, so will the wind discount. Consequently, as highlighted in Figure 1.2, depending on its location relative to the rest of the fleet, a new wind farm built in Alberta has the potential to lower not only its own, but also

the average wind fleet capture price. In other words, building new wind farms can have negative implications for existing ones and the risk of a future wind farm being built nearby may dissuade new investment. Coupling of existing wind farms with an energy storage asset could increase their value factor through energy arbitrage [23]: a benefit which parallels recent project announcements out of California [24].

1.2   Motivation

Electrical grids dependant on variable renewable energy, wind and solar, may require significant amounts of firming power to eliminate the risk of brownouts. As their levelized costs decline, many are looking to energy storage as one solution to this problem, with energy arbitrage, moving electricity from low to high demand (price) hours, providing financial incentive. This thesis seeks to determine whether wind-driven hydrogen energy storage, selling hydrogen, power, or both, will be financially feasible in the coming decade.

1.3   Thesis Overview

The remainder of this thesis is comprised of 3 additional chapters. Chapter 2 provides a background on energy storage, summarizing relevant literature and the burgeoning interest in the decarbonization potential of green hydrogen[2]. Chapter 3 contains a manuscript, *Mapping Canada's Wind Energy Fleet*, submitted to *Renewable and Sustainable Energy Reviews* in August 2020.[3] The paper describes the data collection process for the Canadian Wind Turbine Database [25], whereby we mapped and indexed Canada's entire[4] operational wind fleet. Though wind energy is the focal point of this chapter, much of the overarching discussion is generally relevant to novel energy technologies; in the coming decade it is likely that hydrogen will see similar

---

[2]Hydrogen produced through the electrolysis of water, powered by a renewable energy source
[3]Awaiting review at the time of writing
[4]As of mid 2020

development trends to which wind and solar were, and still are, subject. Chapter 4, the principal chapter of this thesis, outlines the performance of a small wind-hydrogen hybrid plant, using existing and proposed wind farms in Alberta, operating under various future market scenarios.

Chapter 2

Literature Review

2.1 Introduction to Energy Storage

People have been harnessing energy for millennia, with one of the first examples of energy storage being the Roman aqueducts and hydro-powered grain mills [26]. In the early 20th century, closely following the discovery of electricity, a surge of pumped hydro facilities began development across Europe; by the time the first pumped hydro plant had been constructed in the United States in 1928, it is estimated that over 40 were operational in European countries such as Germany, Switzerland, and France [26, 27]. Electricity cannot be stored in the same way that a physical substance, e.g. water, can; rather, it must be converted into a storable form of energy, then converted back when needed [28]. Energy can be stored through a variety of techniques: mechanically, through pumped hydro, compressed air, and flywheels; electrically through supercapacitors and superconducting magnetic energy storage; chemically through batteries, typically lithium-ion or lead-acid, flow batteries, and hydrogen [2]; thermochemically, through solar fuels; and thermally, as latent and sensible heat [29]. Each of the energy storage systems have pros and cons with respect to efficiency, storage duration, and costs. In 2020, the global energy storage fleet reached a total installed capacity of about 175 GW, an overwhelming majority being pumped hydro (97%), followed by thermal storage and batteries (1% each) [27]. Figure 2.1 gives the evolution of global energy storage over time, with a separate (smaller) axis

showing the development of non-hydro resources. Note here that the *other* category consists of flow batteries, capacitors, and hydrogen storage technologies.
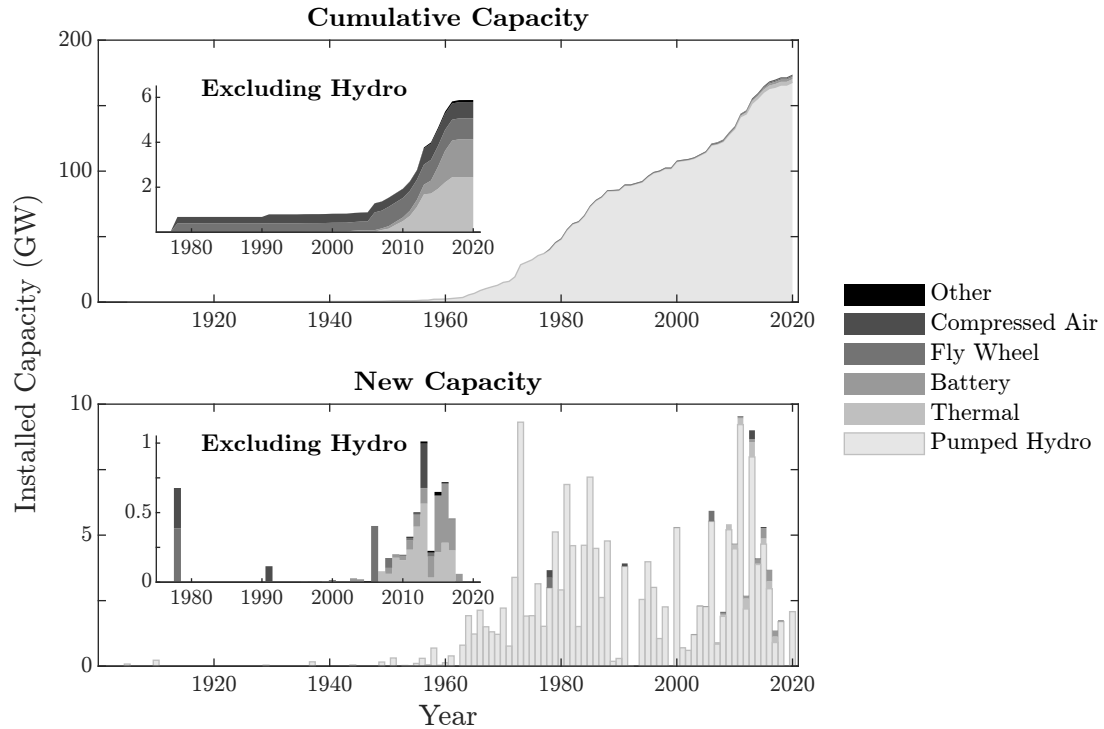
Figure 2.1: Cumulative (top) and new (bottom) installed capacity of the operational global energy storage fleet [27]

Since the early 1900's, pumped hydro has held the majority share of global storage capacity, although recently, in the past decade, the aggregate non-hydro storage fleet has tripled in size (see Figure 2.1). Pumped hydro is geographically constrained, meaning the number of suitable sites declines as more hydro facilities are erected. As a result, one could make the argument that the gap between hydro and non-hydro energy storage facilities will soon begin to shrink.

As of November 2020, according to the Global Energy Storage Database [27], there are 1363 operational energy storage projects in 78 unique countries: outlined in *black* as shown in Figure 2.2a. Of the 175 GW of total capacity, nearly 50% of it is installed in 3 countries: China (31.5 GW), Japan (27.7 GW) and the United States (24.5 GW). Canada's storage fleet, shown in Figure 2.2b, consists of 211 MW of storage from 21 facilities: 14 (204 MW) of which can be found in Ontario. It should be noted here

that this data does not contain Canada's entire hydro fleet, rather just one pumped hydro plant. A portion of Canada's hydro fleet, which provided between 59% [30] and 61% [31] of electricity consumed in 2018, may store energy through withholding dispatch, rather than pumping.

(a) Global Storage Fleet

(b) Canadian Storage Fleet
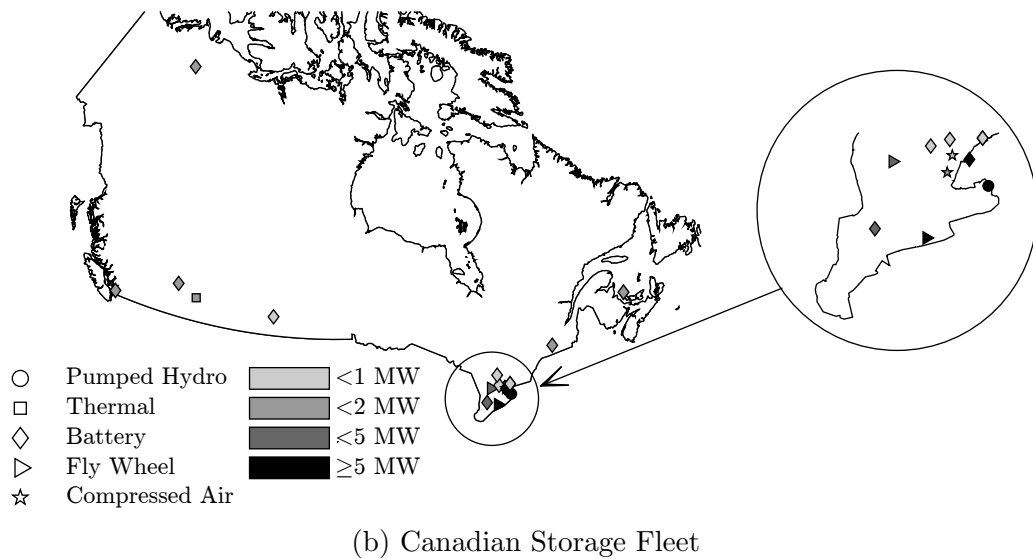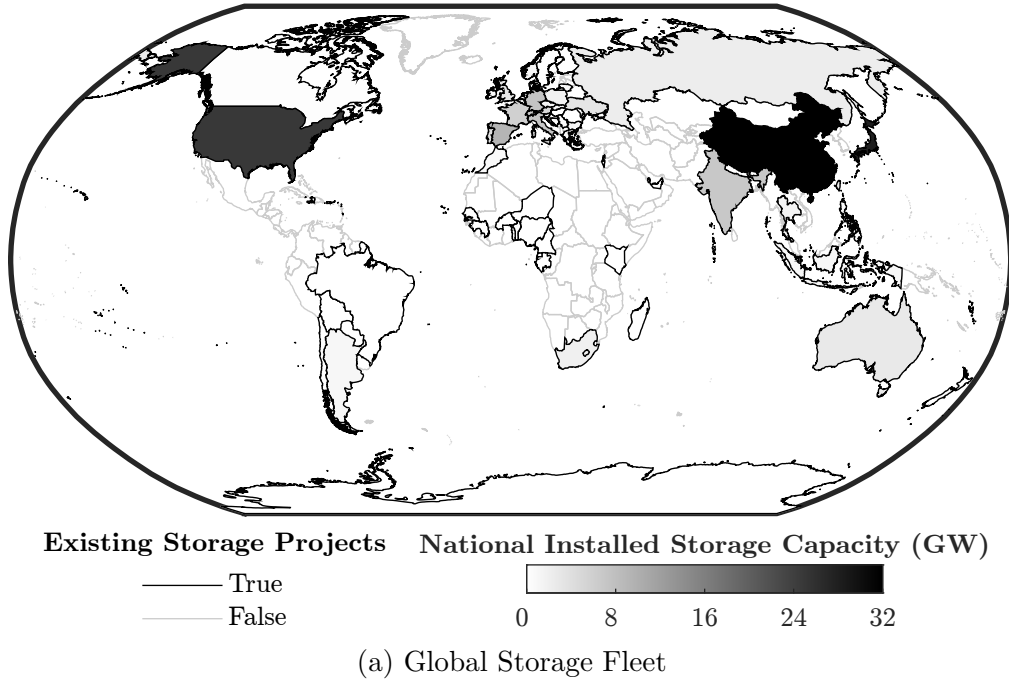
Figure 2.2: National Installed capacity of energy storage by country (a) and operational energy storage projects in Canada (b)

Different storage technologies are suited to different applications [28], often as a function of technical and economic considerations. Figure 2.3 groups storage technologies into broad categories based on technological characteristics, installed capacity and duration, with ranges sourced from existing literature [2, 28, 29]. Figure 2.4 shows the evolution of the cheapest (based on levelized costs) storage technologies over the next 2 decades, with respect to depth and frequency of charge-discharge cycles [32].
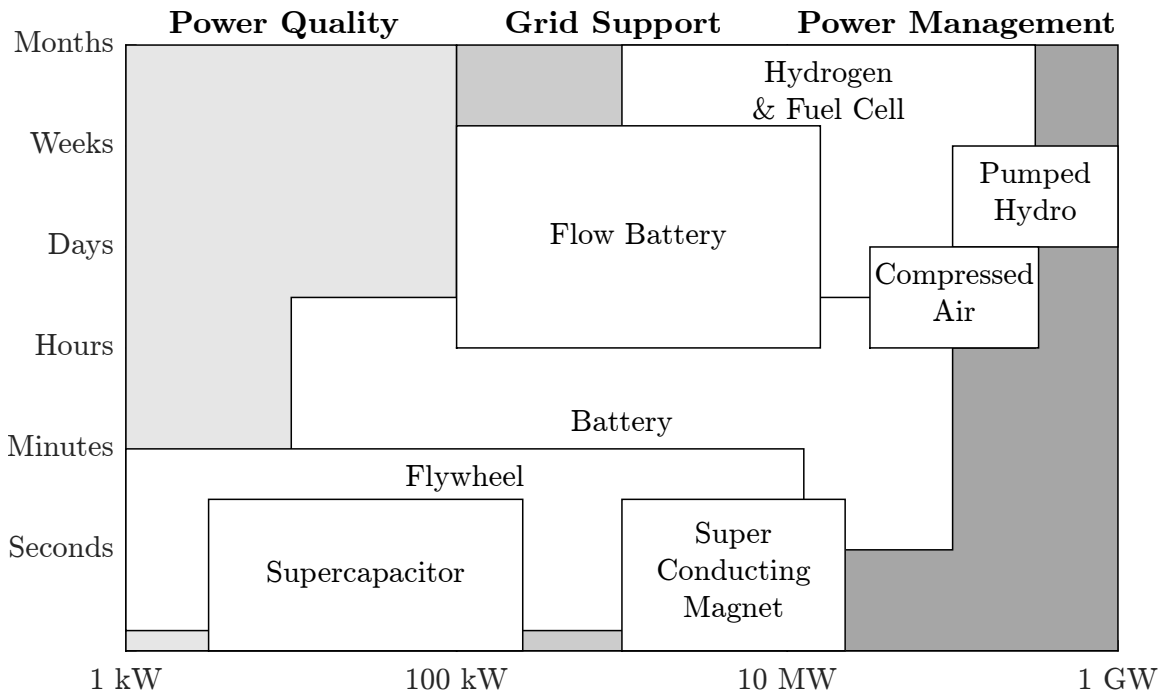
Figure 2.3: Energy storage technologies grouped by installed capacity and duration

Energy storage allows for power to be moved from low price hours to high price hours. Its energy market value is both a function of the difference in price, or arbitrage, and frequency at which it can cycle between charging and discharging. Note also, that auxiliary values are also possible, as demonstrated by the Tesla battery which captured over half of the ancillary market revenues of the South Australian market in 2018 [33]. Although longer-term energy storage technologies, such as pumped hydro and compressed air, are able to provide all the same services as batteries, they are subject to higher capital costs and construction times, as well as a limited availability of suitable sites [23]. This, paired with declining battery costs, may drive

13
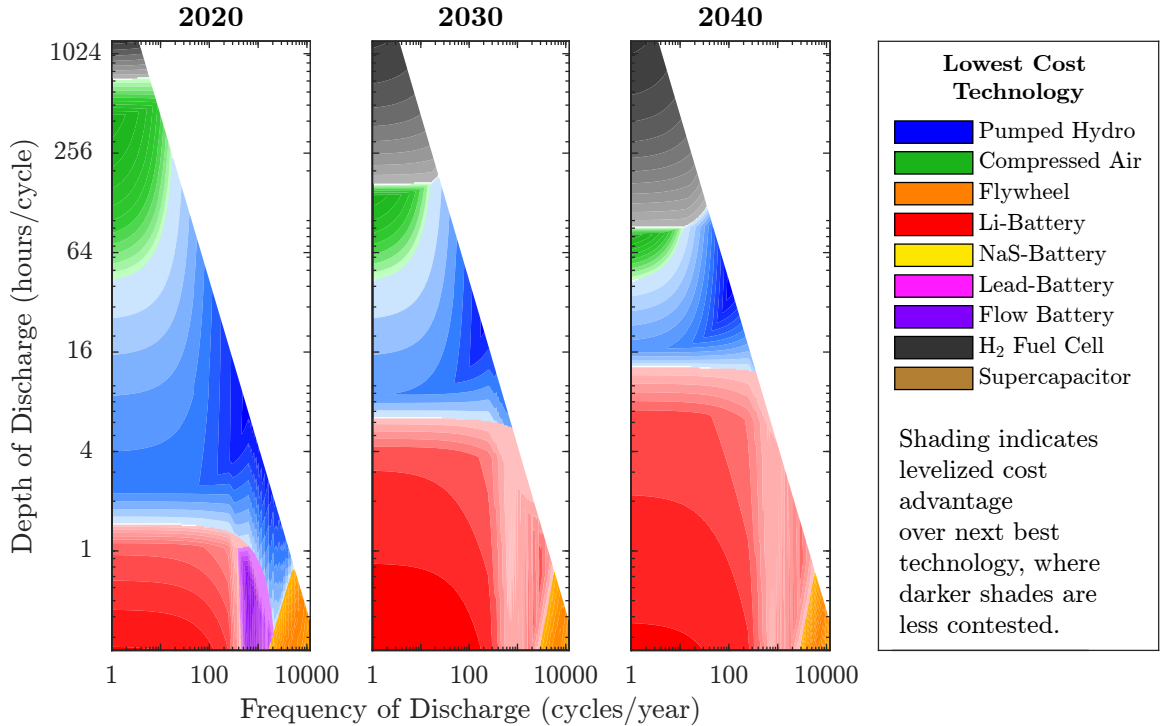
Figure 2.4: Energy storage technologies with lowest levelized cost for 2020, 2030, and 2040, based on cycling conditions - data and image adapted from [32]

the energy storage paradigm toward more small-scale, fast-response systems [34], though some have argued otherwise [35, 36]. The following subsections provide short descriptions of those technologies which most closely rival hydrogen in application (Figure 2.3) and are economically relevant based on future cost projections (Figure 2.4): pumped hydro, compressed air storage, and lithium-ion batteries. Further information on the remaining technologies can be found in abundance in the literature, often in review articles [2, 28, 29].

2.1.1 Hydrogen Energy Storage

A hydrogen energy storage (HES) system consists of two independent processes for producing and consuming hydrogen [29]. On the front end of the system, an electrolyser produces hydrogen using electricity. The hydrogen is then compressed and stored in a tank, "charging" the system. From here, stored hydrogen can be used to generate electricity through traditional combustion or a fuel cell [2, 28, 37]. Alternatively, the

hydrogen itself may be sold as a commodity [29, 38], allowing for arbitrage outside the power market: an opportunity unique to HES systems. For example, green hydrogen could be used to offset upstream emissions of bitumen upgrading in the Alberta industrial heartland [38–40]. Similarly, U.S. nuclear asset owners are considering using hydrogen to avoid premature decommissioning, with several demonstration projects planned for the near future [41].

There are six major types of fuel cells: alkaline (AFC), polymer exchange membrane (PEMFC), direct methanol (DMFC), phosphoric acid (PAFC), molten carbonate (MCFC), and solid oxide (SOFC). Fuel cell types are characterized by different fuels, operating temperatures, [42], and capacities [43], shown in Table 2.1.

Type	Fuel	Temperature Range	Capacity Scale
AFC	H_2	50 - 200°C	kW - 10 KW
PEMFC	H_2	0 - 100°C	W - kW
DMFC	CH_3OH	20 - 90°C	W - 100 W
PAFC	H_2	220°C	10 kW - MW
MCFC	H_2 & CO	650°C	MW - 10 MW
SOFC	H_2, CO, & CH_4	500 - 1000°C	kW - 10 MW

Table 2.1: Characteristics of different fuel cell types.

Different fuel cell types answer to a range of applications [28, 44]. Those in the watt (W) range have a high energy density and are fast to recharge, making them useful in portable electronics. Fuel cells in the kilowatt (kW) range have a low startup time and are fast response, often being used in cars, boats, and for domestic combined heat and power (CHP). Larger fuel cells, those in the megawatt range (MW), are high efficiency and quiet, with applications such as buses, heavy duty transit, and distributed power generation [42, 45].

Fuel cells generate power by "organizing combustion" into two separate steps at the anode and cathode. As a result, they are able to operate at much lower temperatures

than traditional combustion and are not subject to the Carnot cycle [42]. Electrical potential of a fuel cell operating under standard conditions is limited by the change in the Gibbs free energy of the overall reaction, or the difference between the enthalpy of the reaction and the entropic heat loss. Power output is then determined by a polarization curve, which describes the relationship of voltage and current density (current per unit area). Compared to fossil fuel combustion, fuel cell operation is quiet and efficient [29]. A HES system, on the other hand, is subject to both charge (electrolyser) and discharge (fuel cell) efficiencies, resulting in an overall lower round trip efficiency than most other electrical energy storage systems [38].

2.1.2 Long Term Energy Storage

Long duration energy storage systems, such as pumped hydro and compressed air, are able to store up to weeks, or even months, worth of energy. In a pumped hydro storage (PHS) facility, the potential energy of water changes with height as it moves vertically between two basins. Charging is achieved through pumping water from lower to the upper basin, raising its gravitational potential energy; this energy is discharged when the water is run through a turbine as it returns to the lower basin. The maximum output of the facility, i.e. the power it can supply, is largely dependant on the height difference between the basins, often referred to as pressure head. The duration of the facility, i.e. the amount of energy it can provide, is related to the physical volume of the basins [2].

PHS is characterized by high (65%-80%) round trip efficiencies [28] and long life cycles; however, its large physical size may introduce difficulties in finding suitable sites and can drive up capital costs [29]. When implemented in warmer climates, evaporation and precipitation can cause significant fluctuations in operational costs [2]. Pumped hydro systems, particularly existing hydro assets, can lower their life-cycle carbon emission by using renewable energy, e.g. wind and solar, to power their pumps. Large storage duration and quick response times of PHS systems make them

well suited for applications such as seasonal energy storage, peak load shaving, and smoothing the power output of variable renewable energy sources [29].

In a compressed air energy storage (CAES) system, energy is stored as pressurized gas. Charging occurs by running air through a series of compressors, storing it in underground caverns. Energy is discharged by preheating, often through a natural gas heater, then expanding the compressed gas through a turbine. Operation of a CAES system resembles that of a Brayton cycle, with the compressor and turbine operating separately. Similar to pumped hydro systems, the duration of CAES systems is related to the volume of the cavern; the power it can supply relates to the thermodynamic properties of the air as it expands through the turbine. Due to similarities in capacity and response time, large scale CAES are suited to similar applications as PHS [29].

While CAES does not suffer from evaporative losses, they may be subject to small amounts of leakage [2, 28], depending on the pressure of the system as well as the material properties (e.g. permeability) of the surrounding cavern. Further (heat) losses occur as the compressed gas cools to the ambient temperature of the storage vessel. Similar to PHS, geographic availability of suitable sites remains one of the largest barriers in developing a CAES system [29].

2.1.3 Short Term Energy Storage

Coupling of energy costs ($/MWh) and power costs ($/MW) for short term energy storage systems, such as batteries, make them too expensive for long duration applications (> 24 hours) [36]. Battery energy storage (BES) is one of the most common forms of energy storage technology, having been used in portable electronics and vehicles for several decades [2, 29]. In more recent years, the deployment of BES systems has increased. Utility-scale BES are used for a variety of functions, such as smoothing renewable power output, emergency backup power, and operating reserves [29].

A battery's function depends on the direction of the electrical current. Charging occurs when an external potential is applied to the electrodes, and discharge occurs

due to an electrochemical reaction within the battery; the exact reaction which occurs depends on the electrode materials and chosen electrolyte [29]. BES are classified as having high technical maturity [28], low construction times [29, 46], and flexible installation location [29], making them an attractive option for a wide range of fast-response applications.

2.2 Existing Studies on Energy Storage in an Electricity Market

Previous work examining the impact of large scale deployment of renewable generators is well documented; a number of studies have recognized that the success of high renewable penetration is contingent on increasing the flexibility of electrical grids, which can be achieved through integration of utility scale energy storage [23, 35, 47–50]. This section reviews such literature, paying close attention to any assumptions, methodologies, and conclusions which may be relevant to this work.

2.2.1 Hydrogen Energy Storage

Over the past decade, an extensive literature has developed on the use of hydrogen energy storage to augment variable renewable generation. Previous studies have explored a broad scope of applications, from distributed power in buildings [51], micro-grids in indigenous communities [52] and islands [53], as well as entire cities [54], states [3], and countries [55]. Many of these studies follow a similar approach, simulating power system operations using a popular distributed-generation modelling software, HOMER (Hybrid Optimization of Multiple Energy Resources) Pro [56]. HOMER Pro allows for the simulation of annual micro-grid operations, examining all user-defined system combinations to meet a given set of load profiles. Simulation results present a list of feasible systems, sorted by descending net-present cost.

Contemporary work by Kharel [3] compares the techno-economics of hydrogen and lithium-ion batteries for large-scale energy storage in South Australia. As outlined

by the authors, this region gets its base load power from natural gas and coal fired generators, with the remaining demand met by solar and wind; as the share of variable renewable generation increases to meet renewable energy targets, and coal plants are retired, large-scale long-duration energy storage may be required to maintain grid reliability. For this purpose, 2 unique storage systems, a stand-alone battery bank and a battery plus hydrogen system, are sized to provide up to 4 days of autonomous operation [3].

Results of Kharel [3] demonstrate the growing potential for long-term energy storage as a cost-effective solution to back up renewable generation, and highlight the ability of hydrogen to fill that need. Here, the addition of a 2400 MW electrolyser, 2400 MW fuel cell, and 10,000 t[1] of hydrogen storage capacity is used to replace 172 GW (307 GWh) of battery[2] capacity, resulting in a 75% decrease in the cost of energy for the proposed system. In an alternative scenario where the system is given the option to use excess hydrogen to displace natural gas generation or to export to neighbouring states, an additional 22%, or 81% overall, reduction in the cost of energy is observed. Alberta and South Australia are similar in their electricity supply mix: dependant on thermal generation, but targeting higher renewable penetration in the near future. Consequently, Kharel's results show positive implications for the potential of long-duration hydrogen storage to displace gas generation in Alberta.

HOMER is well suited for a wide range of energy system research, as evidenced by the growing body of literature that uses it; however, like most closed source software packages, it is subject to a number of limiting factors. For instance, while HOMER Pro does allow for a grid connection to be considered in its energy systems, its current algorithm does not give proper consideration to the grid sell back price. Here, for any given hour, the grid is always used as the final option when no other energy sources or sinks are available. While this dispatch logic makes sense for micro-grid operations,

---

[1]Equivalent to 333 GWh, based on the lower heating value of hydrogen (33.3 kWh/kg)
[2]Assuming 130 kW/232 kWh Tesla Power Packs [57] are used

HOMER's target audience, for certain applications (e.g. energy arbitrage) it may lead to sub-optimal results: for example, a wind or solar asset generating during a period of high grid prices should not divert any energy to storage unless absolutely necessary. An alternative HOMER software, HOMER grid [58], corrects this issue, but does not currently support hydrogen assets. For the purpose of this work, a storage optimization algorithm has been developed in-house to more accurately represent the ideal behaviour of a grid-connected wind-hydrogen hybrid plant. Details regarding the algorithm are outlined in Chapter 4 of this thesis.

2.2.2 Long-term Energy Storage

Power systems with a high share of variable renewable energy require sufficient storage capacity, up to days or weeks in duration, to maintain reliability during periods of low renewable output [36]. Previous work has shown a sharp increase in required capacity in systems with heavy reliance variable renewable energy ($\gtrsim 80\%$) [59], or with strict emissions limits ($\lesssim 50$ kg-CO_2/MWh) [23, 60]. The ability of long-term energy storage to enable high build-out of wind and solar generation has seen a recent surge in interest [36], with studies showing the need for low-cost (500 - 1000\$USD/kW, 20 - 40\$USD/kWh) storage with durations greater than 100 hours to ensure power system reliability [61, 62].

Recent work by Sepulveda [36] models future power markets under various combinations of long-duration energy storage and low-carbon firm power. Electricity demand and weather profiles, based off Texas and New England, are considered under reference/high-electrification and reference/high/low scenarios respectively. Impacts of varying renewable and lithium-ion costs are also included. Simulations are performed using GenX [63], an MIT-copyrighted capacity expansion model, which bases power system performance on the assumption of perfect knowledge regarding future electricity demand and renewable energy profiles: a common approximation, according to the authors [23, 36].

The principal focus of Sepulveda [36] is to determine the system value of various long-term energy storage technologies across five dimensions: energy capacity cost ($USD/kWh), as well as power capacity cost ($USD/kW) and efficiency (%) for both charging and discharging. Here, system value refers to the decrease in total electric system cost due to the introduction of each new technology. Their results highlight the relative importance of each dimension. Energy storage technologies characterized by low energy capacity cost and high discharge efficiency are shown to have the most favourable impact on system value, with discharge power capacity cost and charge efficiency playing a secondary role [36]. Future scenarios considered feasible under current technologies see cost reductions from 10 - 40%, with greater reductions achieved by technologies that are geographically constrained (e.g. pumped hydro) and systems with durations over 100 hours. Due to its high capital cost and low flexibility, systems dependant on nuclear for their firming power see the largest benefit of long-term energy storage. At current demand levels, a full replacement of firm power capacity by long-duration storage requires energy capacity costs to fall below $USD 1/kWh [36].

Limitations, as identified by the authors, fall into three categories. First, this work covers the broad scope of firming power and long-duration storage, missing potential complementary interactions between combinations of storage technologies. Second, with transmission left out of the analysis, potential benefits such as the reduction of network congestion by energy storage have not been accounted for. Third, in accordance with similar studies, analyses focus solely on techno-economics, not accounting for the environmental risks or societal push back inherent in real-life electricity projects [36].

2.2.3 Short-term Energy Storage

A 2020 study by Mallapragada [23] models the performance of stand-alone lithium-ion batteries in a pseudo-American electricity market, closely resembling the U.S.

Northeast and Texas power systems, with simulations are performed using GenX [63]. Here, batteries are sized by discrete incremental durations (2, 4, and 8 hours) with an aggregated capacity to provide up to 40% of peak demand over various study scenarios, spanning a range of renewable penetration levels (40-60% by annual demand). All else held constant, simulations show that increasing storage capacity and renewable penetration will lower and raise the captured value of storage respectively. In other words, existing storage projects will see greater revenue as more renewables are brought online, but less as more storage projects emerge. However, even in high renewable scenarios, the captured value of storage is not enough to offset the capital costs of installing the batteries, which, according to the authors, is consistent with similar studies [48, 49, 64–66].

Mallapragada [23] demonstrates that short-duration storage operating in an optimized system will derive the majority of its value from reducing renewable curtailment and replacing natural gas plants during on-peak hours. Here, energy storage performs better in systems with high amounts of wind or solar, but not both; in particular, solar-centric systems derive the greatest benefits from the addition of storage, due to their predictable diurnal profiles [23]. Short term energy storage will likely play an important role in future energy systems, but it is not a one-size-fits-all solution: for example, exclusive use of lithium ion batteries is not a cost-effective decarbonization strategy [35]. Also, the interaction between energy- and power-capacity costs of batteries make them ill-suited for long-term ($\gtrsim$ 24 hour) applications [67].

Results of Mallapragada [23] are limited by assumptions restricting renewable generation profiles to a single representative time-series, and truncating grid operations to characteristic weeks. That is to say that wind (solar) fleets are treated as single generating units with a capacity equal to the sum of all individual parts, and annual grid operations are represented by extrapolating results from 7 weeks for each year of simulated data. Discussion surrounding storage performance is also limited to short term applications, with the study considering only 2 - 8 hours of storage duration.

Work performed in this thesis, though subject to its own limitations, presents a more realistic representation of electricity market operations: every wind and solar asset included in simulations has been given a unique hourly generation schedule, and grid operations are run for every hour across the simulation horizon. Additionally, storage capacity (power and energy) is optimized, rather than being simulated at discrete intervals.

2.3   Introduction to (Green) Hydrogen

Hydrogen is a colour- and odour-free gas with a specific energy approximately three times greater than conventional fuels [68, 69]. On its own, this metric can be somewhat misleading; the volumetric energy density of hydrogen gas is relatively small due to its low molecular weight, meaning an equivalent volume of another hydrocarbon contains more energy. The low energy density of hydrogen can be counteracted through compression or liquefaction, often performed for transportation and distribution purposes [68]. Figure 2.5 summarizes the energy properties of hydrogen as compared to other conventional fuels under standard conditions.
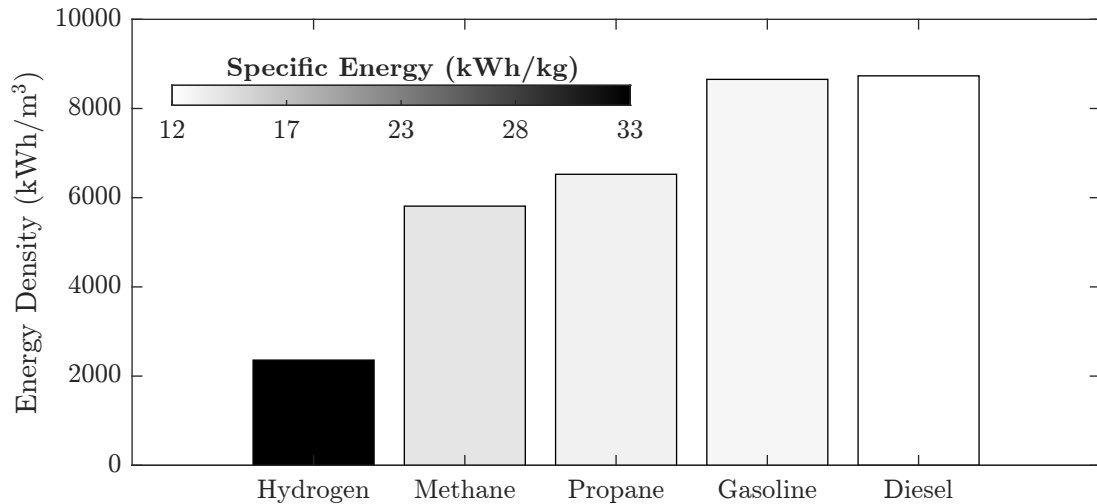
Figure 2.5: Comparison of specific energy (per unit mass) and energy density (per unit volume) for several fuels based on lower heating values [70]

Typically, hydrogen is found in compounds, e.g. water, methane, and other hydro-

carbons, requiring it to be extracted before use. The method in which it is extracted, as well as the carbon intensity of the process, is often used to distinguish four different "types" of hydrogen; in ascending order of emission intensity, these are: green, blue, grey, and brown/black[3]. Brown or black hydrogen come from the gasification of coal, lignite and bituminous respectively [72, 73], and will be omitted from further discussion as they are the most carbon-intensive processes, not widely considered as environmentally beneficial.

Grey and blue hydrogen are similar to each other, in that they are both a result of steam-methane reforming (SMR); the difference comes from the addition of carbon capture and sequestration (CCS) on the downstream side of blue hydrogen production. SMR is a two-part reaction using water (steam) to generate hydrogen and carbon dioxide [74]. The process occurs at very high temperatures (800 - 1000°C) achieved through combustion of additional natural gas [2] and is described by:

$$Heat + CH_4 + H_2O \longrightarrow 3H_2 + CO, \text{ and} \tag{2.1}$$

$$3H_2 + CO + H_2O \longrightarrow 4H_2 + CO_2. \tag{2.2}$$
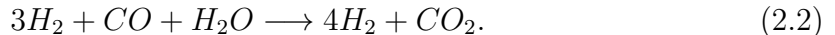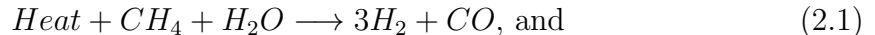
Green hydrogen, the least carbon-intensive of the four options, is generated through wind-, solar-, or hydro-powered electrolysis of water: an oxidation-reduction (redox) process, driven by an electric potential across two electrodes. The oxidation process occurs at the anode, resulting in a loss of electrons as described by $(2H_2O \longrightarrow O_2 + 4H^+ + 4e^-)$ for proton exchange membrane (PEM) electrolysers and $(4OH^- \longrightarrow O_2 + 2H_2O + 4e^-)$ for alkaline electrolysers. At the cathode, the reduction process results in a gain of electrons, as described by $(4H^+ + 4e^- \longrightarrow 2H_2)$ and $(4H_2O + 4e^- \longrightarrow 2H_2 + 4OH^-)$ for PEM and alkaline electrolysers respectively. By balancing the equations, it can be shown that the overall reaction for types of electrolysers can be written as a simple decomposition of water into gaseous hydrogen

---

[3]There is no standardized classifications for H_2 colours, and while this nomenclature may be common in industry and scientific literature [71], the terms are subjective and hold different meaning to different groups.

and oxygen: $(2H_2O \longrightarrow O_2 + 2H_2)$.

Today, carbon dioxide emissions are inversely related to the cost of hydrogen production, though this may soon be subject to change. Using the results of previous work, Table 2.2 summarizes production costs [75] and carbon intensities [76] for grey, blue, and green hydrogen. Note here that cost estimates are provided in 2016 $CAD and do not consider distribution or dispensing processes. Carbon intensity estimates account for electricity usage and, where applicable, natural gas consumption and carbon capture rates [68].

Hydrogen Colour	Specific Cost ($CAD/kg)	Energy Cost (CAD/GJ_\text{HHV}$)	Carbon Intensity (kg-CO$_2$e/kg-H$_2$)
Grey	0.91 - 1.42	6.41 - 10.01	11.4 - 12.2
Blue	1.34 - 1.85	9.44 - 13.04	2.4 - 4.2
Green	3.10 - 5.01	21.85 - 35.31	0 - 0.6*

*Upper range a result of methane emissions from hydro reservoirs [68]

Table 2.2: Wholesale cost and carbon intensity ranges of grey, blue, and green hydrogen, assuming no carbon pricing

Hydrogen can be distributed by truck, rail, and, to some extent, through already existing pipeline networks; current natural gas systems can accommodate up to 15% hydrogen blending, with higher percentages (or pure H$_2$) likely requiring new infrastructure [68]. The chosen mode of transport and storage conditions will be strongly influenced by demand and desired transportation distances. For example, the cost of distributing H$_2$ by truck can range from $3 - $10 per kilogram, depending on the distance travelled and mode of storage [76]; distribution by pipeline is expected to be the cheapest option ($\sim$ $USD 1/1500km/kg-H$_2$) [77] once demand levels justify their construction.

2.4 The Potential for a Hydrogen Economy

The uses of hydrogen can be grouped into two broad categories: as a stored energy fuel, through combustion or using a fuel cell, and as a blending agent for chemical and fossil fuel upgrading, with the latter use being much more common today[4] [77]. Like the majority of renewable/alternative energies, the potential for hydrogen to add value is heavily influenced by its decarbonization potentials: especially in historically carbon-intensive industries [68]. In 2018, nearly 2/3 of global hydrogen supply was still produced using natural gas (48%) and coal (18%) [77]. Alberta's current hydrogen market follows a similar pathway, with the majority of hydrogen production coming from SMR for production of synthetic crude oil (SCO) [38], i.e. grey hydrogen.

Outside of the oil-sands, there are a number of potential uses for hydrogen in Alberta: residential heating and household appliances, for example. Between 2011 and 2015, natural gas consumption in Albertan households ranged from 79% - 81% [78] of total energy usage. By blending appropriate amounts of hydrogen into the existing natural gas supply, the resulting fuel could still be used for many applications such as furnaces, stoves, and barbecues. Hydrogen can also be used in electricity generation and heavy duty transport (freight) [68]; here, either fuel cell or blended fuel combustion could be applied, depending on the specific application. Alternatively, hydrogen can be used as a feed stock in chemical (e.g. methanol) and fertilizer (i.e. ammonia) production. In fact, current projections show demand for Canadian hydrogen reaching 2 - 4 Mt/year by 2030, and up to 8 - 20 Mt/year in 2050 [5].

As more countries pledge to reduce, or even eliminate, carbon emissions in the coming decades, many are turning to hydrogen as part of the solution. A recent op-ed out of Bloomberg advocates for green hydrogen as a contender, alongside wind, solar, and lithium-ion batteries, to receive a portion of the U.S. coronavirus relief funding

---

[4]From IEA Future of Hydrogen Report [77]: "The top four single uses of hydrogen today ... are: oil refining (33%), ammonia production (27%), methanol production (11%) and steel production ... (3%)."

[79]: an opinion which parallels the climate plan of the 47th U.S. President, Joe Biden. In May 2021, President Biden revealed plans for his next budget, including $800M for fighting climate change [80]. The Biden infrastructure plan, or American Jobs Plan [81], states that the United States will be "supporting carbon capture as well as new sources of hydrogen — produced from renewable energy, nuclear energy or waste" [82]. Here, the main support for hydrogen lies in is its ability to decarbonize industrial sectors outside of electricity generation and passenger transportation: with the latter two being better suited to wind + solar and batteries respectively. According to the 2019 Global Carbon Budget [83], a complete decarbonization of global electricity and transportation sectors would still leave around half of the world's CO_2 emissions untouched, further solidifying the need for green hydrogen.

At this point, the promise of a hydrogen-driven economy is decades old [84], urging the question: why the renewed interest? As reported in a recent review out of MIT, the short answer is: the falling costs of renewables and advancements in electrolyser technology [85]. Current projections cite green hydrogen becoming cost competitive within the next 10 years in areas with high renewable penetration [86], and by 2030 elsewhere [77]; through proper policy deployment, costs of solar generated hydrogen may reach as low as $2 USD/kg across much of the continental United States [87] in the coming decade. In fact, results presented in the final chapter of this thesis show wind-driven green hydrogen achieved at costs below $2 CAD/kg in the next 5 years.

2.4.1 The Future of Freight

In a three-part series entitled *The Future of Freight*, Lof [74, 75] and Layzell [45] investigate the potential for emission reductions in Canada's freight industry. As one would expect, much of the discussion involves alternatives to diesel for use in internal combustion engines (ICE): a tangent, though not unrelated, to this work. The latter half of the most recent report in this series evaluates the possibility of offsetting, or replacing, the Albertan diesel market through an aggregation of green and blue

hydrogen [45]. Alberta is a net exporter of diesel, with around 90% of its production ($3.7 billion CAD of revenue in 2014 [88]) being consumed in other provinces; as a result, a replacement industry would need to provide similar economic benefits, as well as offset carbon emissions, to be considered in future investments.

When considering blue hydrogen (SMR + 90% CCS) as an alternative to diesel, Layzell found that 2016 Albertan natural gas production was marginally lower than its total diesel demand (including exports) for the same year [45]. That is to say that, strictly on the basis of energy, Alberta has sufficient resources (i.e. natural gas reserves) to effectively replace its diesel industry with blue hydrogen[5], all while maintaining its internal supply commitments. Assuming a retail price of $5 CAD/kg-$H_2$[6] [74], hydrogen sales would net on the order of $7 billion CAD [45] annually. It is also worth noting that while overall CO_2 emissions will decrease with a shift to blue hydrogen, 100% of associated emissions will occur in Alberta, where the hydrogen is generated; while water is the only emission generated by hydrogen consumption, through combustion or using a fuel cell, the SMR process generates 2 - 4 kg of CO_2 for every kg of hydrogen produced [2, 74]. Alternatively, when compared to natural gas, by using green hydrogen the process could be made effectively carbon neutral.

In 2018, wind and solar accounted for 6% and <0.1% of the total 81 TWh of electricity generated in Alberta respectively [89]. As discussed in section 1.3 of this work, Alberta's wind fleet receives a lower price than the rest of the generating pool due to their operation during off-peak hours; this effect is further amplified by the fact that wind infrastructure is highly concentrated in a small area of the province [18]. A similar phenomena can arise when a large amount of solar is added to a system, i.e. the "Duck Curve" [21, 90]; however, at the time of this work Alberta's current solar fleet was far too small to influence the power price in this manner [20], although

---

[5]Assuming an SMR/CCS efficiency of 78% based on higher heating values [71]

[6]From Future of Freight Part B [74]: "To calculate the retail price for H_2, we estimated the cost of ... producing ..., distributing, ..., compressing [,] and storing the H_2 ..., providing an additional 10% margin for the fueling station."

it has recently begun to grow rapidly. Pairing a hydrogen system, consisting of an electrolyser, compressor, and storage tank, with existing (and new) renewable assets would offer an additional revenue stream, similar to other energy storage technologies. Here, a portion of the renewable generation can be allocated to producing hydrogen during low demand (low price) hours, which in turn can be sold as fuel [45]; with the addition of a fuel cell stack, hydrogen could also be converted back into electricity to sell back to the grid.

Contrary to the blue hydrogen case, Alberta's current renewable fleet does not have the generating capacity to replace diesel demands entirely with green hydrogen. Table 2.3 summarizes findings based off Layzell's work [45, 91], outlining the additional infrastructure required to meet the 2016 internal diesel demands for Alberta and all of Alberta's 2016 production (9x internal demands) via green hydrogen (75% wind, 25% solar). For wind, calculations consider a fleet of General Electric 4.8 MW turbines with a rotor diameter of 158 m, a capacity factor of 36% [92], and direct land requirement of 0.003 km^2/MW [93], which includes associated infrastructure (e.g. access roads). Note, however, that the total land use for wind is much larger than the direct land use; with an assumed power density of 1.12 MW/km^2 [94], wind turbines would need to be spread across 4,360 km^2 to meet internal diesel demands, for example. Solar calculations are based off an assumed capacity factor of 17% [95], and land requirement of 0.04 km^2/MW [91].

A significant limitation of Layzell [45] and Loff [74, 75] originates from their treatment of renewable asset owners in an electricity market: assuming they will operate for the sole purpose of generating hydrogen. In Alberta, wind and solar farms are currently not allowed to offer their power above \$0/MWh; they can, however, divert their power from the grid to an energy storage device or electrolyser during low-price hours. If a wind or solar asset is generating during high-price hours (e.g. above their levelized cost), it is likely in their best interest to dedicate their entire capability to the grid for that time. Here, the gain in energy revenue counterbalances the lower

Parameter	Internal Demand	Plus Exports
Wind		
Number of Turbines Required	3,881	34,910
Installed Capacity (GW)	19	168
Estimated Energy Output (TWh/yr)*	59	529
Direct Land Use (km^2)**	57	504
Solar		
Installed Capacity (GW)	13	118
Estimated Energy Output (TWh/yr)*	20	176
Direct Land Use (km^2)**	520	4720

*Energy Output = (Installed Capacity)(Capacity Factor)(8760 hrs/yr)(1 TW/1000 GW)

**Land Requirement = (Installed Capacity)(Power Density)(1000 MW/1 GW)

Table 2.3: Additional infrastructure requirements to replace 2016 diesel demands with green hydrogen through wind and solar-driven electrolysis of water

yield of hydrogen, inherent in this strategy, likely resulting in an overall lower cost per unit of hydrogen.

2.4.2 Large Scale Wind Hydrogen Production with Energy Storage in Western Canada

Previous work by Olateju et al. [38–40] models hydrogen production by wind-driven electrolysis as an alternative to steam-methane reforming in Alberta. In the most recent study [38], an in-house techno-economic model was developed using MAT-LAB, utilizing historical market inputs, hourly average wind energy production, and grid pool prices, all obtained through AESO. The objective of this model, on top of determining the feasibility of such a project, is to determine the optimal plant configuration: electrolyser size, number of electrolysers, and battery capacity, resulting in the minimal hydrogen production cost.

A wind-hydrogen pathway was chosen for this particular study [38] as it incurs the lowest greenhouse gas emissions of all available (as of 2016) hydrogen production methods [96–99]. In addition to wind and hydrogen units, energy storage, i.e. a battery bank, is used to better capture the dynamic pricing inherent in the Alberta electricity market. Electrical energy storage, rather than a hydrogen storage-fuel cell configuration, was selected as the latter pathway is more expensive and has a round trip efficiency on the order of 25-30% [38, 55, 100–103]. Also, without the aid of a flexible mediator (the battery), the electrolyser's efficiency and lifespan will be negatively impacted by the volatility of the wind energy input [104, 105], increasing the potential for over and under estimation of modelled hydrogen production and operational costs respectively [38].

Key findings of Olateju [38] indicate the optimal electrolyser-battery configuration as one where the capacity factors of each of the units are approximately equal, regardless of electrolyser size. According to the authors, in order to understand this result, it is important to note that an electrolyser's productivity is directly related to the battery's ability to supply it with energy: i.e. an undersized battery will lead to under-utilization of the electrolyser. For a given size of electrolyser, as battery size increases, electrolyser capacity factor will also increase until it is no longer constrained by the battery. Past this juncture, as battery capacity is further augmented, its capacity factor will begin to decrease: optimal electrolyser and battery sizing is subject to a trade-off between these events [38].

The addition of a battery to a wind-hydrogen plant has been shown to increase electrolyser capacity factor and allows for more consistent capturing of on-peak electricity prices; the marginal magnitude of the benefits decreases with increasing electrolyser capacity. With respect to energy arbitrage, it was found that such benefits were not enough to cover the costs of the battery, providing only 2.3% decrease in hydrogen productions costs when compared to a previous model, however, the increase in electrolyzer durability may make the addition of a battery worthwhile [40]. Olateju's

work is limited by the inherent assumption that the market does not react to the addition of storage to the grid. In other words, market players (generators), including those on the margin, are considered indifferent to the additional generating capacity being added. For the chosen case study, however, the effects of this approximation are relatively small as the added capacity in on the order of a couple megawatts [38]. The effects are lessened further by the fact that much of the additional power is dedicated to hydrogen production for bitumen upgrading, rather than electricity production.

2.5 Conclusions

This chapter presents a review of energy storage and hydrogen, emphasizing their role in future electricity markets and the broader economy. Having recently released a national hydrogen strategy [5], Canada aims to position itself as a global leader in hydrogen production, export, and use. The overwhelming majority of Canada's current hydrogen economy exists in the province of Alberta, producing more than 5 kt of hydrogen per day, 2/3 of which is consumed on site [106]. Historically, Alberta's hydrogen production comes from steam methane reforming, resulting in in approximately 18 Mt of CO_2-equivalent emissions per year [106].

Renewable energy produced by wind and solar is inherently variable and, in the case of wind, often inversely proportional to the power price. As such, a wind-hydrogen hybrid plant, could prove to be mutually beneficial. Diverting wind energy from the grid to an electrolyser during instances of near-zero power prices would increase the captured price of wind; the byproduct, low-cost zero emission hydrogen, can be converted back to electricity, through combustion or a fuel cell, once the price of power has rebounded, or sold itself as a raw material. With ongoing improvements in electrolyser technology [85], decreasing costs of wind and solar [1], and increasing carbon pricing in Canada [14], it is no longer a question of if electrolysis will become cost-competitive with steam methane reforming, but when.

Renewable energy has seen significant economic and technological breakthroughs

in the past, and this trend is showing no indication of changing. For example, utility-scale solar has seen a 90% decrease in levelized cost since 2009 [1]. Similarly, the average wind turbine installed in Canada has doubled in height and more than tripled in rotor diameter and nameplate capacity since the early 1990's; further discussion on the evolution of the Canadian wind fleet can be found in the next chapter of this thesis. As a result, previous work regarding renewable technologies, such as Olateju [38–40] or Khare [3], are condemned to obsolescence in relatively short order. The final chapter of this thesis expands upon this previous work: forecasting power market composition and electricity prices to inform future opportunity in hydrogen energy storage technologies.

Chapter 3

Mapping Canada's Wind Energy Fleet

William Noel[a], Timothy M. Weis[a,*], Qiulin Yu[a], Andrew Leach[b] and Brian A. Fleck[a]

[a] Department of Mechanical Engineering, University of Alberta, Edmonton, AB, Canada T6G 1H9

[b] Alberta School of Business, University of Alberta, Edmonton, AB, Canada T6G 2R6

* Corresponding author; *Email:* tweis@ualberta.ca

Abstract

This paper describes the development of a data set mapping all commercial wind turbines in Canada: the 9th largest onshore wind energy fleet in the world. Details contained in the map outline the evolution of commercially deployed technology in a large North American market, as well as the differences in development patterns across the country in part resulting from the introduction and cessation of various policies. In total, 6711 turbines spanning 263 projects and 13.4 GW of generating capacity were indexed including coordinates, model, manufacturer, owner, tower height and commissioning date. Data were compiled from publicly available sources including planning documents, technical reports, environmental impact studies and acoustic emission reports. In 2019, average rotor diameters were 131 m with 102 m tall towers, roughly double the average size of both 20 years ago, while the typical installed capacity density has remained close to 1.65 MW/km^2. Commercial wind farms have trended towards large turbines and installed capacities, while the emergence of community-led

projects in the past decade have simultaneously resulted in smaller projects in recent years. This work serves as a benchmark for the evolution of wind energy in Canada and a framework for similar analyses in other jurisdictions.

3.1 Introduction

Despite wind energy being a significant and growing contributor to the Canadian electricity supply, until recently there was no comprehensive map or index of wind energy infrastructure with sufficient granularity to detail individual turbine locations at a national level. Regional inventories that do exist, for example in the province of Nova Scotia (NS) [107], often give wind farm locations as a single representative point. Maps of higher accuracy can be found in jurisdictions such as the United States [108], the United Kingdom [109], Denmark [110, 111], and some sub-national regions of Canada such as Ontario (ON) [112, 113], to name a few. A Texas-based company, IntelStor, has set out to map the geographic locations of the global wind fleet, having already catalogued over 100,000 turbines as of April 2019 [114, 115]. To better document Canada's wind energy fleet, the University of Alberta, in collaboration with Natural Resources Canada (NRCan) and the Ottawa branch of the Canada Centre for Mineral and Energy Technology (CanmetENERGY), sought to consolidate fleet information regarding the Canadian wind industry into a more comprehensive database. The results of this work are presented here along with a overview of the evolution and state of wind energy infrastructure in Canada. Data resulting from this study are publicly available via NRCan [25]. Screenshots of the map for Canada, and a zoomed in portion of Southern Alberta, are shown in Figures C.1 and C.2 in the Appendix respectively.

As of 2019, Canada was ranked 9th in the world for onshore wind energy, with a total installed capacity of 13.4 GW across all 10 provinces and 2 of the 3 northern

territories. Figure 3.1 provides a map of Canada annotated with provincial installed wind [116] and total generation [12] capacities, with colour representing provincial wind penetration. For the most part Canada's provinces operate their electricity systems predominantly to serve their domestic loads, however there are a few notable outliers including Newfoundland and Labrador (NL) where over 5000 MW of its generation capacity is purchased by Hydro Quebec, and Prince Edward Island (PE) imports just under 2/3 of its electricity from New Brunswick (NB) [12]. Outside of these two provinces, wind energy fleets range from 5% to 10% of installed provincial system capacities. Combined, wind energy generated 5% of electrical energy generated in Canada in 2018 [12], making it the 5th largest electricity source behind hydro (61%), nuclear (15%), natural gas (9%) and coal (8%).

3.2   Background

3.2.1   Significance of a Wind Turbine Map

Recent projects in Canada have been announced with winning bid prices as low as 37 CAD/MWh in Alberta and 35 CAD/MWh in Saskatchewan for 20-year contracts announced in 2017 and 2018 respectively. These costs are consistent with North American data showing that wind energy has become one of the lowest levelized cost of energy for new electrical generation [117]. The Canadian wind industry expects cost declines to continue into the future [118]. The low energy cost of new wind generation combined with continued efforts to reduce carbon emissions in the electricity sector and to increase electrification will likely result in increased wind energy growth in Canada in the coming years.

The publication of this database can be useful in Canada as wind energy grows and is scrutinized during development and operation. As many scientific journals are not open-sourced, the general public does not have free access to the majority of peer-reviewed articles. As such, those seeking information will often obtain it from popular
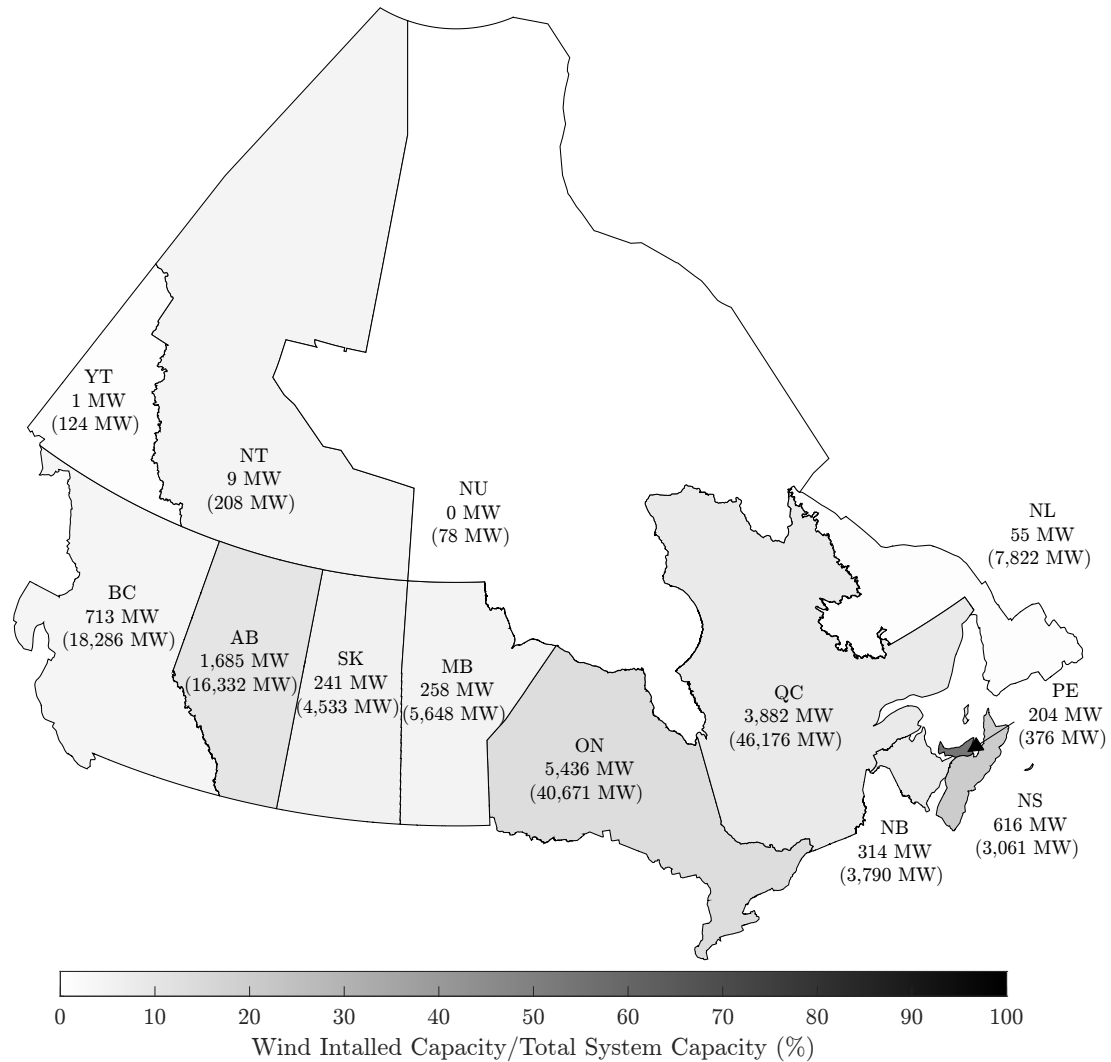
Figure 3.1: Provincial installed wind capacity and total system capacity, 2019

literature and the internet; unfortunately, many of these sources of information are subject to high levels of bias and a lack of scientific evidence [119]. Publicly available data resulting from this work may help to contribute to a better understanding of the effect of wind turbines on human health and their surrounding environment, among other things.

In spite of its growth in recent years, wind energy in Canada has not always been without detractors, many of who point to issues of visibility, acoustic emissions and risks to avian wildlife [120, 121], including the formation of anti-wind energy development organizations. In Ontario, Canada's most populous province, orga-

nized groups fighting wind energy development were able to convince a newly elected provincial government to take an unusual step of cancelling multiple wind projects mid-construction [122, 123]. Similar occurrences have been documented in France, where community resistance to some wind projects has been a major contributor to delayed development of individual projects [124].

Sometimes resistance to wind energy comes from concerns regarding potential human health impacts. Studies on community perceived health-effects attributed to nearby wind farms are well documented. A common finding of these studies is that a proportion of people living near operational wind turbines consider them an auditory annoyance. It has been suggested, however, that this annoyance is not only related to sound, but also a conglomeration of subjective factors such as visual impact of and preexisting attitudes towards wind turbines as well as noise sensitivity [119]. Many of the self-reported ailments including loss of sleep, headaches, and irritability, for example, are also symptoms of anxiety and annoyance [119, 125]. Another common complaint of wind farm adjacent communities is infrasound exposure; while wind turbines do emit measurable levels of infrasound (sound below 20 Hz), there is currently no conclusive evidence linking exposure to any adverse health effects [126]. A complete turbine location database may help to further track continued health related research as it allows the comparison of turbine sizes and distances to dwellings all across the country.

As is the case with any power generation infrastructure, wind turbines have the potential to cause unintended impacts to their local environment. While not a leading cause of avian fatalities in Canada, wind farms can have impacts on bird and bat populations [127]. As wind farms proliferate and turbine sizes increase, birds and bats fatality rates may also change in part part due to a difference in their migratory altitudes [120, 128]. There are still gaps in understanding of wind turbines' negative impacts on avian population and as such research is going into its prevention and mitigation. While siting new wind farms away from sensitive avian habitats and

migration corridors is common practice, strategies to minimize cumulative impacts and mitigation of existing infrastructure must also be developed. For this latter case, there does not seem to be a catch-all prevention approach as various species react to mitigation methods differently [129]. One potential solution to this problem relates to a recovery of ecological conditions to reinforce prey population and encourage improved roosting and mating conditions [130].

Finally, the publication of a detailed wind energy inventory may help to promote more geographically detailed and was as inter-provincial comparative research. The database also catalogues development patterns and technological deployment across Canada and is the focus of the latter half of this paper.

3.3 Methodology

Although Canada is the focal case study for this paper, the methodologies and evaluation metrics defined below are not region specific. That is to say that many of the developed methods and their associated analyses could be applied to further operational wind fleets, regardless of jurisdiction.

3.3.1 Generating a Comprehensive Wind Turbine Map

In Canada, there are no national bodies which governs the entire electricity sector; rather, provinces and territories have jurisdiction over the infrastructure, proposed and existing, within their own borders. Most, with the exception of Saskatchewan, have a provincial utility commission which must approve the construction or alteration of any electricity generation, transmission, or distribution facilities [131]. Through these administrations, one is able to access records: applications, filings, and proceedings, for all electrical generation projects in the given province. These documents provide initial information necessary to locate wind farms. Further insight may also be gained from Crown utility companies: BC Hydro and NB Power, for example, or electrical grid operators such as Alberta Electric System Operator (AESO) or Ontario's

Independent Electricity System Operator (IESO).

Data Collection

At the time of this study, there were over 6700 commercial-scale wind turbines operating in Canada, grouped into more than 260 individual projects. In order to efficiently map and index each turbine, one should start by locating project sites and their associated turbine count. From here, individual turbines can be tracked down on a farm-by-farm basis [113]. For the purpose of this work, a list of operational wind farms has been obtained through the Canadian Wind Energy Association (CanWEA). The number of turbines per farm, as well as turbine characteristics (manufacturer, height, rotor diameter) are collected directly from project documents for each wind farm where possible. Documentation is generally found through the provincial utility commission or one of the project developer, owner, or operator web pages. In the case where project documentation is lacking (or difficult to find), information can often be found in technical reports, such as acoustic emissions studies, from adjacent wind projects. International databases such as The Wind Power website [132] can also be used as primers for less readily available data.

Mapping Individual Wind Turbines

The level of specificity on turbine locations given in documentation varies greatly between projects, ranging from vague descriptions (nearest county or township) to annotated maps or lists of specific geographic locations (latitude-longitude/northing-easting). In cases where coordinates are not readily available, wind turbines can typically be located directly from satellite images due to their large physical size and familiar shape as shown in Figure 3.2a, for example. When geographic information can be taken directly from project documentation, locations are still verified against satellite images to ensure accuracy, as projects may change between planning and construction. The use of multiple satellite image providers is often necessary due to

outdated imagery, e.g. if the photo is taken before the turbines have been erected. This study uses Google Maps, Apple Map, Yandex Map, and Esri Map. Building off of the information provided, individual turbines are mapped using Google Earth, as demonstrated in Figure 3.2b.

(a) Blackspring Ridge Wind Farm, AB (Latitude: 50.067°, Longitude: -112.923°)

(b) Glen Dhu Wind Farm, NS (Latitude: 45.665°, Longitude: -62.222°)

Figure 3.2: Satellite images of wind infrastructure showing individual turbines (a) and wind farm layout (b)

3.3.2 Analyzing Infrastructure Density

In order to minimize wake effects, a general practice when siting wind turbines is to leave 6-10 rotor diameters and 3-4 rotor diameters between turbines in the prevailing and cross wind direction respectively [133]. As a result, the closest any wind farm expansion, or adjacent wind farm could be built would be at a distance of at least 10 rotor diameters from an existing wind farm. In order to develop a metric to define the geographic size of a wind farm, the area of influence for each turbine is set as 10 rotor diameters.

Capacity and Turbine Density

For the purpose of this study, the term "capacity density" will be used to denote the ratio of the nameplate capacity of installed wind turbines and the geographic area of land that they occupy. Such terminology is used to circumvent any confusion, as

the term "power density" (or power potential) typically refers to the power available in the wind for a given location, and is based off factors such as: air density, wind speed, and the probability frequency distribution of wind for the selected area [134]. Similarly, "turbine density" refers to the ratio of the number of turbines for a given wind farm compared to the land area that the wind farm occupies. Finally, wind power classes are used to classify the quality of the wind resource for each wind farm. Here, power class ranges can be found in Table 3.1 as defined by the NREL [135].

Wind Power Class	Average Annual Wind Speed at 50 m
1	≤ 5.6 m/s
2	≤ 6.4 m/s
3	≤ 7.0 m/s
4	≤ 7.5 m/s
5	≤ 8.0 m/s
6	≤ 8.8 m/s
7	≤ 11.9 m/s

Table 3.1: NREL wind power classifications, based on wind speed at 50 m [135]

Wind farm geographic area analysis was performed using ArcMap on a 1983 North American Datum (NAD) projection. Wind project data are converted to a comma-separated variable (.csv) file and imported into the Geographic Information System (GIS) software. From here, wind farms are split into individual layers, whereby each turbine consists of a circular area with a diameter 10 times that of its rotor. Using the buffer and dissolve functions, turbine areas are combined into a single polygon; for the cases where visible gaps are present in this larger polygon, the null areas are filled by connecting outer adjacent circles with tangential lines. Figure 3.3 gives an example of the finished polygons for the Caribou and Lameque wind farms located in NB. For wind farms with varying rotor diameters, turbines are grouped by diameter and combined by the same method as described above. Any areas which overlap are

only accounted for once. Finally, capacity density measured in megawatts per square kilometre, and turbine density measured in turbines per square kilometre, for each wind farm is found by taking the ratio of the wind farm capacity and number of turbines to the total polygon area respectively.
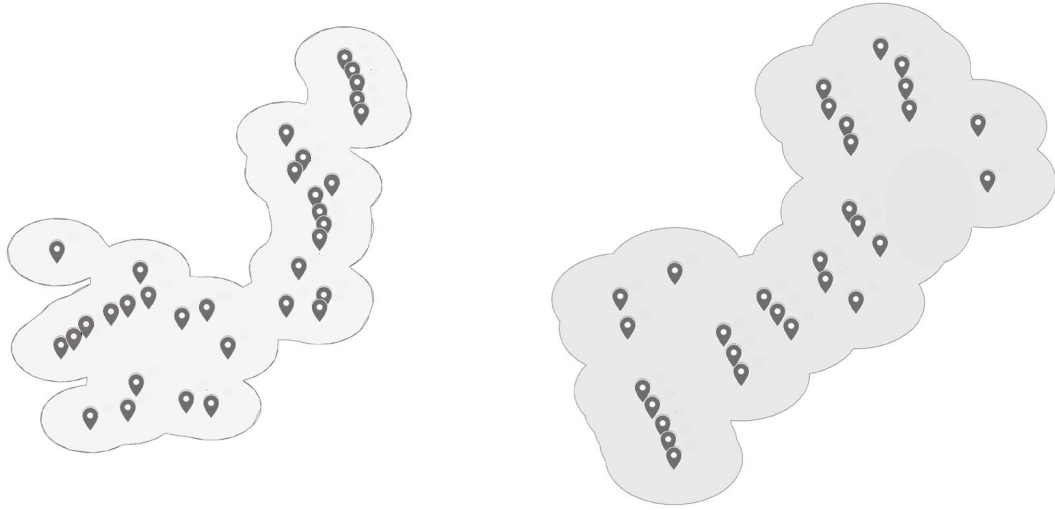
(a) Caribou Wind Farm, NB
(Polygon area = 35.6 km^2)

(b) Lameque Wind Farm, NB
(Polygon area = 22.3 km^2)

Figure 3.3: Example of polygons used to define wind farm areas

Wind Power Class

Defining a wind power class for a given location requires a characteristic wind speed at a height of 50 m. For the purpose of this study, this information was sourced using the Global Wind Atlas' modelled wind speeds [136]. The Global Wind Atlas is a public data set of simulated annual mean wind speeds from a down-scaled generalized atmospheric model [137] using 0.25 km horizontal grid spacing, developed by the Technical University of Denmark and the World Bank Group. These data are not validated as part of this work, but offer a consistent source to characterize overall wind regimes. Using this tool, wind speeds at each wind farm site are found for 50 m above ground.

From the Global Wind Atlas website, 50 m wind speed data for Canada are down-

loaded as a Tagged Image File Format (.tiff), and imported into ArcMap on a 1983 NAD projection. With the wind speed map overlaid by turbine locations, a characteristic wind speed is found for each wind farm using the pixel inspector tool; this tool allows for a user defined grid of pixel values (i.e. wind speeds) to be examined simultaneously. Here, the strategic siting of wind turbines was accounted for by altering the grid size and shape for each individual farm: for example, the grid for a wind farm located on a mountain ridge would have few columns and many rows as to exclusively capture the high-speed wind regime in which the turbines operate. Wind speed values from each grid are averaged to compute a representative wind speed for each site, allowing for each farm to be categorized into an NREL power class.

3.4 Results

3.4.1 Canadian Wind Map

Data for each wind farm are sourced from project documents, concatenated into a spreadsheet, and visualized on Google Earth; information such as project name, year commissioned, location, number of turbines, owner, and operator are tabulated. From here, individual turbine data are collected and listed by characteristics such as: geographic location, power rating, rotor diameter, hub height, manufacturer, and model. For indexing purposes, each turbine is given a unique identification number corresponding to the project to which it belongs, and its number out of the total fleet of turbines for the given farm. Finally, an indication of confidence in the accuracy of turbine locations is given, with associated explanations (e.g. outdated imagery) where required.

A total of 263 projects, comprised of 6711 individual turbines with 13.3 GW of installed capacity have been accounted for, and additional projects will be added to the NRCan database as they are commissioned. Figure 3.4 shows the progression of wind capacity in Canada from 1998 to 2019, split by province. To avoid crowding in

figures, NB, NS, NL, and PE have been combined into Atlantic Canada (ATL). Similarly, Saskatchewan (SK) and Manitoba (MB) have been consolidated into a single jurisdiction (SK+MB). It should be noted that this study does not consider projects in any of the territories: Yukon (YT), Northwest Territories (NT), and Nunavut (NU), as these regions make up less than 1% of the total installed capacity in Canada [116].
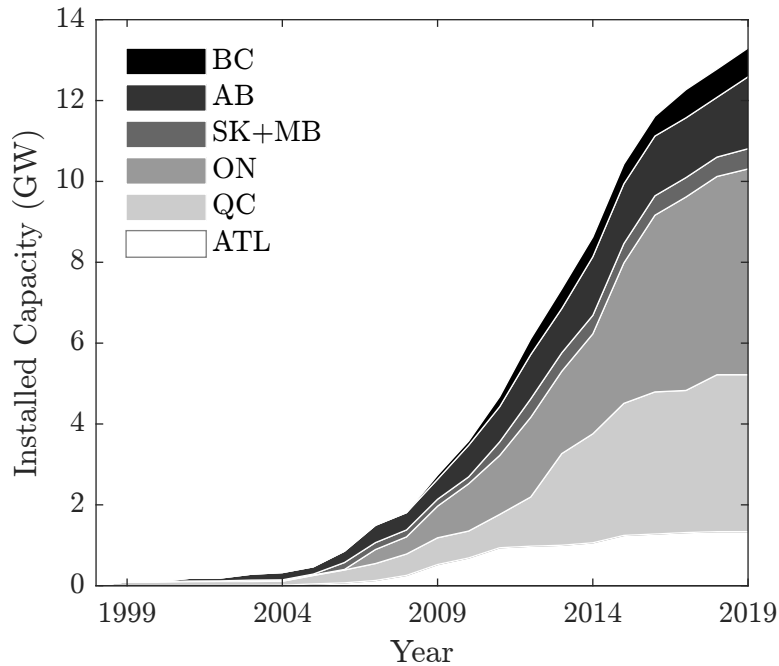
Figure 3.4: Annual time series of cumulative installed wind capacity by province

As investment into wind infrastructure increases, technological advancements follow suit. Wind turbines benefit heavily from scale; the power output of a turbine is proportional to wind speed cubed and rotor diameter squared, where wind speed increases with height inside the atmospheric boundary layer. Figure 3.5 shows the progression of wind turbine technology (height, diameter, installed capacity) in Canada over the past 25 years. Note here, that height of the circles gives an average turbine hub height for the given year, the bubble size provides a representation of average diameter, to scale with the *y-axis*, and bubble colour shows the average turbine capacity for that year.
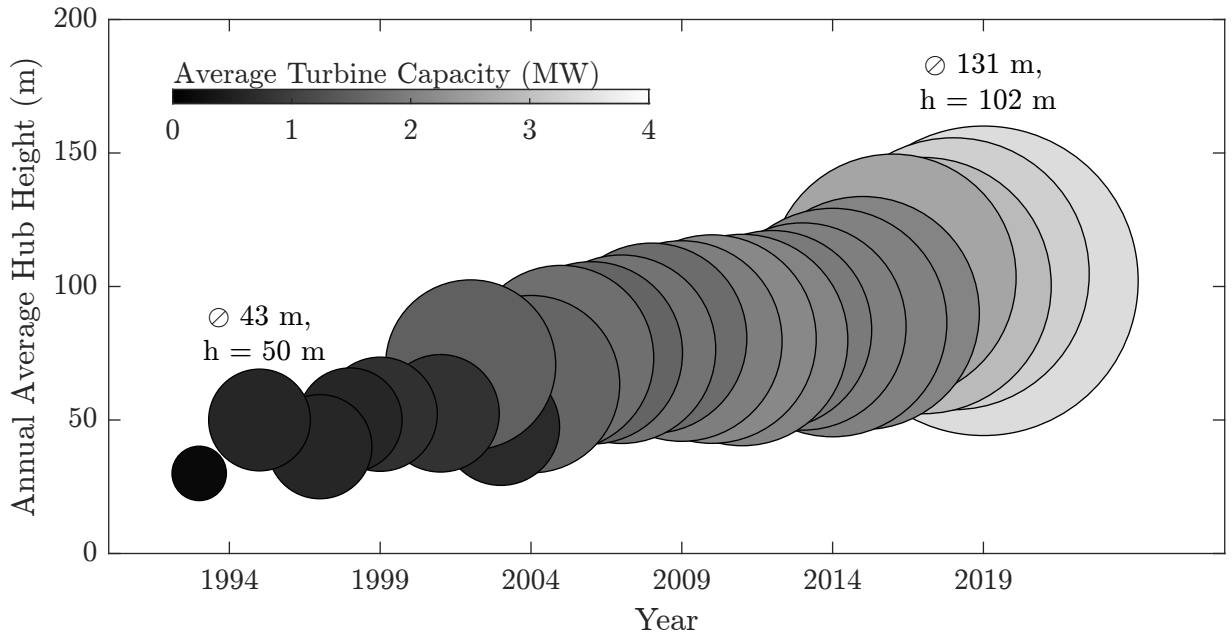
Figure 3.5: Annual average turbine capacity, turbine diameter, and hub height

Figure 3.6 provides a range of wind farm sizes installed every year; the shaded area shows median bounded by the 25th and 75th percentiles, i.e. the Interquartile Range (IQR). The '+' symbols show the largest installed wind farm for a given year. The bar graph on the lower axis gives the national annual installed capacity.

Of the turbines which were mapped, 97% of them are manufactured by 5 companies: General Electric (GE), Vestas, Siemens, ENERCON, and Senvion, with the remaining 3% being produced by various smaller companies. Figure 3.7 gives an account of provincial wind fleets by manufacturer. Note that the capacity installed by smaller companies, omitted from the plot, comes from a combination of: Acciona, Bonus, DeWind, Emergya Wind Technologies (EWT), Gamesa, Lagerwey, Leitwind, Nordtank Energy Group (NEG) Micron, Nordex, Pfleiderer, Samsung, Suzlon, Tacke, Turbowinds, and Vensys, some of whom have been subsequently purchased by the aforementioned manufacturers.
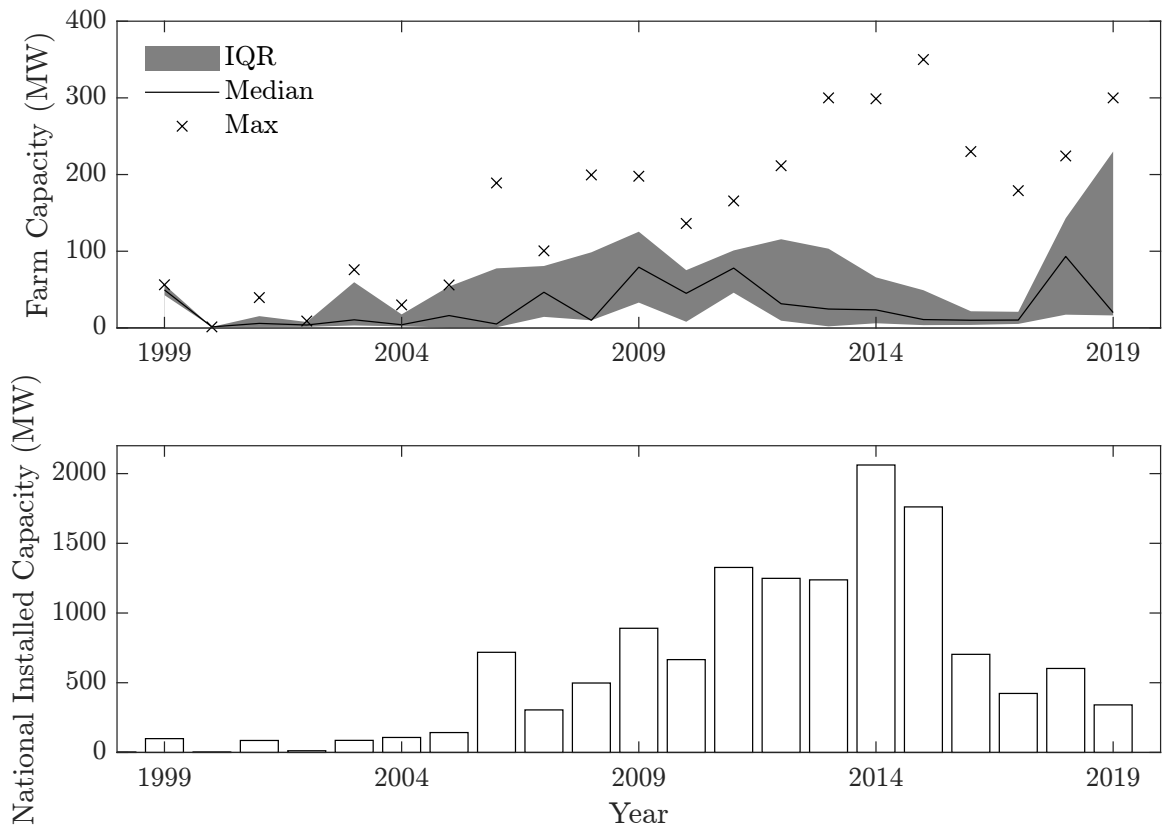
Figure 3.6: National annual installed farm capacity
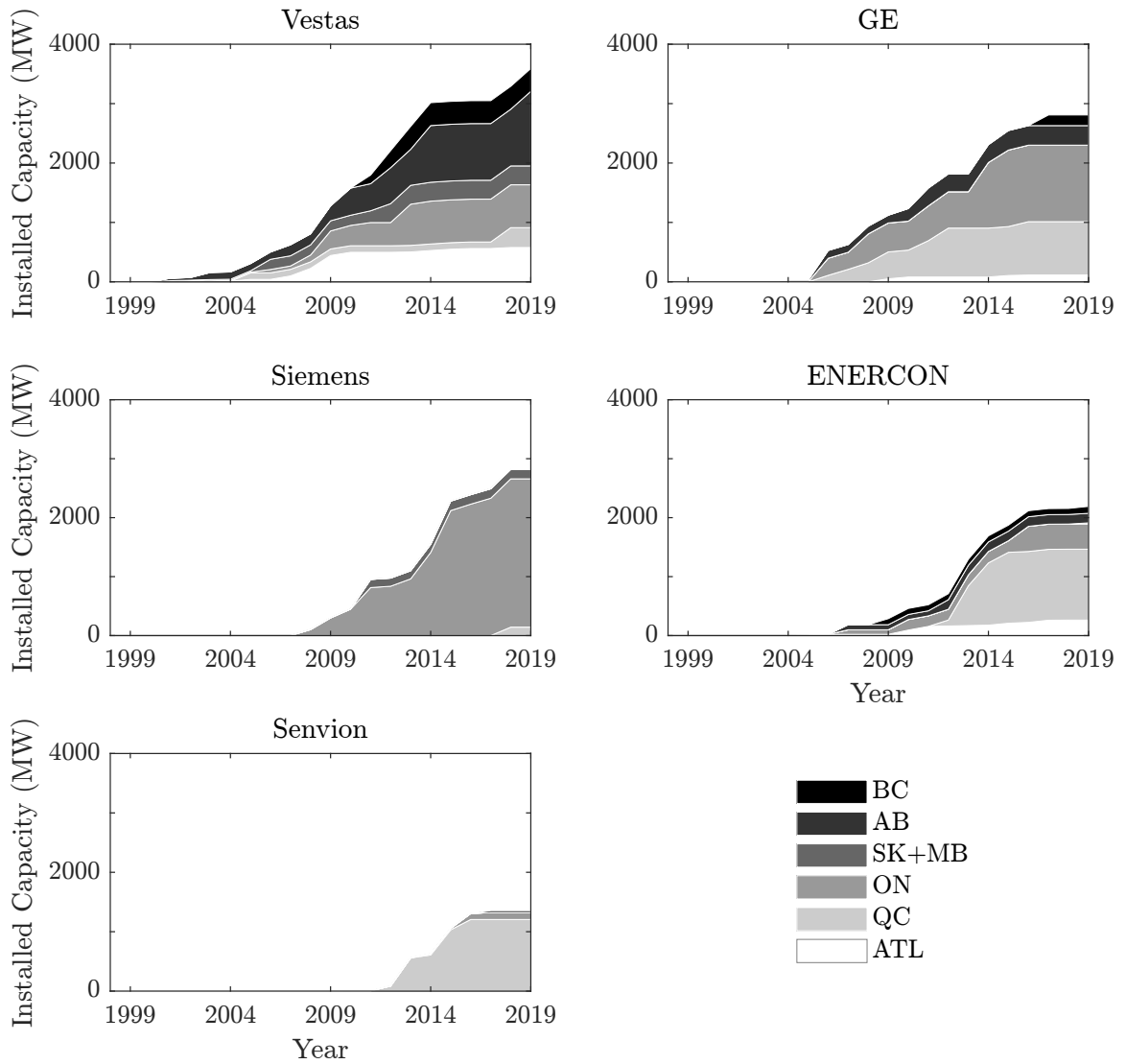
Figure 3.7: Proportion of installed wind capacity by major (>1000 MW cumulative installations) manufacturers

3.4.2   Canadian Wind Power Potential

Additional metrics are analyzed in ArcMap using turbine locations, rotor diameter, nameplate capacity and wind farm land area. Turbines are grouped by wind farm and given an estimated land area calculated based off their physical spacing with a buffer around each farm characterized by ten rotor diameters from the outer most turbines. This land area can then be used to analyze the turbine density and capacity density of each wind farm. Each of these measures provide a slightly different representation of historical project layouts; for a given portion of land, one can find a reasonable assumption of the number of turbines, or installed capacity, that will fit. Figure 3.8 shows the time progression of wind farm size, both physical (bubble height) and capacity (bubble size), split by jurisdiction. Figure 3.9 gives a timeline of the evolution of provincial infrastructure density, characterized by an IQR, median, as well as annual minimum and maximum values. Here, both plots are based on wind farm areas, as demonstrated in Figure 3.3.

Wind turbine output is significantly influenced by the quality of the wind resource in which it operates. The available energy in the wind is proportional to its speed cubed, as such, relatively small increase in average wind speeds results in considerable increase in turbine productivity. Conversely small reductions in average wind speeds can result in significantly lower annual production. For this reason wind farms are generally sited in areas with higher wind speeds. Using NREL's wind classes (see Table 3.1) the variations of wind resource that wind farms are operating in across the country can be observed. Figure 3.10 shows the proportion of provincial wind farm installations per wind class. Figure 3.11 gives a timeline of the installed capacity of infrastructure per power class, where the size of the bubbles represents the installed capacity for the given wind farm.
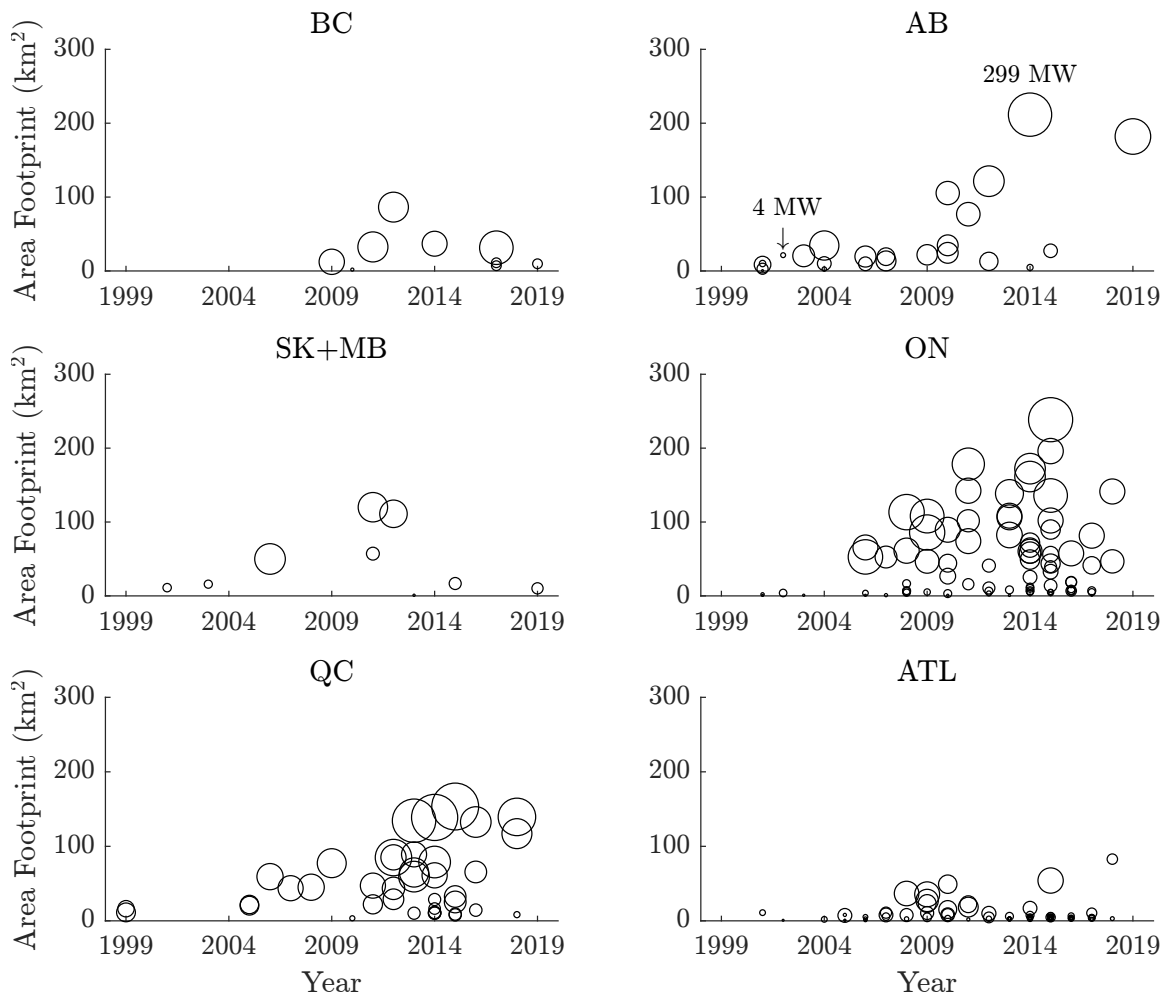
Figure 3.8: Wind farm area footprint (and capacity) by year
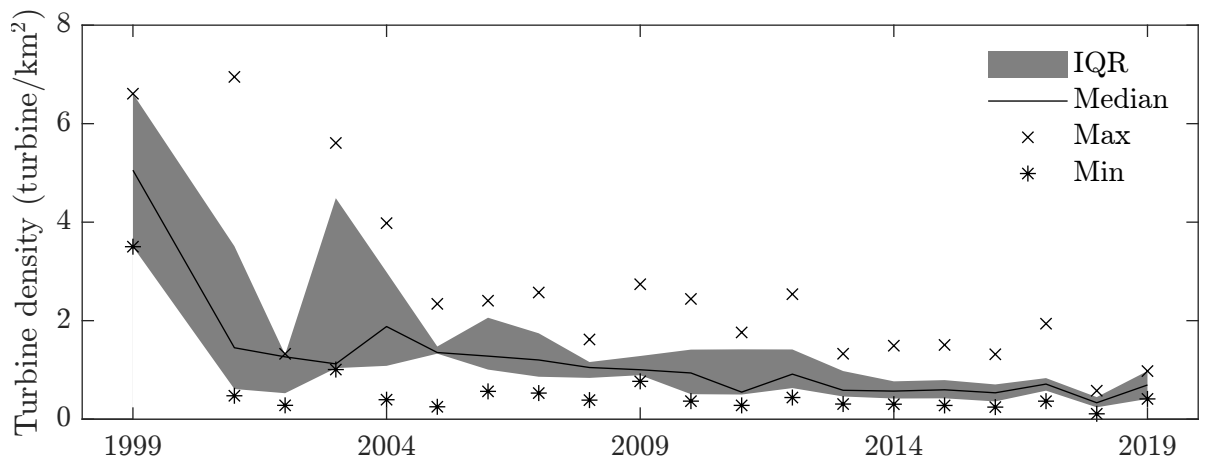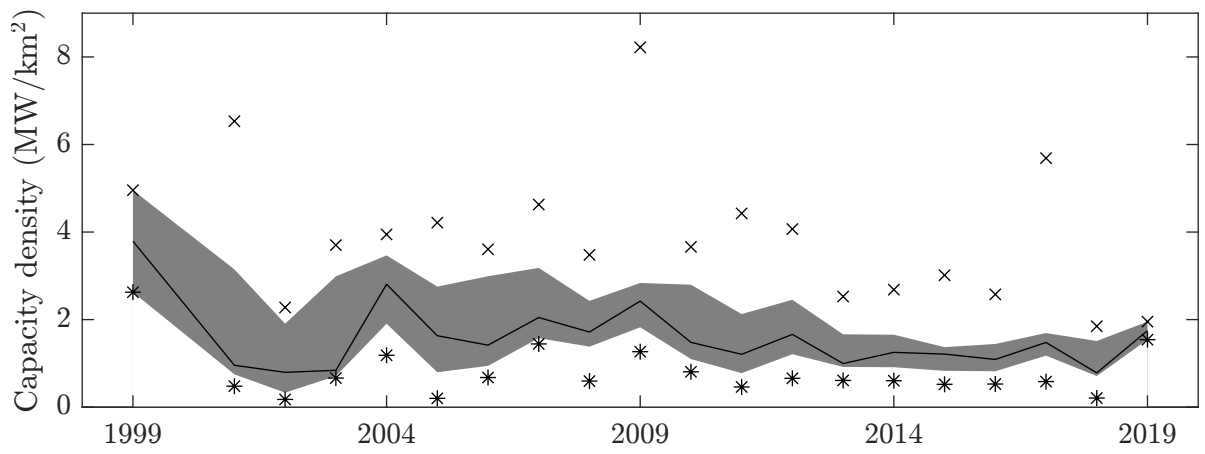
Figure 3.9: Annual time series of provincial infrastructure density split by type

51
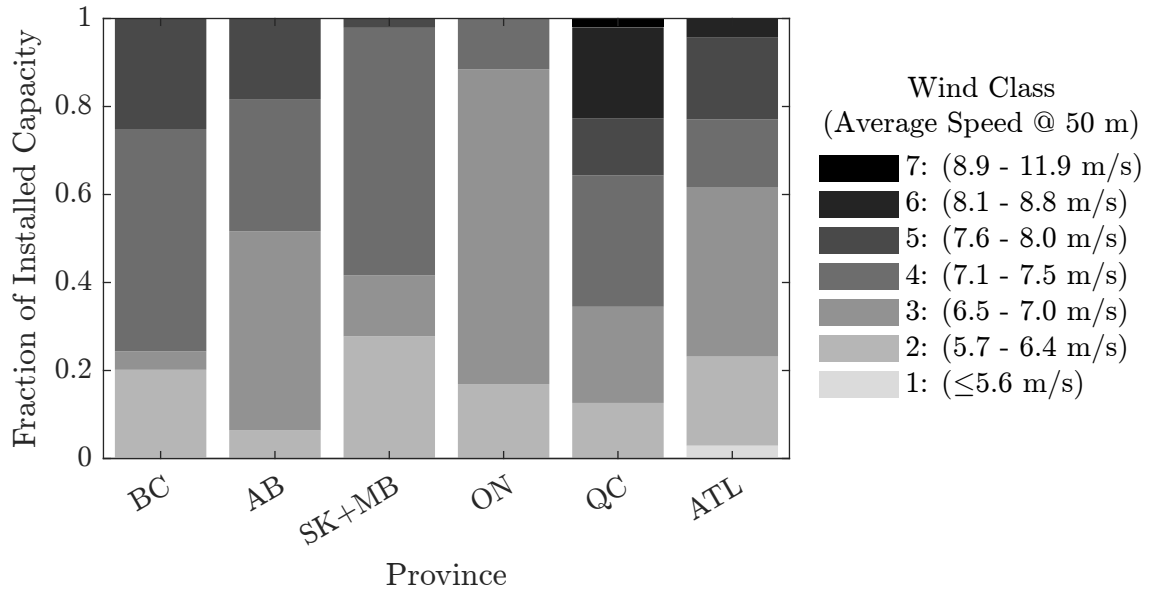
Figure 3.10: Proportion of provincial installed wind capacity, categorized by NREL wind power class
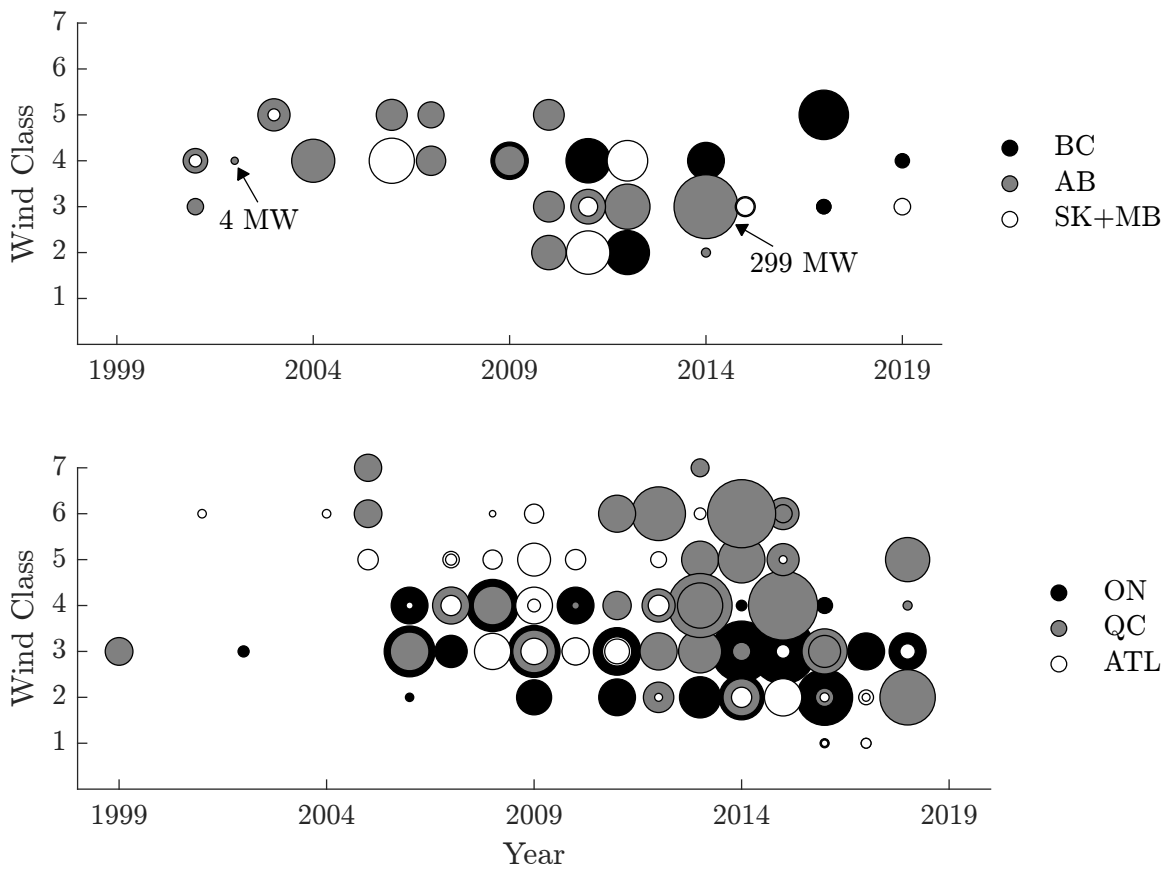
Figure 3.11: Annual time series of provincial wind infrastructure by wind class and installed capacity (bubble size)

3.5 Discussion

3.5.1 Wind Development in Canada

In 1993, Canada's wind industry was pioneered in Pincher Creek, Alberta (AB), with a single Bonus AN150/30 turbine providing 150 kW of renewable capacity to the surrounding communities. Two years later, a second turbine was erected in Tiverton, ON, with a nameplate capacity 4 times that of the first. The first commercial wind farm in Canada also began operating in 1993 and operated until 2016. The AB wind farm, which consisted of 57, 375 kW turbines, remains the only wind farm that has been decommissioned in Canada [138].

After the completion of the first wind farm there was minimal development in Canada until 2002, when the federal government introduced the Wind Power Production Incentive (WPPI), designed to encourage up to 1000 MW of wind energy. WPPI provided a 10-12 CAD/MWh subsidy (amount depended on project start date) for the first ten years of operation [139]. This $330 million CAD program was replaced in 2007 by the ecoENERGY for Renewable Power (ecoERP), following a change in government. This new program expanded eligibility to include biomass, low-impact hydro, geothermal, solar photovoltaic (PV), and tidal, all of which qualified for 10 CAD/MWh for the first ten years of operation. The 1.4 billion CAD ecoERP program supported almost 4500 MW of new renewable projects, and by 2010 approximately 3800 MW of the 4000 MW of wind farms in Canada we receiving funding from one of the two federal programs [140].

While federal production incentives ended in 2011, provincial programs had begun to spur development notably in Quebec (QC) and ON, Canada's two most populous provinces. In 2006 the government of Quebec implemented an energy strategy with a target of 4000 MW of wind by 2015 [141]. To achieve this target, they conducted four competitive procurements between 2008 and 2015 including blocks reserved for independent power producers, community and indigenous community partnerships

and the provincial utility. The projects brought the total installed capacity to 3880 MW, just short of the 4000 MW target. Also beginning in 2006, Ontario began the first of various forms of 20-year fixed price contract feed-in tariffs targeting projects less than 10 MW in capacity. In 2009 Ontario passed a Green Energy Act establishing feed-in tariffs for wind, solar, biogas and small hydro, leading to the the largest growth in wind energy in Canada until the program ceased new applicants in 2017 [142]. As can be seen in Figure 3.4, the most significant growth of wind energy in Canada occurred between 2012 - 2016 during the height of these policies. During that time frame, between 63% (0.9 GW) and 97% (1.6 GW) of the national growth occurred in ON and QC. The policies in both provinces also encouraged local manufacturing, which explains in part some of the regional differences in turbine make.

The third largest wind fleet in Canada belongs to the province of AB. Provincial carbon pricing mechanisms have been the primary driver of wind projects in AB in addition to the aforementioned federal programs. However, in 2015, the government of Alberta implemented a climate change plan that involved phasing out coal and targeting 30% renewable energy by 2030. While this policy has been repealed after a change in government, three competitive procurements were issued in 2017 and 2018 for close to 1360 MW of new projects in Alberta, the first of which was commissioned in late 2019 [143].

Between 2011 and 2016, NS implemented a feed-in-tariff program similar Ontario's dedicated to small, community-owned projects, through which 150 MW of wind, biomass, and small hydro was installed [144]. These two programs are in part responsible for the prevalence of smaller projects seen in both NS and ON, but less so throughout the rest of the country.

By the end of 2019, Canada's total wind fleet capacity reached 13.4 GW - enough to supply electricity to 3.4 million homes [116]. There remains very few provincial or federal programs targeting new wind projects in Canada, but future development will likely be sought based on energy prices as well as national carbon pricing policy.

[145]

Over the course of the past two and a half decades, wind turbines have increased in size significantly. As demonstrated in Figure 3.5, the average turbine height and rotor diameter have doubled and tripled respectively since 1995. Average installed turbine capacity has also grown from 0.66 MW turbines in the early 2000s, to turbines over 3 MW in size for the most recently installed wind farms. However, while the largest wind farms commissioned annually has been, for the most part, steadily increasing, the median wind farm capacity has remained bounded below 100 MW. Shown in Figure 3.6, a typical year in Canadian wind development shows growth from numerous small projects and the occasional large one.

Figure 3.7 splits provincial installed capacity by manufacturer. Here, it can be seen that Vestas and GE turbines are spread uniformly across the country, while the bulk of Siemens turbines have been commissioned in ON and the majority of ENERCON and Senvion infrastructure are in QC. Until recently, Siemens manufactured turbine blades locally in Tillsonburg, ON. Similarly, both ENERCON and Senvion have headquarters in Montreal, QC. However, requirements for locally manufactured turbines has not been adopted nationally, and so while Vestas and GE began installations about 5-10 years earlier than the other major manufacturers large-scale manufacturing for either is not present in Canada. There also exists other turbine manufacturers not shown in the figure, some of who have subsequently been bought by other manufacturers. The largest increase for this small segment of development occurred between 2010 and 2012, around the time the community feed-in tariff programs were active in Eastern Canada.

3.5.2 Power Potential

As the Canadian wind industry expands and technology advances, the size (both physical and capacity) of projects has grown, as demonstrated in Figure 3.8. Wind farms in British Columbia (BC), however, are somewhat of an anomaly; since the

majority of these projects are built on the ridges of mountainous terrains with strong prevailing winds, turbines are erected in a single row rather than a cluster. With wake effects being less of an issue for this particular siting strategy, turbines are packed tightly together. Note also that the small community projects resulting from government subsidies as described in section 5.1, can be observed along the bottom of subplots for ON, QC, and ATL (includes NS). As a final point, one should notice that the *y-axis* for each of the panels in Figure 3.8 is equivalent, and as such, development of wind projects along the east coast appears smaller in comparison to ON and QC. Referring back at Figure 3.1 however, this disparity in project size can be attributed to differences both provincial topography and total electrical system capacity.

Figure 3.9 gives an account of how densely packed turbines are (per farm) and how this has changed over time. Here, it can be seen that both capacity and turbine density have flattened out, showing little variation after the early 2010's. Note also that the points that fall well above the IQR (more evident with capacity density) are wind farms from BC; the explanation for this is similar to the one presented for Figure 3.8. From the plots, one can make a reasonable estimate at how much wind infrastructure will fit on a given area: i.e. 1 - 3 MW/km^2 or 1 - 2 turbines/km^2.

Figures 3.10 and 3.11 relate to the quality of the harnessed wind resource, as found using Wind Atlas models and classified using NREL definitions. Here, in Figure 3.10, it can be seen that the majority of Canadian wind farms (84% by capacity) are operating in greater than class 2 wind regimes, with the most common being class 3 (44%). From this plot, it can also be seen that QC has the highest quality wind, with 36% of its capacity operating in class 5 or above, followed closely by BC (25%), ATL (23%), and AB (18%). As more wind farms are commissioned, one would expect that the earlier projects would be located in the best wind regimes, with a downward trend over time as these locations are claimed. This is not the case however, with no obvious trends appearing in Figure 3.11. Rather, it seems as though a typical wind farm in Canada, regardless of its commissioning date, lies in a wind class between 2

and 5 inclusive. Also, there does not appear to be any noticeable bias with respect to wind farm capacity and wind class: projects of all sizes are shown to span wind power classifications 2 through 7, with only a couple of small Atlantic projects located in class 1 regimes.

3.5.3   Challenges of this Work

Mapping wind infrastructure on a per-turbine basis presents a variety of challenges, many of which could be circumvented if wind farm documentation was more standardized and accessibility was more centralized. Web pages belonging to provincial utility commissions are often overwhelming and difficult to navigate, as they vary from province to province. Although many of these databases behave similarly, no two are exactly alike in terms of where and which data are reported. Also, while many developers link these documents directly to their website, others are not voluntarily forthcoming. This issue is exacerbated further when wind farm ownership is shared or changes hands.

Wind farm documentation generally contains the location and physical characteristics of turbines as they were compiled for this work. A model number is all one needs to determine rotor diameter and nameplate capacity, however hub height can vary for a given turbine model, and is not always reported without examining technical reports such as acoustic or environmental impacts. Information regarding turbine locations varies from project to project, with the majority of publicly available technical reports providing only a single representative point for the entire farm. Occasionally the more detailed reports do provide exact geographic locations for each turbine. In either case the locations are verified using satellite images, generally Google Earth. During this verification process, it was noted that newer wind farms may be absent from the satellite images if they were erected after the photos were taken. Old images may also show turbines which have since been decommissioned.

3.6   Conclusions

The purpose of this work was to create an exhaustive data set of Canadian wind power infrastructure, discuss the methods used, challenges encountered, and document the historical growth of the industry. Through the combined efforts of NRCan, CanmetENERGY-Ottawa, and the University of Alberta, the entire Canadian wind fleet has been, and will continue to be, accounted for; at the time of this project, an aggregate of 6711 turbines have been mapped and indexed by their physical characteristics. This map, freely available through the Government of Canada's open data portal [25], is intended to assist future research, modelling, and development of the wind industry, while also promoting an increased public knowledge base: an effort intended to dispel myths and improve perceptions of the technology.

Acknowledgements

Funding Sources

Chapter 4

Modelling a wind-hydrogen hybrid plant in Alberta

This chapter quantifies the potential for wind-driven electrolysis for hydrogen production in Alberta. Known for its fossil fuel based economy, Alberta is well established in hydrogen production through steam-methane reforming [106]. According to the Natural Gas Vision and Strategy [146], the Government of Alberta intends to increase its investment in to steam-methane reforming, disregarding the opportunity of pairing renewable energy with electrolysis. By simulating potential future electricity prices and wind generation schedules, we quantify the future costs of generating green hydrogen using wind. Results show electrolysis being competitive with steam methane reforming by 2025, with costs reaching as low as $1.50/kg under specific conditions.

4.1 Electricity Market Forecasting

Alberta's wholesale electricity market operates under a competitive, deregulated scheme for electrical generators. A province-wide power price is determined every minute through an economic merit order, administered by the Alberta Electric System Operator (AESO) [9], as a result all new electricity projects are subject to market price risk. The hourly market price is dependent on many factors, some of which can be anticipated, such as daily demand peaks. Other factors, which are more difficult

to predict, may be a result of human behaviour[1], unexpected equipment failure, or weather events. In this chapter, we project a set of power price series as a function of future macro trends and historic stochasticity.

The goal of this paper is not to predict the exact behaviour of Alberta's electrical grid over the next decade, an unachievable task at best, but rather to explore a wide variety of potential outcomes and their implications on the future of hydrogen. For this work, the Alberta electricity market is simulated using an industry standard long-term capacity expansion software, Aurora [147], developed and maintained by Energy Exemplar. Simulations cover 4 potential scenarios over the next decade, with a focus on future price trends. Aurora solves hourly electrical dispatch as a minimization problem, set to achieve the lowest total system cost for the given demand profile. As a result, Aurora's reported market price lacks the volatility observed in Alberta's deregulated electricity market. Historic price shocks, derived from AESO market data, are applied to the predicted future average power prices to better capture hourly market dynamics.

4.1.1 Simulation Logic

The first step in the process of predicting future price trends is the Aurora model. Aurora's simulation logic can be broken into three steps: commitment, dispatch, and capacity expansion (CE). The following section provides a high-level overview of each algorithm, with further discussion on Aurora model inputs and simulation results to follow.

The Aurora dispatch algorithm seeks to minimize the cost of electricity generation, determining the optimal schedule for each plant and intertie in the system. Feasibility is contingent on plant capacities, transmission flow limits, and any user defined constraints. In each hour, the model reports the marginal plant as most expensive dispatchable resource operating, and electricity price as the shadow price of the solution.

---

[1]Particularly in how a particular electrical generator, or group of generators owned by the same company, will structure their offer prices for any given hour

In other words, electricity cost is determined in the same way as in the Alberta deregulated electricity market: by the incremental value of increasing electricity demand by one unit.

In electricity system planning, CE models are used to forecast the commissioning and retirement schedule of a power market. The standard, or traditional, CE model in Aurora builds and retires resources based on financial viability. Each iteration, the existing power market is simulated with a small set of additional new resources, with the first set being chosen based on fixed costs. At the end of each iteration, following commitment and dispatch operations, the value (revenue minus costs) for each resource in the system is calculated. Existing resources with the most negative value are retired, replaced by new resources with the highest value. The next iteration begins by selecting a different set of new resources, including the winning ones from the previous iteration. This process is repeated until the optimal set of resources converges, or the user-defined maximum number of iterations is met.

Aurora allows for three types of plant characterization: cycling, non-cycling, and must run. The power capability of a cycling unit is independent of its previous operations, limited only by its installed capacity. Non-cycling resources, i.e. plants unable to easily ramp up and down between hours, are subject to a commitment schedule, based on week-ahead internal price forecasts[2]. Commitment decisions are made prior to the dispatch algorithm, and are only broken to avoid an infeasible solution, meaning a resource that does not fulfill its generation commitment will incur a steep financial penalty. To avoid non-commit penalties, committed units must at least run at their minimum stable generation and for their minimum up time. Must run units are similar to non-cycling plants, but do not have a commitment schedule; rather, they are always required to run at their minimum stable generation. Any capacity above the minimum stable generation, for both non-cycling and must-run,

---

[2]From the Aurora help function: "... price history in conjunction with other observed simulation parameters ... [such as] demand, fuel prices, and hydro conditions ... produce the 168 hour-ahead forecast."

is dispatchable based on economics.

4.1.2 Model Inputs

Aurora's objective function seeks to meet electricity demand at the lowest possible cost across the entire study horizon. The optimal solution to this function will also depend on a set of user-defined inputs and constraints which, when correctly applied, allow for the simulation of any perceivable market design, within reason. Good models are subject to the quality of their inputs; although Aurora comes prepackaged with an existing Alberta model [148], to ensure accuracy, we update the existing data set as follows.

Generating Resources

Alberta's current electricity supply is predominantly from the combustion of fossil fuels: in terms of installed capacity, natural gas and coal make up 57% and 17% of Alberta's total fleet (16,817 MW) respectively [22]. As Canada moves to phase-out coal-fired power by 2030 [13], the share of coal plants in Alberta has already started to decline, often replaced by dual- (gas + coal) or gas-fired steam cycles. As of August 2021, 7 coal units have been converted: Keephills 2, Sundance 6, Sheerness 1 and 2, Battle River 4 and 5, and H.R. Milner [149–151]. As a result, an update of Aurora fuel types, conversion dates, and occasional installed capacities is required for the aforementioned units. A large portion of the natural gas capacity exists behind-the-fence at oil-sands operations, using excess steam to serve on-site power demand. As electricity generation is a secondary function of these cogeneration facilities, in Aurora, these units are treated such that they will not be considered for retirement during capacity expansion runs.

At the time of writing, Alberta's renewable fleet consists of wind (2085 MW), solar (336 MW), and hydro (894 MW) facilities [22]. For the purpose of this work, hydro resources are left as-is according to the Aurora data set. Variable renewable generators,

wind and solar, are given a unique hourly generating schedule using historic climate data: wind speeds from the Canada Wind Atlas [136], and insolation data from the National Solar Radiation Database (NSRDB) [152]. For the sake of consistency, as wind and insolation are correlated, all weather data is taken from the same year. Previous work by Vergara Bonilla [153] demonstrates that wind generation schedules using 2009 weather data are best suited to modelling the Alberta wind fleet.

Following the methodology presented by Vergara Bonilla [153], a wind turbines output is described by a piece-wise polynomial representation of its power curve, with wind speeds at turbine hub height found using the power law [154]. For every hour of data, the wind shear coefficient, α is calculated as:

$$\alpha = \ln\left(\frac{u_1}{u_2}\right) - \ln\left(\frac{z_1}{z_2}\right), \tag{4.1}$$

where u_1 and u_2 are the wind speeds corresponding to heights z_1 and z_2. Next we approximate the hourly wind speed at hub height, u^* using:

$$u^* = u_i \left(\frac{z^*}{z_i}\right)^\alpha, \tag{4.2}$$

where z^* is the turbine hub height, and $z_i = z_1$ or z_2 is chosen as the value closest to the hub height. Turbine gross power output, P_G is then found according to the following piece-wise equation:

$$P_G = \begin{cases} 0 & u^* < u_{cut-in} \ || \ u^* \geq u_{cut-out} \\ \sum_k a_k(u^*)^k & u_{cut-in} \leq u^* < u_{rated} \\ P_{rated} & u_{rated} \leq u^* < u_{cut-out} \end{cases}, \tag{4.3}$$

where u_{cut-in} and $u_{cut-out}$ are the turbine cut-in and cut-out speeds respectively, P_{rated} is the turbines rated output power, achieved at its rated wind speed, u_{rated}, and a_k are empirically derived coefficients, unique to each turbine model [153]. Turbine power curves are often given at standard atmospheric conditions, i.e. temperature (T°) and pressure (p°) [153, 155]. Assuming air acts as an ideal gas, we apply the following density correction:

$$P'_G = P_G \left(\frac{T^\circ}{T}\right)\left(\frac{p}{p^\circ}\right), \tag{4.4}$$

where P'_G is the expected power under operating temperature, T and pressure, p. Finally, a generic loss coefficient, L is applied such that net wind farm power output, $P_N = NP'_G(1 - L)$, where N is the number of turbines for the given wind farm. Turbine losses are a result of an aggregate of factors, e.g. wake effects, grid availability, and curtailments, and can be approximated by the following [153]:

$$
L = \begin{cases} 0 & u^* < u_{cut-in} \parallel u^* \geq 1.4u_{rated} \\ u_{rated}^{-1} \sum_k b_k(u^*)^k & u_{cut-in} \leq u^* < 1.4u_{rated} \end{cases}, \tag{4.5}
$$

where b_k and the "loss cut-off" factor of 1.4 are empirically derived [153].

Solar output profiles are approximated using the methodology outlined by Durán [20], using the System Advisor Model (SAM) [156] and NSRDB [152], both developed by the National Renewable Energy Laboratory (NREL). Hourly solar generation profiles are approximated for historic (2009) weather patterns, with photovoltaic (PV) DC to AC ratios ranging from 1 to 1.8, incremented by 0.2^3.

Through intertie connections, Alberta has the ability to import or export power to three adjacent electrical grids: British Columbia (BC), Saskatchewan (SK), and Montana (MT), where BC and MT pass through a shared flow gate [158]. To cut down on computational time, each intertie, SK and BC/MT, is modelled as a basic market with a single generator and demand. By setting both the market demand and link limit to half of the generator capacity, we ensure that each reduced system is able to offer a full export while still meeting internal supply commitments. In this way, we model the entire BC/MT and SK electrical systems as gas plants with installed capacities of 2200 MW and 306 MW respectively, with the BC/MT system increasing to 3020 MW in 2023 [159]. This serves to remove the complexity of modelling full adjacent grids, and will remain a reasonable assumption so long as there are no periods of tight supply constraints in Alberta's import markets.

---

[3]Range is in agreement with recent solar project announcements in Alberta [157]

New Generators for Capacity Expansion

During the capacity expansion process, Aurora chooses from a set of available resources to consider for commissioning. For the same reasons as outlined above, i.e. Canada's coal phase out [13], new coal plants are removed from consideration. Similarly, all new resources must be constructed in Alberta, rather than BC/MT or SK, such that the proxy markets remain a single source of supply and demand. Using the same methods as outlined above, additional wind and solar resources are added for consideration. Figures 4.1 and 4.2 provides a map of all existing and proposed [157] wind and solar projects used for in this work.
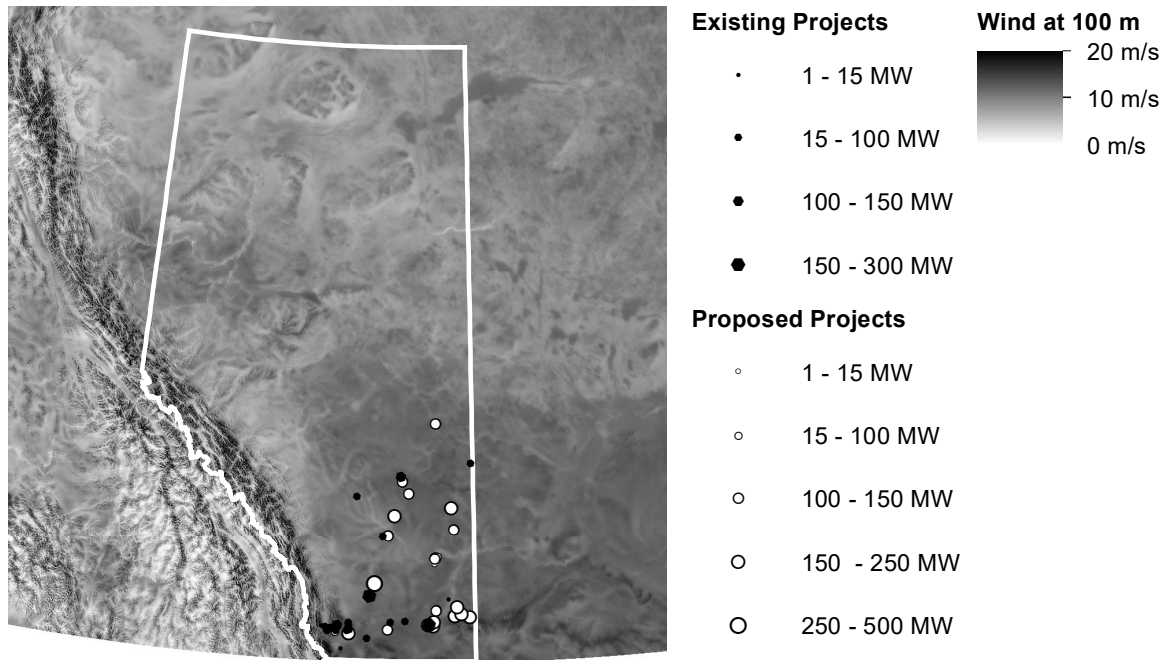
Figure 4.1: Existing and proposed wind power projects in Alberta, mapped over wind speeds at 100m

Overnight capital cost is one of the primary economic factors considered in the capacity expansion process. These costs come as part of the Aurora database, calculated using data from the Energy Information Administration (EIA) [160], separated by National Energy Modelling System (NEMS) regions [161]. As the NEMS analysis only contains regions from the continental United States, costs from a geographic
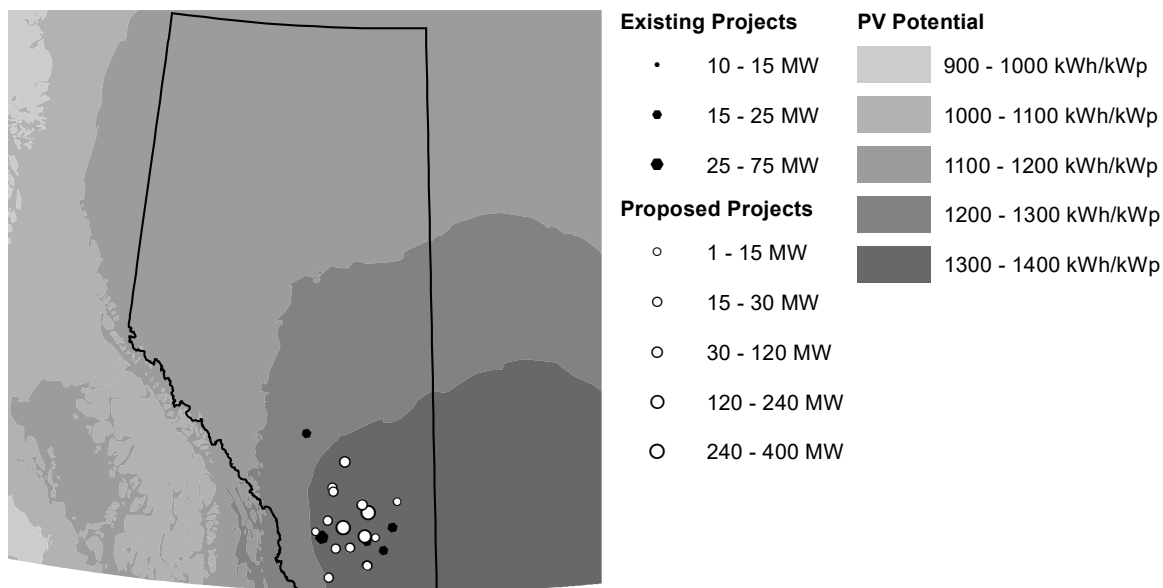
Figure 4.2: Existing and proposed solar power projects in Alberta, mapped over photovoltaic (PV) potential

region most akin to Alberta, i.e. the Northwest Power Pool (NWPP), are used to approximate build costs for our model. This assumption has been verified by comparing Aurora database costs to electricity project costs in Alberta [162–186], as shown in Table B.1 in the Appendix.

Electricity Demand and Emissions Pricing

Every 2 years, the AESO publishes a *long-term outlook* [187], whereby they provide a 20 year forecast of electricity demand and power generation by technology. The model used in this paper is based on the AESO 2021 long term outlook demand estimates.

With respect to carbon pricing, our model uses the most recent schedule released by the Government of Canada in December 2020 [14]. Under this new model, the Canadian carbon price will increase by $15/tCO_2e every year until it reaches $170/tCO_2e in 2030. Alberta power generators do not bear the full brunt of this tax, rather, they are subject to an emissions intensity benchmark of 0.37 tCO_2e/MWh, known as "good-as-best-gas" [188]. In other words, we update Aurora such that thermal generators' emissions are only priced over and above 0.37 tCO_2e/MWh.

Custom Scenario Constraints

Using Aurora, we simulate four potential future scenarios. First, we model a base (reference) case, allowing Aurora to run with no extra user-defined constraints, providing a benchmark for the alternative scenarios. Second, we place a maximum annual capacity constraint on renewables; as our base case results in a greater build-out of wind capacity than is predicted in the 2021 AESO LTO [187], we use the LTO values to define the constraint. Third, we place an annual minimum constraint on solar generation, forcing a greater expansion of the solar fleet. Solar constraint limits are defined, borrowing from an analysis by Ben Thibault [189], with data from AESO [15, 187, 190] and the Alberta Government [191]. Finally, we run a scenario with a lower carbon tax, stopping its increase at \$CAD 80/tCO$_2$e in 2024.

4.1.3 Simulation Results

Under the inputs and constraints described above, four potential future scenarios are forecast using Aurora. Pertinent results of the simulations are shown in Figure 4.3 through Figure 4.7 below, outlining the different pathways that the Alberta generating fleet may take in the coming decade. Figures 4.3 and 4.4 give the evolution of annual installed capacity and average monthly generation over the simulation horizon, respectively. Figure 4.5 shows annual equivalent CO$_2$ emissions by technology. Figure 4.6 gives a monthly average power price, as well as a solar and wind capture prices relative to 20% and 50% capture rate ranges, while Figure 4.7 provides a closer look at hourly price data, comparing Aurora base case and historic AESO prices. With the exception of Figures 4.6 and 4.7, all alternate scenarios are framed in relative terms with respect to the base, or reference, case.

Figures 4.3 and 4.4 show significant development in wind energy over the next decade for the reference and low tax cases. Relative to the base case, the low tax scenario builds more wind mid-decade in favour of building solar later (Figure 4.3). This leads to a decrease in thermal generation (Figure 4.4), and its associated emis-
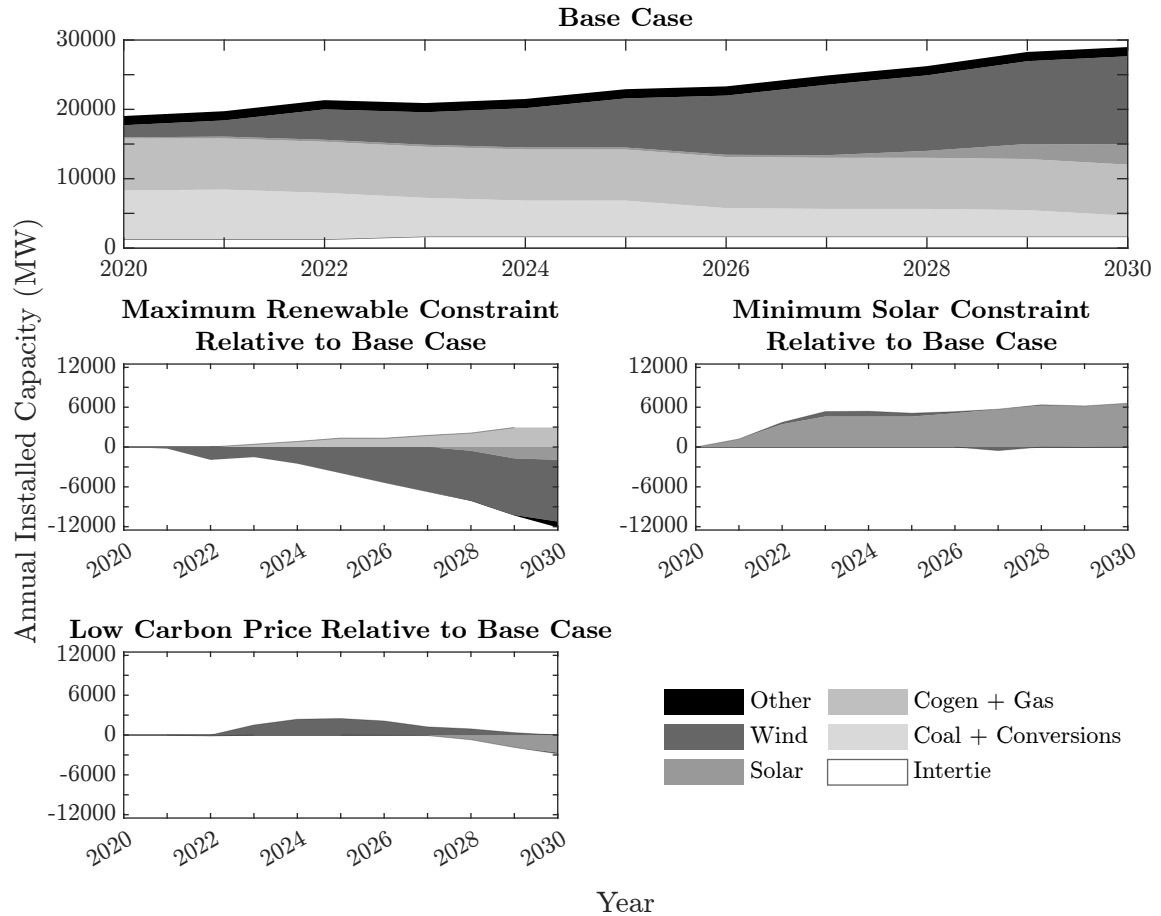
Figure 4.3: Aurora simulation results, annual installed capacity by scenario and technology for 2020 - 2030

sions (Figure 4.5), between 2022 and 2028, followed by an increase to 2030. The base case scenario shows Alberta's electrical generation emissions decreasing by half in the next 10 years, with the bulk of the remaining emissions being a result of cogeneration facilities.

Both constrained scenarios, minimum solar and maximum renewable, behave more or less as one would expect, with their respective constraints having a significant impact on simulation output. The maximum renewable scenario sees a significantly lower renewable deployment, with Figure 4.3 showing 2 GW of gas being built in favour of 7 GW of wind by end of decade. Under this scenario, net CO_2 emissions (Figure 4.5) show a relative increase of up to 10 Mt when compared to the base case. The minimum solar scenario sees significant increases in solar build-out (Figure
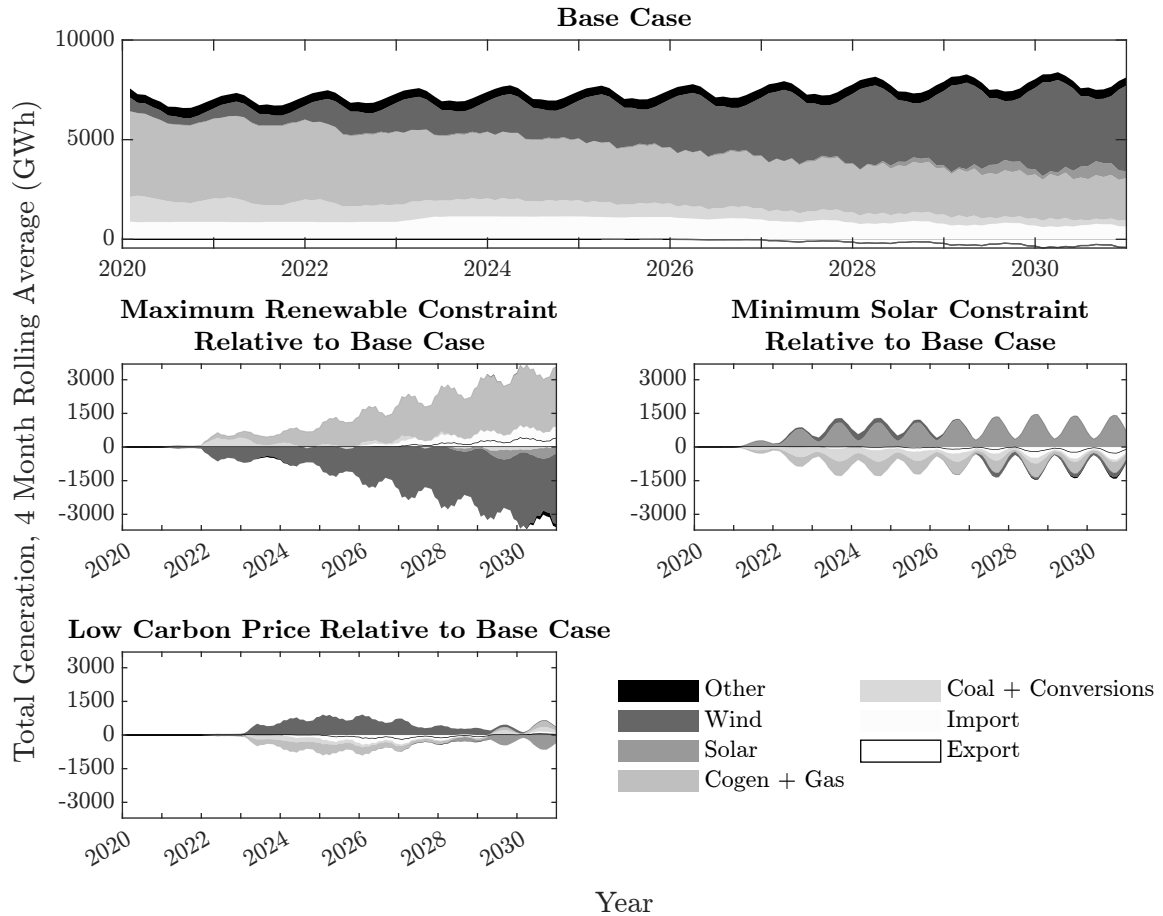
Figure 4.4: Aurora simulation results, monthly rolling-average generation by scenario and technology for 2020 - 2030

4.3): 6 more GW than the base case has by 2030, though no noteworthy changes in capacity for other technologies; this result is likely driven, in part, by the lack of energy storage in the system. In other words, high solar built out without energy storage augmentation will still require large amounts of thermal (gas) firming power. Under this scenario, the increase in emission displacement (Figure 4.5) leads to a relative decrease in net emissions on the order of 2 - 5 $MtCO_2e$, meaning emissions reach half of their current amounts a few years earlier than the reference case.

As shown in Figure 4.6, monthly power prices are relatively similar between the different scenarios, with the minimum solar prices decreasing after 2028. It can also be seen that solar premiums, that is solar capture rates above 1, are only maintained at low ($\lesssim$ 1 GW) installed capacity. Similarly, both wind and solar capture rates
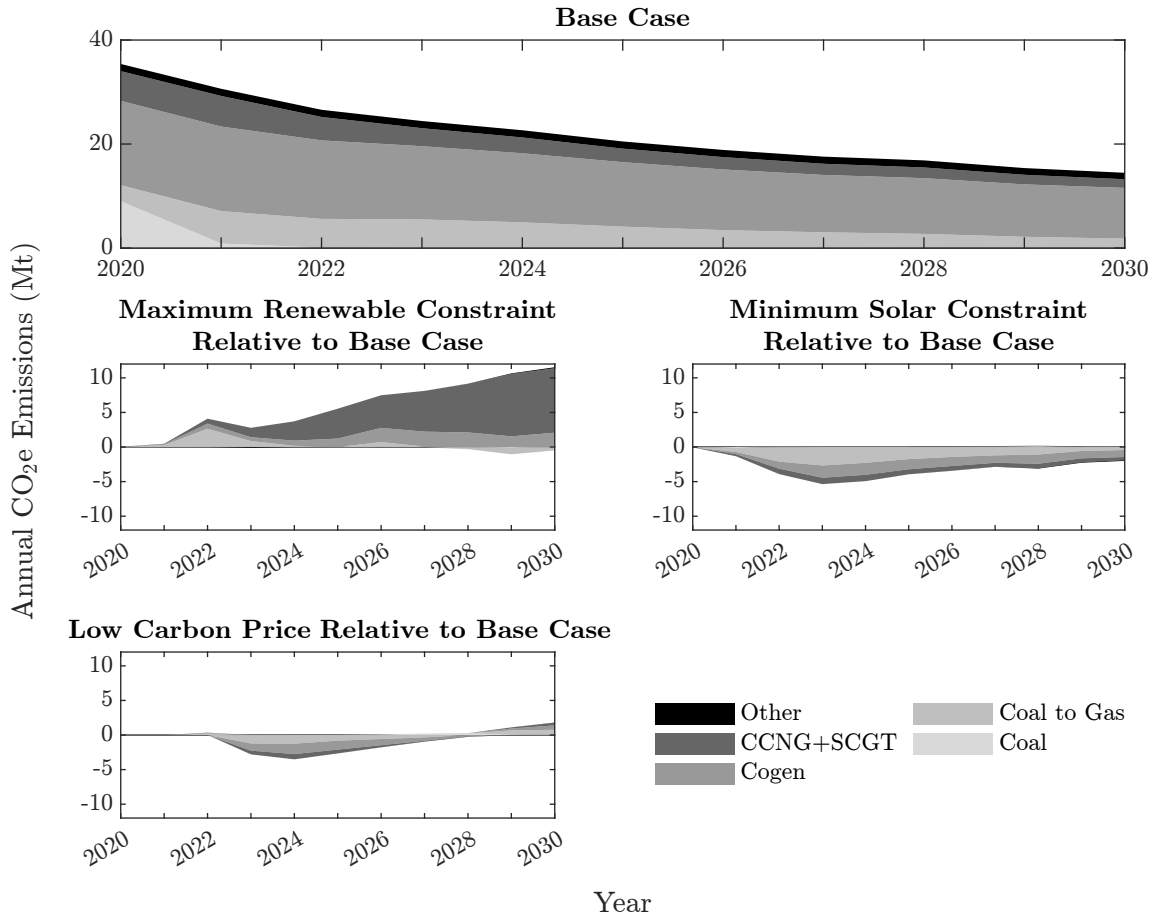
Figure 4.5: Aurora simulation results, annual CO_2-equivalent emissions by scenario for 2020 - 2030

begin to fall as more renewables enter the system, with solar causing a collapse in price after 2028 in the minimum solar constraint scenario. Regardless of scenario, Aurora's hourly price trends tend to be bounded, contingent on power demand and plant operating costs. Figure 4.7 shows a snapshot of Aurora price outputs for January 2020 relative to historic AESO prices for the same time frame. From this plot, one can see the obvious lack of volatility in the Aurora price output, providing justification for application of historic price shocks to these data.
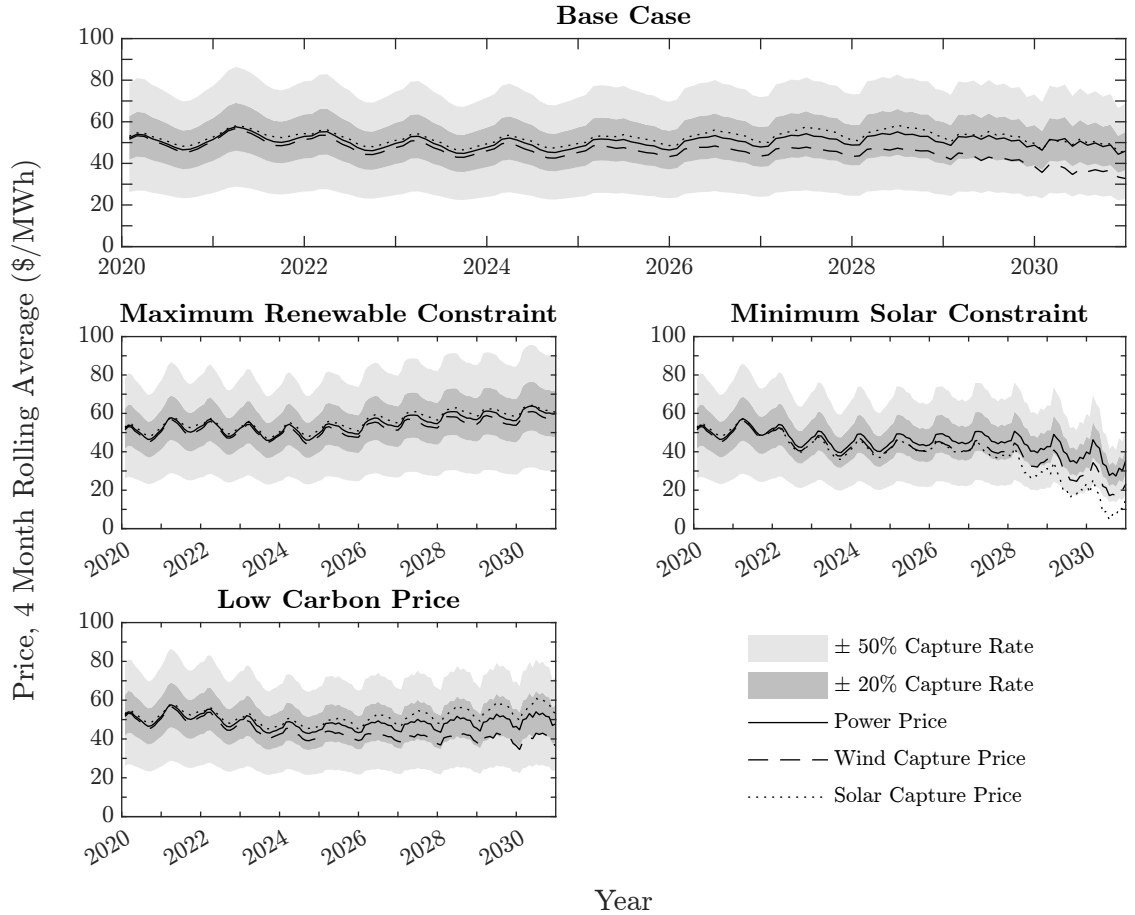
Figure 4.6: Aurora simulation results, monthly rolling-average power price and renewable capture price by scenario for 2020 - 2030
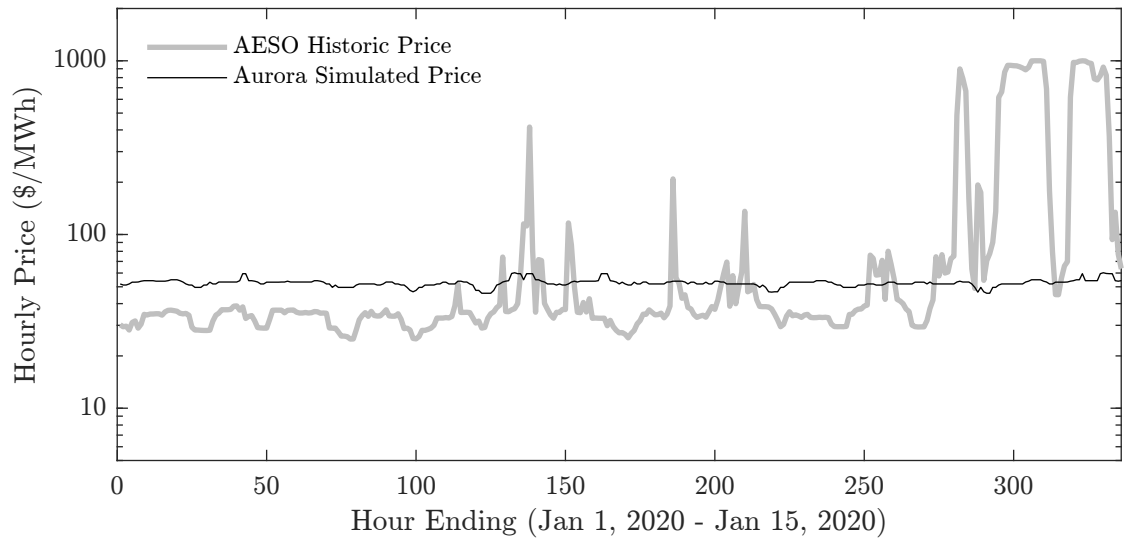
Figure 4.7: Example comparison of hourly Aurora price data and historic (AESO) price data for the first two weeks of January, 2020

4.2 Wind-Hydrogen Plant Operation

4.2.1 Linear Program (LP) Model Formulation

This section presents an algebraic model for a hydrogen system, schematic shown in Figure 4.8, using the following parameters:

- c_X = annualized capital and annual operating costs for equipment X [$/kW];

- e^t = wind generation into electrolyzer for hour t [kWh];

- f^t = fuel cell output for hour t [kWh];

- g^t = grid price for hour t [$/kWh];

- h = price of delivered hydrogen [$/kg];

- HHV_{H_2} = higher heating value of hydrogen (39.4 kWh/kg);

- s^t = hydrogen tank level for hour t [kg];

- w^t = total wind generation for hour t [kWh];

- E = electrolyzer capacity [kW];

- F = fuel cell capacity [kW];

- P^τ = hydrogen production requirement over time period τ [kg/time period];

- S = hydrogen tank capacity [kg];

- η_e = electrolyzer efficiency (0.74 kWh$_{\text{H}_2}$/kWh$_\text{e}$ [38]);

- η_f^t = fuel cell fuel efficiency for hour t [kWh$_\text{e}$/kWh$_{\text{H}_2}$]; and

- η_r = rectifier efficiency (0.95 kW$_\text{DC}$/kW$_\text{AC}$ [38]).

Our in-house linear model minimizes the annualized net cost of operating a wind-hydrogen hybrid plant. Decision variables consist of installed capacities and operating schedules of hydrogen equipment: electrolyzer, fuel cell, and storage tank, providing
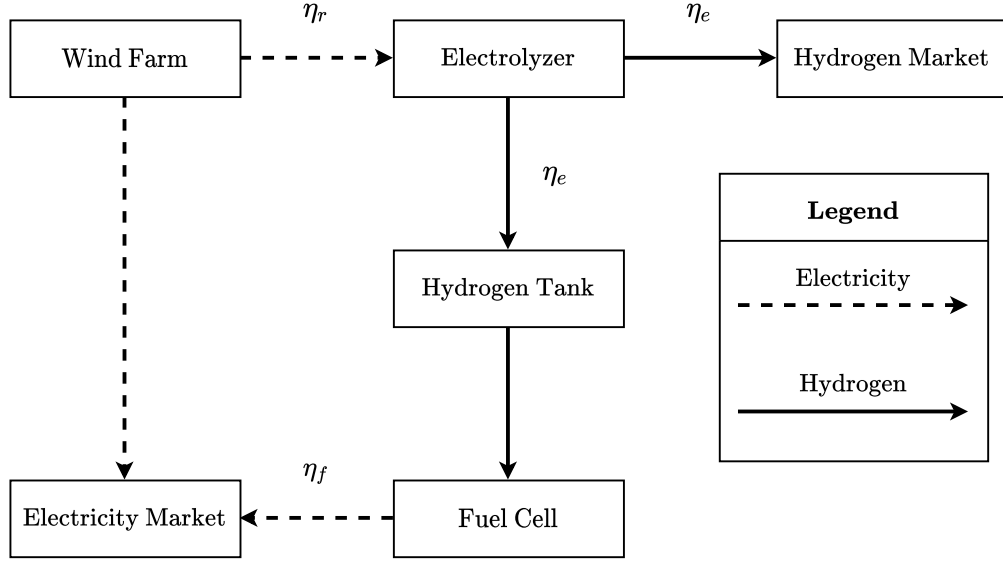
Figure 4.8: Diagram of wind-hydrogen hybrid plant, showing electricity and hydrogen paths and conversion efficiencies between equipment

both an optimized plant size and generating schedule for the given inputs. The optimization is written as:

$$\text{minimize} \sum_X \sum_t X \cdot c_X + g^t \cdot \left(e^t - f^t\right) + h \cdot \left(\frac{f^t}{\eta_f^t} - \frac{\eta_r \eta_e e^t}{\text{HHV}_{\text{H}_2}}\right), \forall t, X \in \{E, F, S\} \quad (4.6)$$

Subject to the following constraints:

$$\eta_r e^t \leq E, \quad \forall t \tag{4.7}$$

$$e^t \leq w^t, \quad \forall t \tag{4.8}$$

$$f^t \leq F, \quad \forall t \tag{4.9}$$

$$\frac{f^t}{\eta_f^t} \leq s^t \leq S, \quad \forall t \tag{4.10}$$

$$\eta_r \eta_e e^t - \frac{f^t}{\eta_f^t} \geq s^t - s^{t-1}, \quad t > 0 \tag{4.11}$$

$$\sum_t \eta_r \eta_e e^t - \frac{f^t}{\eta_f^t} - s^\tau \geq P^\tau, \quad \forall t, t \in \{t_1, t_2, ..., \tau\} \tag{4.12}$$

$$\left\{E, F, S, e^t, f^t, s^t\right\} \in \mathbb{R}^+ \tag{4.13}$$

The objective function in equation (4.6) weighs capital and operating costs of hydrogen equipment against their potential revenue streams. Here, opportunity costs of wind and fuel cell generation have been accounted for to strike a balance between the electricity and hydrogen markets. Such opportunity costs allow the model to determine if it is more lucrative to offer wind generation into the electricity market, run the electrolyzer and sell the hydrogen as a commodity, run the electrolyzer to generate stored hydrogen for energy arbitrage, or some combination of the above. Arbitrage value, in both the hydrogen and electricity markets, is hindered by the second law of thermodynamics. Conversion between hydrogen and electricity results in an entropic loss: i.e., a kilowatt-hour of electrical energy will always generate less than a kilowatt-hour of hydrogen and vice versa. As a result, in order to be economically viable, the value obtained through arbitrage must offset both equipment cost and irreversible energy losses. Equations (4.7) and (4.8) require the hourly electrolyzer generation to be less than both the electrolyzer installed capacity and the available wind generation. Similarly, equation (4.9) limits fuel cell generation by the fuel cells installed capacity, while (4.10) bounds the hydrogen available in the tank between hourly fuel cell output and max storage capacity; that is to say that the fuel cell can't use more hydrogen than is available, and that the amount of stored hydrogen is limited by the volume of the tank. Equation (4.11) performs a mass balance on the hydrogen tank, requiring the change in mass in the tank between chronological hours to be less than the difference between electrolyzer output and fuel cell input to the tank. Writing the mass balance as an inequality, rather than an equality, allows for excess hydrogen, over what is sent to storage, to be sold as a commodity. Finally, equation (4.12) requires the system to meet a predetermined annual hydrogen demand, and equation (4.13) defines all decision variables as positive real numbers, preventing non-physical results such as a negative installed capacity or generation.

4.2.2 Model inputs

Equipment and Hydrogen Costs

Parameters representing the capital and operating costs are taken from various sources from both academic literature and industry reports. Table 4.1 provides the total range of costs found within such sources. Some challenges were faced during the data collection process, including a lack of manufacturer-specified costs, as many companies are not willing to share such information with those not looking to buy. Also, as can be seen in Table 4.1, capital costs presented in the literature cover a wide range of values: for example, the highest electrolyzer capital cost ($3000/kW) is 25 times larger than the lowest ($120/kW), though these values may be outliers. Electrolyzer (as well fuel cell and storage tank) capital costs are dependant on a number factors, e.g. type and size; as verification of equipment cost is not the focus of this paper, differences in costs have been included as sensitivity studies, using mean and 25$^{\text{th}}$ percentile values, also present in Table 4.1, as upper and lower bounds respectively. For this work, maintenance costs have been approximated as a fixed annual value that scales with installed capacity, while any variable operating cost have been accounted for through opportunity costs, as described in the previous section. To maintain consistency in costs, all values have been converted to nominal 2020 $CAD using historic inflation rates [192] and, where necessary, exchange rates from appropriate years [193].

For this study, the market price of blue and green hydrogen is assumed to be equal, meaning that the model will only generate green hydrogen when it is economically competitive with blue. This assumption can be sidestepped through the use of equation (4.12), whereby the model generates enough green hydrogen to meet the specified demand at the lowest cost, regardless of the cost of blue hydrogen. Any additional green hydrogen above the demand specified in equation (4.12), however, will once again be competing with blue hydrogen. Hydrogen costs used in the model are also summarized in Table 4.1. Here, the model uses mean delivered cost and emissions,

and a carbon price which varies based on the year being studied.

Parameter	25th pctl.[*]	Mean[*]	Range	Unit	References
Capital Costs					
Fuel Cell	800	1,650	510 - 6,000	$/kW	[3, 51–54, 102, 194]
Electrolyzer	500	1,600	120 - 3,000	$/kW	[3, 51–54, 102, 194, 195]
Storage Tank	500	850	320 - 1,685	$/kg-$H_2$	[51, 52, 54, 194]
Operating Costs					
Fuel Cell	32	34	30 - 40	$/kW/yr	[52, 53, 196, 197]
Electrolyzer	20	25	13 - 31	$/kW/yr	[3, 51–54, 102]
Storage Tank	20	38	12 - 82	$/(kg-$H_2$/yr)	[51, 52, 54]
Hydrogen Costs					
Delivered Cost	-	1.60	1.34 - 1.85	$/kg-$H_2$	[74]
Emissions	-	3.3	2.4 - 4.2	kg-CO_2e/kg-H_2	[74]
Carbon Price	-	-	30 - 170	$/t$CO_2$e	[14]
Total Cost[**]	1.66	1.90	1.41 - 2.56	$/kg-$H_2$	

[*]Used to defined upper and lower limits in study

[**]Total Cost = Delivered Cost + (Emissions)(Carbon Price)(1 t/1000 kg)

Table 4.1: Equipment capital expenditure, operating expenditure, and value of hydrogen estimates, with mean and 25th percentile values used as coefficients in the LP objective function, equation (4.6)

Economic Assumptions

As each simulation is only run for a single year, all economic inputs are converted to an annual frame of reference. With an assumed project length of $N = 20$ years, inflation rate of $f = 2\%$ [192], and nominal discount rate of $i' = 8\%$, the real discount rate, i and capital recovery factor, CRF are calculated as[4]:

---

[4]Assumptions align with similar studies found in the literature: see Kharel [3], for example.

$$i = \frac{i' - f}{1 + f} = 5.88\%, \text{ and}$$

$$\text{CRF} = \frac{i(1 + i)^N}{(1 + i)^N - 1} = 8.64\%,$$

such that the annualized capital cost of hydrogen equipment is equal to 8.64% of the total capital cost.

Fuel Cell Efficiency

Hydrogen consumption by a fuel cell, or fuel efficiency, depends on its energy output relative to installed capacity. For this work, the polarization curve from the Ballard 140 kW FCgen©-HPS [198] fuel cell is used to derive fuel efficiency as a function of capacity factor. Technical specifications for this fuel cell can be found in the Appendix. The following equations are used in converting from polarization to fuel efficiency:

$$P = IV, \tag{4.14}$$

$$\dot{m}_{H_2} = NI \left(\frac{M_{H_2}}{n_e F} \right), \text{ and} \tag{4.15}$$

$$\eta_f = \frac{P}{\text{LHV}_{H_2} \dot{m}_{H_2}}, \tag{4.16}$$

where:

- $\dot{m}_{H_2}$ = hydrogen consumption [g/s];

- n_e = moles of electrons per mole of hydrogen (2 $\text{mol}_e/\text{mol}_{H_2}$ for PEM);

- F = Faraday's constant (96485 C/mol_e);

- I = total current [A];

- LHV_{H_2} = lower heating value of hydrogen (120 MJ/kg);

- M_{H_2} = molar mass of hydrogen (2.016 g/mol);

- N = number of cells in the fuel cell stack (309 [198]);

- P = power output [kW]; and

- V = cell voltage [V].

While a continuous efficiency curve would be more accurate, in order to maintain linearity in the model, the fuel cell capacity has been broken in the three separate blocks, each with a discrete efficiency. Note that as efficiency decreases with output, shown in Figure 4.9, no additional constraints are required to ensure the fuel cell blocks operate in chronological order: i.e. block 1 will operate at full capacity before block 2 comes online, and blocks 1 and 2 will operate at full capacity before block 3 comes online.
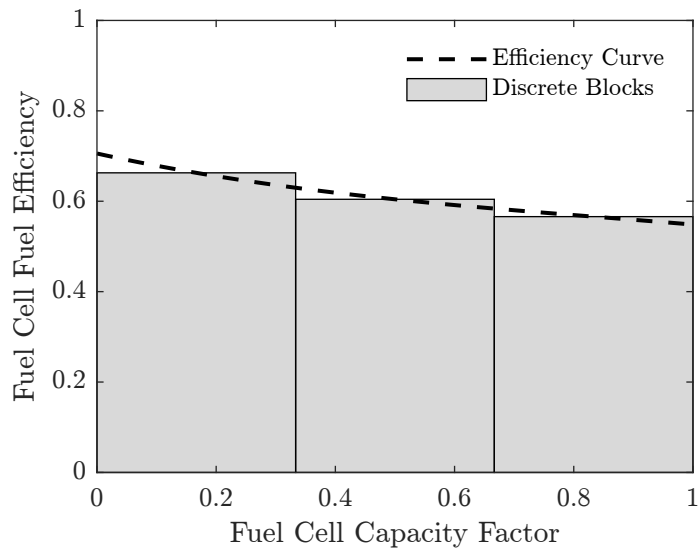
Figure 4.9: Fuel cell fuel efficiency as a continuous function and discrete blocks

There is an important distinction in defining the efficiencies of an electrolyzer in converting electricity to hydrogen (final term in equation 4.6) and a fuel cell in converting hydrogen back to electricity (equation 4.16). A fuel cell's efficiency should always be defined using the lower heating value (LHV) of hydrogen as the water is being output as steam; using the latent heat in the steam output for another purpose (e.g. combined heat and power) is one potential way to increase the thermal efficiency

of a fuel cell. An electrolyzer's efficiency, on the other hand, depends on the type of electrolyzer being used. A PEM electrolyzer's efficiency is defined using the higher heating value (HHV) of hydrogen as it operates with steam as an input, often using the waste heat from the process to generate the steam. The efficiency of alkaline electrolyzers is defined by the LHV of hydrogen due to their operation using liquid water [199].

Wind Generation

The electricity opportunity cost of wind-generated green hydrogen, that is the revenue that the wind farm is giving up in order to power the electrolyzer, is heavily influenced by both the wind farm's annual output, as well as its generation schedule relative to the price of electricity. To properly study this relationship, three wind farms with differing characteristics, outlined in Table 4.2, were used in simulating the hydrogen system. Here, two existing wind farms, Castle Rock and Ghost Pine, and one proposed wind farm, Jenner 2, were chosen as they have similar installed capacities (77 MW $\pm$ 6 MW) , but differing capacity factors and/or correlations to the bulk wind fleet. In this way, simulation results should provide insight into the effect to which wind farm location, age, and performance have on the cost of producing green hydrogen.

Electricity Price and Shock Series

Value obtained from energy arbitrage is highly dependent on volatility in electricity price. For example, a market with a fixed power price would present no arbitrage opportunity, as there would be no price difference between charging and discharging. Alternatively, a market price which alternates between its maximum and minimum, $0/MWh and $999/MWh in Alberta, would allow for maximum theoretical arbitrage. Alberta's electricity market operates somewhere between these two extreme cases, with each year having a different level of arbitrage opportunity. This subsection presents the method to which the volatility, or randomness, in Alberta's electricity

Wind Farm	Castle Rock	Ghost Pine	Jenner 2
Year in Service	2012	2010	2022 - 2023*
Installed Capacity (MW)	77 MW	82 MW	71 MW*
Turbine Manufacturer	ENERCON	General Electric	ENERCON
Turbine Model	E70	GE 1.6 MW	5.X MW**
Capacity Factor	0.30	0.29	0.45
Output Correlation to Total Alberta Wind Generation	0.78	0.45	0.69***

*According to Jenner Wind Power Project website [200], date subject to change

**Power curves are not currently available, so Vestas V136 are used as a proxy for this work

***Value simulated using 2009 Wind Atlas data. Real value expected to be lower due to proximity relative to bulk wind fleet

Table 4.2: Characteristics of wind farms used in LP simulations

price is characterized.

Electricity price may depend on a number of observable factors. Many factors relate to the time period being considered: hour of the day, day of the week, and month of year, for example. On peak hours, those where electricity demand is typically highest, off peak times such as stat holidays, and day-ahead demand forecasts will also have an impact. Air temperature, readily available through Environment and Climate Change Canada [201], has a well known correlation to electricity price, especially in the winter months. Lower temperatures improve the efficiency of thermal generation by lowering the amount of cooling required, but raise heating demand, causing an increase in both natural gas and electricity prices.

By combining the factors described above into a least-squares linear-regression, the observable portion of electricity price is quantified. The residuals, or difference between modelled and posted price, provide an approximation of the left-over randomness, or volatility in historic electricity price. Figure 4.10 shows annual duration curves for these random shocks between 2010 and 2020, at 4, 12, 48, and 168 hours

ahead.
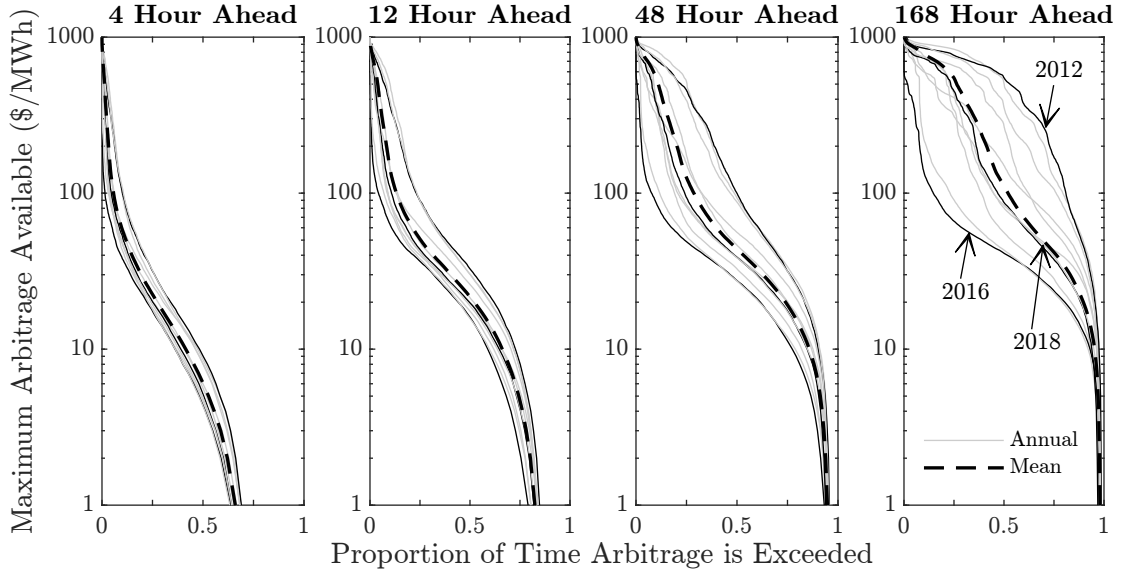
Figure 4.10: Annual modelled arbitrage opportunity in Alberta, 2010 - 2020

To decrease computation time, a subset of available price series is chosen for the linear optimization; Aurora hourly price outputs in 2025 and 2030 for each of the four scenarios are paired with historic shocks from 2012, 2016, and 2018, for a total of 24 unique price series. As highlighted in Figure 4.10, the random shock series are chosen such that the hydrogen plant is subject to under- and over-supplied as well as approximately median market conditions.

4.2.3 Model Construction

The optimization model outlined above is solved as a single linear program using the MATLAB optimization toolbox[5] [203] for each set of inputs. The model is solved in the following format [204]:

$$\text{minimize } z = c^T x$$

$$\text{subject to } Ax \leq b,$$

---

[5]Here, the MATLAB *linprog* function is used [202]

where z is the function to be minimized, c is the vector of objective function coefficients, x is the vector of decision variables, A is the matrix of constraint coefficients, and b is the solution vector. The hydrogen system being considered is comprised of 3 potential pieces of equipment (electrolyzer, tank, fuel, cell), each with a unique capacity and annual operating schedule which, ignoring leap years, are 8760 hours in duration. As described earlier, the fuel cell is broken into 3 blocks, each with a discrete efficiency and unique generating schedule.

The linear program is written such that the entire year is solved simultaneously, a requirement for energy storage optimization, rather than hour by hour. As a result, equations (4.7) - (4.11) are each written as a set of 8760 constraints, with equation (4.10) representing 17520 total constraints as each inequality must be solved individually. The number of equations required to solve the production constraint, described by equation (4.12), depends on time frame being considered: an annual constraint, used in this work, only requires a single equation, while a monthly constraint would require 12. The resulting coefficient matrix, $A \in \mathbb{R}^+_{m \times n}$ vector of decision variables, $x \in \mathbb{R}^+_n$ and solution vector, $b \in \mathbb{R}^+_m$ are comprised of $m = 78,841$ equations, and $n = 43,803$ variables.

4.2.4 Model Solution Procedure

Unless otherwise specified, MATLAB uses a dual-simplex algorithm in solving linear programs [202]. The following section provides an overview of the simplex algorithm in the form of a basic example, with discussion on the similarities between dual and primal simplex methods to follow.

Both dual and primal-simplex algorithms begin by converting a linear program to standard canonical form, whereby all inequalities are written as equalities, all variables are non-negative, and each equation contains a unique variable with a coefficient of one [204]. Here, *less than* constraints are converted to equality constraints through the use of a slack variable, s: for example, the inequality $x_1 + x_2 \leq 1$ can be rewritten

as $x_1 + x_2 + s = 1$, so long as $(x_1, x_2, s) \geq 0$. Similarly, *greater than* constraints are converted to equality constraints using excess variables, e, where $x_1 - x_2 \geq 5$ is equivalent to $x_1 - x_2 - e = 5$ if $(x_1, x_2, e) \geq 0$.

With the LP in standard form, a basic solution to the problem must be found by setting a number of (non-basic) variables to zero, such that the remaining (basic) variables are linearly independent. This basic solution is feasible if the non-negative constraint is maintained [204]. Consider the following LP, written in standard form[6]:

$$
\begin{aligned}
\text{Maximize} \quad & z = 2x_1 + 3x_2 \\
\text{Subject to} \quad & x + 2x_2 + s_1 = 6 \\
& 2x_1 + x_2 + s_2 = 8 \\
& (x_1, x_2, s_1, s_2) \geq 0
\end{aligned}
$$

Alternatively, moving all variables to the left-hand side of their equations and constants to the right, the above LP can be expressed as a matrix:

$$
\begin{pmatrix}
1 & -2 & -3 & 0 & 0 \\
0 & 1 & 2 & 1 & 0 \\
0 & 2 & 1 & 0 & 1
\end{pmatrix}
\begin{pmatrix}
z \\ x_1 \\ x_2 \\ s_1 \\ s_2
\end{pmatrix}
=
\begin{pmatrix}
0 \\ 6 \\ 8
\end{pmatrix},
$$

or simplex tableau [204]:

Row	z	x_1	x_2	s_1	s_2	RHS
0	$\boxed{1}$	-2	-3	0	0	0
1	0	1	2	$\boxed{1}$	0	6
2	0	2	1	0	$\boxed{1}$	8

where RHS represents the right-hand side of the constraints, and canonical variables for each row have been boxed in. From observation, a basic solution can be achieved by setting non-basic variables $(x_1, x_2) = 0$, such that the remaining basic variables,

---

[6]Example adapted from Operations Research, Applications and Algorithms, (4th edition), page 149. [204]

s_1, s_2, and z, equal 6, 8, and 0 respectively. Note that this solution is also feasible as all decision and slack variables have remained non-negative.

As this is a maximization problem, we determine whether the current solution is optimal by testing if increasing any of the non-basic variables would increase the value of the objective function, z. By observation, this can be done by increasing the value of either x_1 or x_2. Here we choose x_2, as it has the most negative coefficient in row 0 of the simplex tableau. As x_2 will be entered into the basis, a previously basic variable must be removed from the basis in order to maintain linear independence. This so-called *leaving variable* is determined through the root-test [204], whereby we can determine how large the *entering variable*, x_2 can become, all else equal, before a basic variable becomes negative. The root test is performed by dividing the RHS coefficient in each row, excluding row 0, by the coefficient of the *entering variable*, from the same row, then selecting the lowest ratio. In this example, we determine that x_2 can increase by $\frac{6}{2} = 3$ or $\frac{8}{1} = 8$ before s_1 or s_2 become negative, respectively. As a result, we select s_1 as our leaving variable and perform the necessary elementary row operations to arrive at the following (canonical) tableau:

Row	z	x_1	x_2	s_1	s_2	RHS
0	$\boxed{1}$	-1/2	0	3/2	0	9
1	0	1/2	$\boxed{1}$	1/2	0	3
2	0	3/2	0	-1/2	$\boxed{1}$	5

where our new basis is now made up of the basic variables, z, x_2, and s_2. The above process is repeated until there are no more negative coefficients in row 0 and the solution is therefore optimal. Note that the same LP can be written as a minimization problem by multiplying the objective function by -1: for example the maximization of $z = 2x_1 + 3x_2$ is the same as the minimization of $z^* = -2x_1 - 3x_2$.

When using the simplex method to solve a maximization, primal feasibility refers to a tableau with no negative coefficients in the RHS column, while dual feasibility

refers to a tableau with no negative coefficients in the objective function. In the above example, the primal simplex method is applied: the initial tableau is primal feasible and a series of pivots are applied, maintaining primal feasibility, until a dual feasible solution is obtained. As one would expect, the dual simplex method is reversed, starting with a dual feasible solution, pivoting while maintaining dual feasibility until a primal feasible solution is obtained. It can be shown, using the Dual Theorem, that primal and dual problems are mathematically equivalent, such that if an optimal solution exists, the solution to the primal and dual problems are equal [204]. Similarly, if either the primal or dual problem is infeasible, the other is unbounded. Oftentimes, the dual method is preferred as it can alleviate degeneracy caused by a zero RHS coefficient [205, 206].

4.2.5 Simulation Results

Using the methods described above, a small-scale, wind-driven green hydrogen plant is simulated across several permutations of input parameters. The following section outlines the pertinent results of these simulations with special focus given to three parameters: capital cost (c_X in equation (4.6)), hydrogen market value (h in equation (4.6)), and annual green hydrogen demand (P^τ in equation (4.12)). The first analysis is performed using average hydrogen market values (see Table 4.1) and no hydrogen demand constraint, i.e. $P^\tau = 0$. Here, simulations are run across numerous combinations of capital costs, bounded by their respective 25th-percentile and mean values (see Table 4.1). The second analysis is performed using mean capital costs and no hydrogen demand constraint, while increasing the market value of hydrogen from $3/kg to $10/kg in discrete increments. The third analysis uses mean capital costs and hydrogen market values, with increasing levels of green hydrogen demand.

Primary Analysis: Sensitivity to Capital Cost

Under the outlined simulation logic, the model will only build a set of hydrogen equipment if it results in a net increase in revenue: that is, if the value obtained by the new equipment offsets the cost of installing and maintaining the equipment, as well as the loss in electricity revenue incurred by generating hydrogen. This condition is verified through the use of Figure 4.11. Annual revenue and costs are shown on the upper *y-axis*, while system value (revenue minus cost) is given on the lower *y-axis*, with all values normalized by installed electrolyzer capacity. Note that each point along the *x-axis* represents an individual simulation, with results sorted by descending system value.
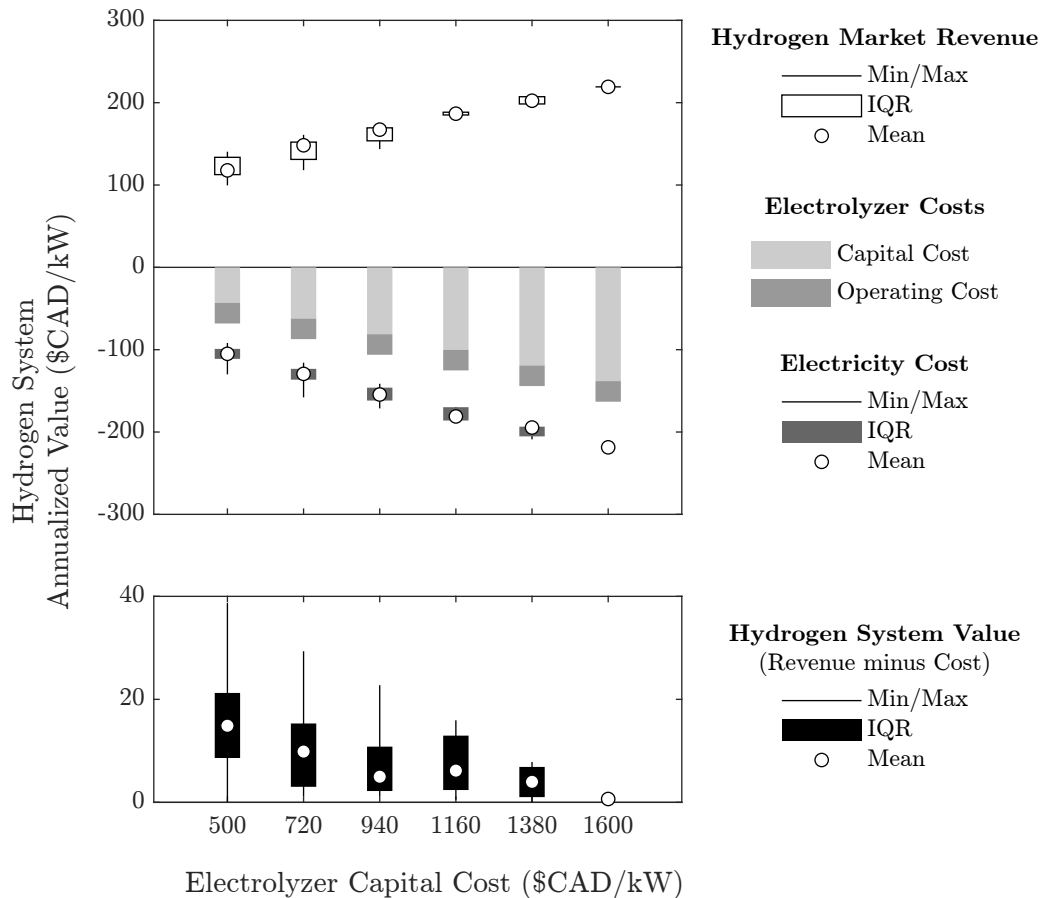

Figure 4.11: Balance of hydrogen system revenue and cost per kilowatt of installed electrolyzer capacity, sorted in increasing order of electrolyzer capital cost

Figure 4.11 shows the contributions of capital, operating, and electricity opportu-

nity costs incurred by installing a hydrogen system. Here, it can be seen that capital expenditure is often the dominant factor in determining system value, with electricity and operating expenses playing a secondary role. For the given inputs, optimal system value is bounded below $40/kW, with the majority of systems seeing values around $10/kW. It can also be seen that the only source of additional revenue is a result of selling hydrogen as a commodity. This result could be interpreted in a couple different ways: either the energy arbitrage available to the system is never great enough to justify purchasing a fuel cell and storage tank, or the arbitrage in the hydrogen market is greater than the arbitrage in the power market, meaning the additional "loss" of energy due to the fuel cell conversion efficiency makes it difficult to justify installing a fuel cell. In either case, results show that a wind-hydrogen plant is only economically feasible when its objective is to sell green hydrogen.

As more wind energy is redirected from the electricity market to power the electrolyzer, the captured price of the wind farm should increase. Note, however, that as less wind energy is being sold overall, the total electricity revenue of the wind farm will begin to decrease. Figure 4.12 shows the increase in the captured price of each wind farm, Castle Rock, Ghost Pine, and Jenner 2, as a function of annual hydrogen production. Here, individual simulation results for a given wind farm are shown as discrete points, with a least-squared best-fit line drawn through each cluster.

The use of a log-log scale in Figure 4.12 gives insight into the order of magnitude increase in wind farm capture price, relative to the order of magnitude increase in hydrogen production. For example, when Jenner 2 is used to produce 6.7 and 72 tonnes of hydrogen per year, it sees a 0.1 and 1.1 percent increase in captured price respectively, meaning a tenfold increase in hydrogen production leads to a slightly larger than tenfold increase in wind farm capture price. The estimated magnitude of this increase is summarized in the data table in Figure 4.12, which shows the captured price of all 3 wind farms increasing at a rate 10% - 12% greater than annual hydrogen production.
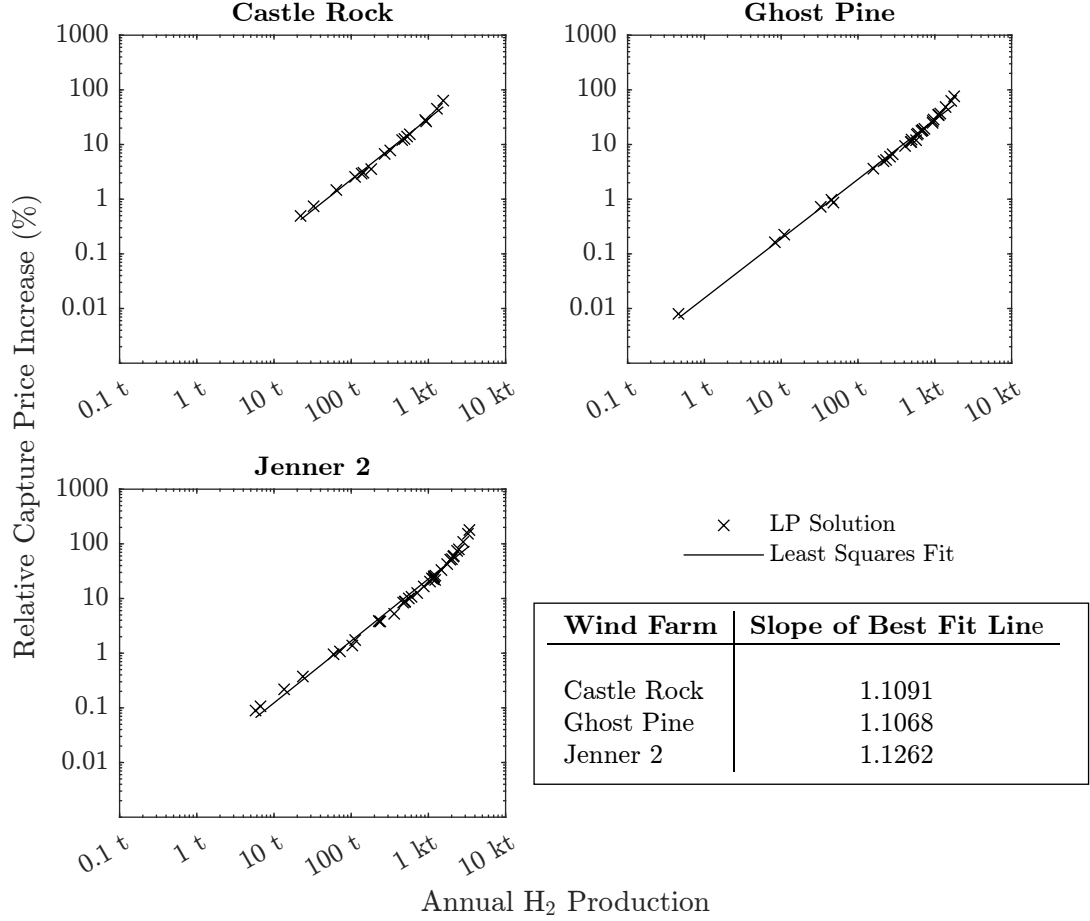
Figure 4.12: Increase in wind farm capture price relative to annual hydrogen production

An optimized green hydrogen plant will only run its electrolyzer when the market value of hydrogen exceeds the market value of the electricity used to produce it. We can determine an upper limit on the electricity price, that is, the maximum power price that a wind farm will generate hydrogen at, by balancing the revenue streams. Using the same variable notation as equation (4.6), we write the following inequality:

$$g^t \cdot \left(e^t - f^t\right) < h \cdot \left(\frac{\eta_r \eta_e e^t}{\text{HHV}_{\text{H}_2}} - \frac{f^t}{\eta_f^t}\right),$$

where the left hand side represents electricity market value and the right hand side represents hydrogen market value. Noting that the fuel cell is not built in any of the simulations, i.e. $f^t = 0$, it can be shown that the above inequality is equivalent to:

$$\frac{g^t}{h} < \frac{\eta_r \eta_e}{\text{HHV}_{\text{H}_2}}.$$

88

Using the range of hydrogen values outlined in Table 4.1, and substituting in the values for η_r (0.95), η_e (0.74), and HHV_{H_2} (39.4 kWh/kg), we can determine the range of electricity prices, over which the electrolyzer should not run:

$$\frac{g^t}{h} \lessgtr 17.8 \quad \& \quad h \in (\$1.41 - \$2.54)/\text{kg},$$

$$\therefore \max(g) \in (\$25.1 - \$45.6)/\text{MWh},$$

where the upper limit on g, i.e. the value of h, depends on the year and scenario being simulated.

Optimal electrolyzer operation is subject to a number of factors: the wind farm to which it is paired, the electricity market in which it operates, and the cost at which it is installed and operated. Figure 4.13 gives a variety of electrolyzer performance indicators with respect to each of these factors. From left to right, we show the proportion of solutions that include an electrolyzer, the electrolyzer capacity relative to the wind farm capacity, the electrolyzer capacity factor, and the annual hydrogen production normalized by electrolyzer capacity. With the exception of the first column, values are shown in terms of statistical ranges, whereby the *bars*, *lines*, and *circles* show the interquartile range, full range of solutions, and the median respectively.

As shown along the top row in Figure 4.13, Jenner 2 has proven to be the most attractive option to pair with an electrolyzer: an intuitive result, due to its high capacity factor. Here, higher amounts of wind energy lends to a larger, on average, electrolyzer capacity and increased annual hydrogen generation. On the other hand, although the two remaining wind farms, Castle Rock and Ghost Pine, are similar in their annual energy production, the latter is clearly the more favourable choice. The discrepancy in their performance is likely a result of their correlations to the bulk wind fleet (Table 4.2).

The second and third rows in Figure 4.13 show electrolyzer performance subject to each Aurora scenario. Here, it can be seen that electricity markets characterized by higher renewable penetration, especially solar, provide a more favourable setting
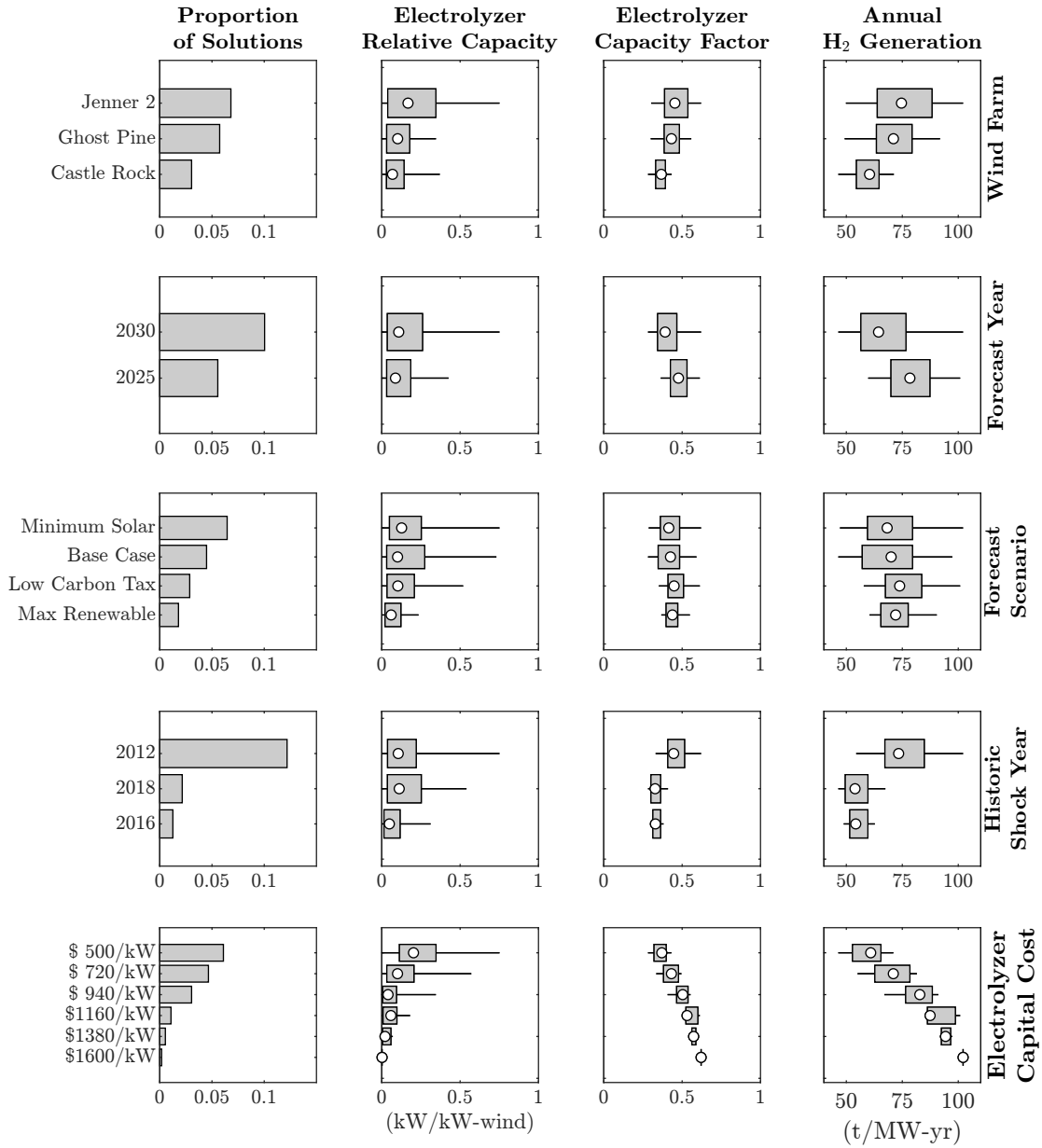
Figure 4.13: Statistical summary of electrolyzer performance parameters for a given set of simulation input parameters, i.e. wind farm, market conditions, and electrolyzer capital costs. Performance indicators show, from left to right: the proportion of optimal solutions for a given input parameter, optimal electrolyzer capacity and capacity factor, and annual hydrogen generation.

than those with less renewable energy. This result is amplified the further you look forward, with more solutions occurring in 2030 than 2025, thereby allowing even more renewables to enter the system. With respect to historic market shocks, shown in the fourth row, results are heavily biased towards the 2012 series. Recall that 2012 is

representative of tight market conditions (see Figure 4.10), while 2018 and 2016 are characteristic average and saturated markets respectively. These results show that a hydrogen plant will generate greater value when subject to higher price volatility.

The final row in Figure 4.13 highlights the influence of capital cost on hydrogen plant performance. At higher costs, e.g. \$1600/kW, the optimal strategy is to install a small (~ 100 kW) electrolyzer and run as often as possible ($> 60\%$ capacity factor). As capital cost decreases, the strategy moves towards building larger electrolyzers that operate at lower capacity factors. Regardless of the scenario being considered, the optimal electrolyzer will have a capacity factor between 40% and 60%, generating between 50 and 100 tonnes of hydrogen per installed megawatt per year.

Energy generation and storage technologies are often compared on the basis of their levelized cost. This metric, e.g. the levelized cost of energy, is an estimate of the average revenue required to cover the costs to build and operate an asset over its expected lifetime. Using a similar approach, for the purpose of this work, we calculate a simplified levelized cost of hydrogen (LCOH) as:

$$\text{LCOH} = \frac{\text{electrolyzer Capital Cost} + \text{electrolyzer Operating Costs} + \text{Electricity Costs}}{\text{Hydrogen Produced}}, \quad (4.17)$$

where capital, operating, and electricity costs are given in terms of *$CAD*, hydrogen production in *kg*, and all four variables are expressed in an annualized frame of reference. Figure 4.14 shows our calculated range of LCOH relative to estimated blue hydrogen costs (see Table 4.1), shown as a *blue shaded area*. Results are broken down in a similar manner as Figure 4.13, showing the relative impacts that wind farm performance, electricity market environment, and electrolyzer capital cost can have on the levelized cost of wind-generated green hydrogen.

Special care should be taken when interpreting the results shown in Figure 4.14. For example, at first glance, it may appear that the lowest LCOH is achieved under a low carbon tax; however, this result is misleading as it is driven by a couple hidden factors. First, it can be shown that the operating low carbon tax scenario only
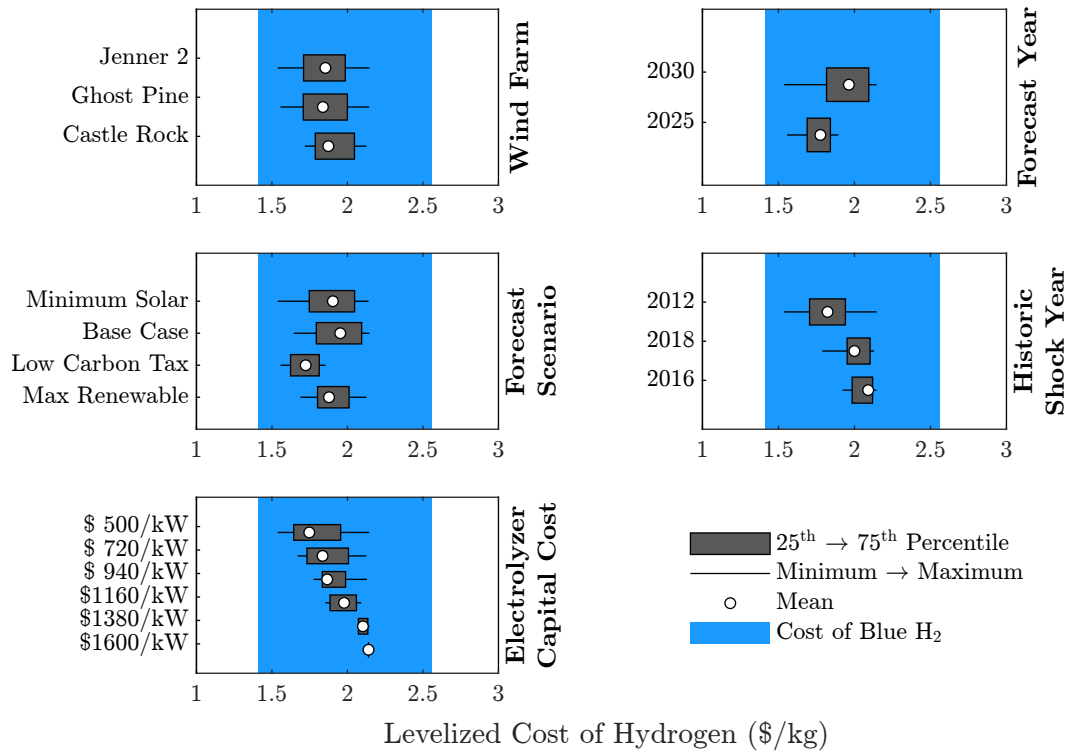
Figure 4.14: Levelized cost of green hydrogen relative to the chosen wind farm, simulation year, Aurora scenario, historic shock series, and electrolyzer capital cost

overlaps with lower cost electrolyzers ($\leq$ \$1160/kW) and favourable price dynamics (2012 shock series). Also, as the value of blue hydrogen is directly proportional to the carbon tax, and the operation of the electrolyzer is contingent on the value of blue hydrogen, the maximum LCOH at which the electrolyzer will operate in this scenario is lower than that of any others. As a result, one should not conclude that the LCOH of green hydrogen is lower under a low carbon tax scenario, but rather that it requires specific conditions to even be possible. Similar reasoning can be applied to explain the difference in LCOH between 2025 and 2030, as seen in the second row of Figure 4.14.

In an optimized system with perfect foresight, the electricity cost contribution to the levelized cost of hydrogen is less than half the cost of installing and operating the electrolyzer. In addition, electricity costs are higher for hydrogen plants operating in electrical grids with low renewables (2025 and Aurora maximum renewable con-

straint), and under saturated market conditions (2016 shock series). As the capital cost of an electrolyzer decreases (bottom row of Figure 4.14), the hydrogen plant can run during less favourable hours, i.e. higher power prices, while maintaining a competitive LCOH.

Alternative Analysis: Sensitivity to Blue Hydrogen Costs

In the previous analysis, the price of hydrogen is based on values from Lof [74], with the addition of a carbon tax [14], and the limiting assumption that this value will not change within the time frame being considered. With global hydrogen demands projected to rise significantly in the next few decades [5, 77], there is a very real possibility that the value of hydrogen will increase in tandem. Figures 4.15 and 4.16 outline the electrolyzer performance, and range of levelized green hydrogen costs achieved under an increasing market value of hydrogen. Note that in Figure 4.16, the value of blue hydrogen is shown as a *dotted line*, rather than a shaded area as in Figure 4.14. Also, the leftmost column of Figure 4.15 shows the proportion of wind energy dedicated to green hydrogen production, rather than the proportion of solutions including an electrolyzer.

Recall that a green hydrogen plant will no longer run its electrolyzer when the price of power (in \$/MWh) is approximately 18-times larger than the cost of blue hydrogen (in \$/kg). Using this result, we can approximate a new range of power price limits for hydrogen values between \$3/kg and \$10/kg (see Table 4.3). As the value of hydrogen overtakes that of electricity, an optimized hydrogen plant will dedicate more energy to powering its electrolyzer. Figure 4.15 shows an equilibrium point around a hydrogen value of \$4.5/kg, whereby wind energy is divided equally between the power and hydrogen markets. Similarly, at a hydrogen value of \$10/kg, an optimized wind farm will dedicate nearly all of its energy to generating hydrogen, regardless of the electricity price. With respect to optimal electrolyzer sizing, results of this analysis are in agreement with the previous section, leading to a capacity factor just above
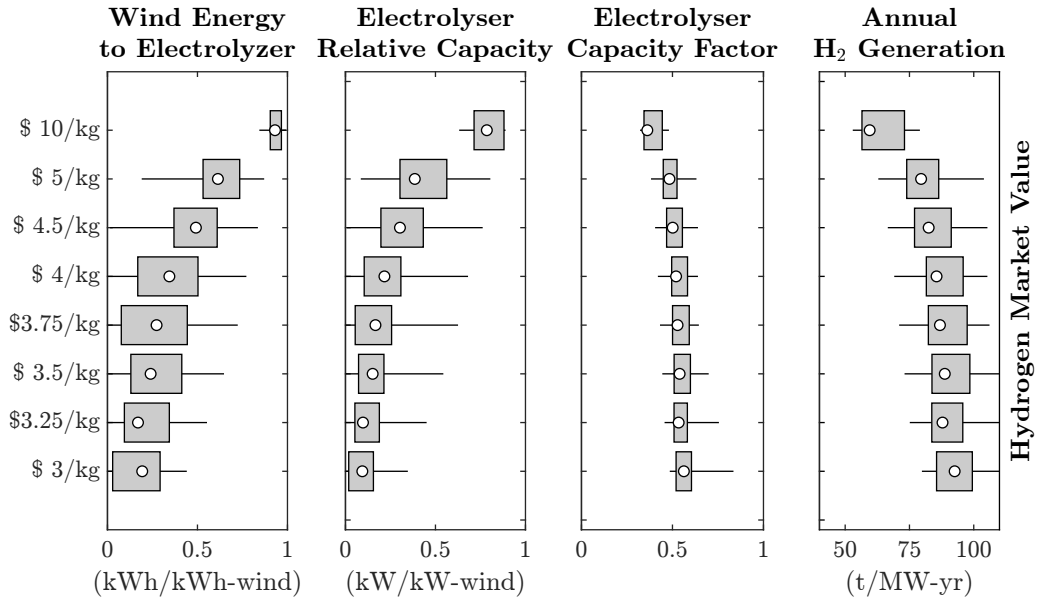
Figure 4.15: Statistical summary of electrolyzer performance parameters for a given range of hydrogen market values. Performance indicators show, from left to right: the proportion of wind energy dedicated to electrolysis, optimal electrolyzer capacity and capacity factor, and annual hydrogen generation.

50%.

To maximize its value through price arbitrage, a green hydrogen plant will power its electrolyzer until the marginal cost and market value of hydrogen are equal, while dumping the remaining wind energy to the electrical grid. In other words, an electrolyzer enables a wind farm to be, in a way, dispatchable. Figure 4.16 highlights the dependence of the levelized cost of green hydrogen on the market value of blue hydrogen. As market price increases, the revenue potential of green hydrogen will eventually outweigh the cost to produce it. In other words, the hydrogen plant will begin to generate hydrogen during higher electricity prices. For example, when hydrogen is valued at \$3.75/kg, the green hydrogen plant will operate at electricity prices at or below \$66.75/MWh (see Table 4.3). As more hydrogen is generated, the marginal cost of that hydrogen increases with increasing electricity prices. At current electrolyzer costs (\$1600/kW), the LCOH is no longer constrained by the market price when it reaches a value of \$4.5/kg. This decoupling effect occurs around the same

Value of Hydrogen ($/kg)	Upper Power Price Limit ($/MWh)
3.00	53.40
3.25	57.85
3.50	62.30
3.75	66.75
4.00	71.20
4.50	80.10
5.00	89.00
10.00	178.00

Table 4.3: Maximum grid price at which an electrolyzer should run relative to the cost of blue hydrogen

point that the plant is producing, on the basis of energy, equal amounts of electricity and hydrogen (Figure 4.15).
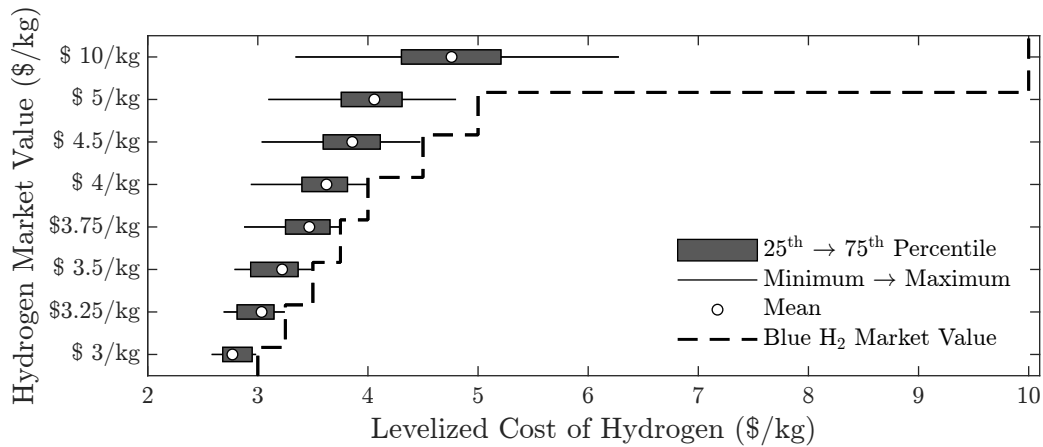
Figure 4.16: Levelized cost of green hydrogen for increasing values of hydrogen market value

Alternative Analysis: Sensitivity to an Annual Demand Constraint

Up to this point, discussion has been focused on a hydrogen plant that operates for the sole purpose of maximizing its revenue, producing and selling hydrogen in response to fluctuations in the price of electricity. The following analysis presents an alternative case study, whereby the plant must produce a defined amount of hydrogen. One could

consider this scenario as akin to a power purchase agreement, by which a contract is drawn between the plant and a buyer: e.g. an industrial consumer of hydrogen. In this case, the LCOH is an indication of the minimum price at which the plant would offer its hydrogen. Figures 4.17 and 4.18 show electrolyzer performance and levelized green hydrogen costs incurred by increasing the annual hydrogen demand constraint, defined by equation (4.12).
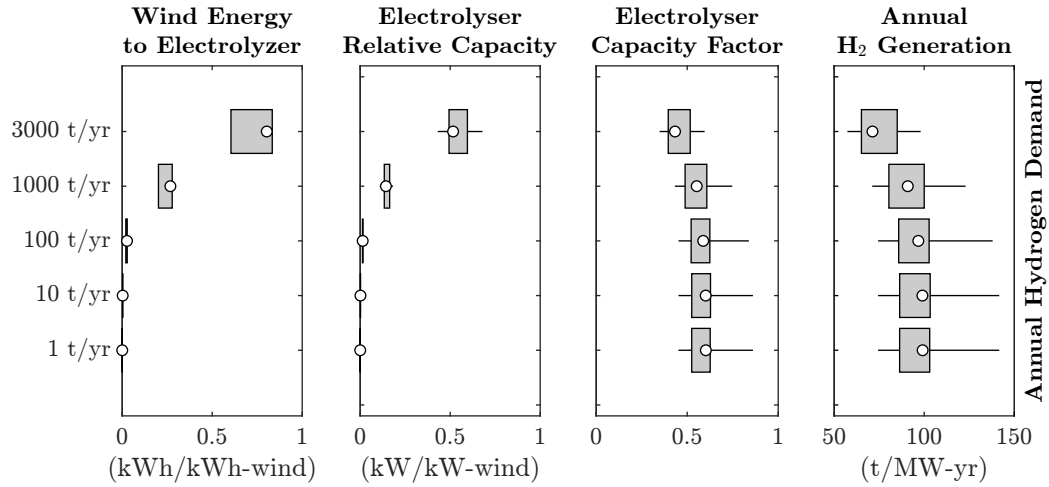
Figure 4.17: Statistical summary of electrolyzer performance parameters for a given range of hydrogen production values. Performance indicators show, from left to right: the proportion of wind energy dedicated to electrolysis, optimal electrolyzer capacity and capacity factor, and annual hydrogen generation.

Results shown in Figure 4.17 mirror those in Figures 4.13 and 4.15. Here, as one should expect, a larger electrolyzer and more wind energy are required to meet increased hydrogen demands, with optimal electrolyzer size contingent on achieving a capacity factor of 50% - 60%. LCOH, shown in Figure 4.18, is bounded between $2 and $6 per kilogram. Systems with higher renewable penetration, characterized by lower average electricity costs, see lower average hydrogen costs (not explicitly shown in Figure 4.18. Similarly, under the annual demand constraint, the cost of electricity is more significant than the unconstrained model, especially in markets with low renewables: in the most extreme cases, the cost of electricity is greater than the annualized capital costs plus operating expenditures.
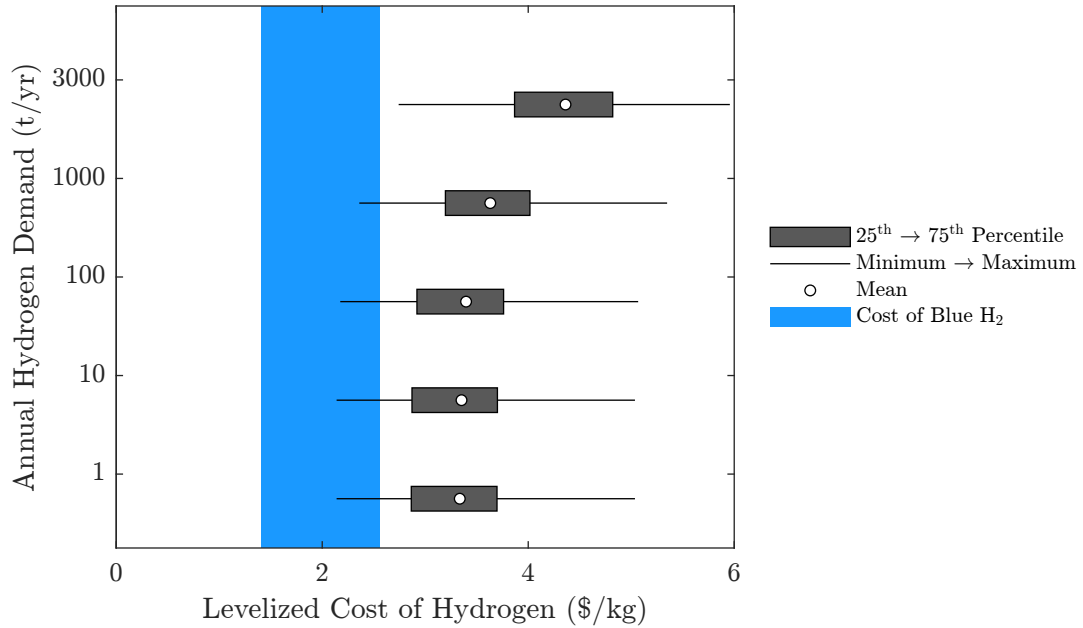
Figure 4.18: Levelized cost of green hydrogen for increasing values of annual hydrogen demand

4.3 Conclusions

This chapter presents an investigation into using wind energy to generate green hydrogen, for energy storage or as a commodity, in Alberta. Aurora is used to forecast future electricity market arrangements under various scenarios. To better represent the inherently dynamic price behaviours of a competitive electricity market, the resulting average price signal, output by Aurora, is augmented with random shocks. Using price data obtained from the Alberta Electric System Operator, market shocks are built by stripping out observable market dependencies, e.g. seasonality, from historic price signals. Renewable generation profiles are modelled using methods taken from Vergara Bonilla [153] and Duran [20], using publically available weather data [136, 152]. Through the use of linear programming, the operation of a wind-hydrogen hybrid plant is optimized with respect to annual revenue. Optimization results are subject to a number of inputs, namely: wind generation, electricity and hydrogen market prices, equipment capital costs, and an annual demand constraint.

Of the scenarios considered, 15% resulted in wind-generated green-hydrogen being

cost competitive with blue hydrogen, made through natural gas reforming, in the next 5 - 10 years. On average, annual green hydrogen sales, sold at cost, are shown to generate value on the order of $10 per installed kilowatt of electrolyzer capacity. The levelized cost of hydrogen (LCOH) is an economic metric which measures the total hydrogen system cost (capital, operating, and electricity) relative to the mass of hydrogen produced over the lifetime of the project. Across all scenarios, the LCOH for wind-driven green hydrogen ranges from $CAD 1.50/kg to $CAD 6.00/kg, showing high sensitivity to electrolyzer capital costs and electricity market dynamics. With respect to the success of a wind-driven hydrogen plant, supply constrained electricity markets subject to high renewable generation, especially solar, are more favourable than saturated power markets with low renewables and/or low carbon pricing. Regardless of the market in which it operates, an optimized electrolyzer should be sized such that it has a capacity factor around 50% - 60%, generating 75 - 100 tonnes of hydrogen per megawatt-year. Of the nearly 1800 unique combinations of input parameters, not a single optimization included in the installation of a fuel cell of hydrogen storage tank, i.e. the value of the hydrogen itself is greater than the electricity it could generate later.

Chapter 5

Conclusion

5.1   Thesis Summary

The goal of this thesis is to investigate the financial feasibility of green (low carbon) hydrogen, generated using wind power in Alberta. Wind farms operating in Alberta's deregulated electricity market often receive a below average price for the power that they generate: a consequence of their near-zero operating costs and their regulator-mandated zero-dollar supply offers. Unlike other energy storage technologies, hydrogen has the dual purpose of electricity generation, creating value through energy arbitrage, as well as being a feed stock for many industrial purposes, e.g. ammonia production. Pairing a wind farm with an energy storage asset, such as hydrogen, may be mutually beneficial: low-cost renewable energy can be stored and sold for a higher price, either as electricity or elsewhere as a commodity. Results of this work gives insight into future costs of generating green hydrogen as well as its feasibility, or lack their of, as an energy storage asset in future electricity markets.

Wind energy is growing rapidly in Canada and the size and location of each turbine and wind farm plays a prominent role in determining the opportunity for utility scale energy storage. The third chapter of this thesis examines trends of the Canadian wind industry, with hopes of helping predict future wind farm output and siting patterns. Results of this chapter show an increasing trend in the physical size of wind turbines, but a convergence of the capacity- and turbine-density of new wind farms.

Here, capacity density refers to the installed capacity (in megawatts) per unit area (in kilometres-squared) for the wind farm. Similarly, turbine density is defined by the number of turbines per unit area of each wind farm. Since the early 2010's, Canadian wind farms tend to have less than 1 turbine per kilometre squared, resulting in a capacity density of approximately 1.5 MW/km^2. From these results, wind energy developers can make a reasonable estimate at how much wind power they can install on a given plot of land.

The purpose of this work is not to predict the future layout and design of the Alberta electricity market, but rather to determine the characteristics of the market which may be advantageous for green hydrogen production. As such, a variety of future market scenarios are simulated using Aurora [147], an industry standard electricity market model. The base, or reference, case is built from inputs that, to our knowledge, are our best guess at how the Alberta market will look in the next 10 years, including parameters such as the federally-mandated coal-phase out [13], renewable generation profiles using historic weather patterns [20, 153], and electricity demand forecasts provided by the Alberta Electric System Operator [187]. Alternative scenarios, looking into the impact of increased solar generation, decreased renewable generation, and a lower carbon pricing scheme are also considered.

Results of this work, using the inputs described in previous chapters, show wind-driven green hydrogen as cost competitive with more traditional methods, i.e. steam-methane reforming, in 15% of the scenarios considered. On the other hand, under the assumed cost structure and efficiency curves, energy arbitrage via a fuel cell was not financially viable in any of the scenarios considered. Electricity markets subject to higher amounts of renewable energy, and the resulting price depression effect, are found to be the most favourable for green hydrogen production. In the most extreme cases, i.e. high renewable penetration (>50% by capacity) and low cost electrolysis ($500/kW), the levelized cost of green hydrogen could be as low as $1.50/kg by 2030.

5.2 Limitations and Future Work

Limitations of this work as well as some recommendations for future research are listed below:

- The design of the hydrogen plant, whose schematic in Figure 4.8, could be improved in a number of ways, namely:

    1. Taking into consideration any parasitic loads of auxiliary hydrogen equipment, such as compression, balance of plant, and dispensing hydrogen;

    2. Adding the option to store oxygen, a byproduct of electrolysis, to be used by the fuel cell, thus increasing its efficiency;

    3. Using a dynamic efficiency for the electrolyzer, as was done for the fuel cell, highlighted in Figure 4.9;

    4. Including the cost of the water feed-stock for electrolysis and transmission/distribution of hydrogen being sold; and

    5. Considering dual purpose electrolyzer-fuel cell, whereby a single piece of equipment can be used to generate and consume hydrogen, thus decreasing the overall capital cost of the system.

- Capital cost estimates for fuel cells and electrolyzers, given in Table 4.1, could be improved. For example, the United States Department of Energy has projected that current and future (2035) capital costs of distributed electrolysis ($\leq$1500 kg/day), including balance of plant, are approximately \$600/kW and \$380/kW respectively [207]: both of which are on the low end when compared to values used in this work.

- Wind discount effects, a primary motivation behind this work, are lost during the electricity price augmentation through historic shocks (see Figure 4.10); in other words, by increasing the volatility of the Aurora price outputs, the

overall price dynamics are overwhelmed by the historic shock series, leading to a decoupling of power price and wind generation. In future iterations of this type of work, it is recommended that wind generation is considered in the development of the historic shock series such that the discount effect is maintained.

Bibliography

[1] Lazard. *Levelized Cost of Energy Analysis - Version 14.0.* Tech. rep. Oct. 2020, pp. 1–21. URL: https://www.lazard.com/perspective/levelized-cost-of-energy-and-levelized-cost-of-storage-2020/.

[2] Riccardo Amirante et al. "Overview on recent developments in energy storage: Mechanical, electrochemical and hydrogen technologies". In: *Energy Conversion and Management* 132 (2017), pp. 372–387. ISSN: 0196-8904. DOI: https://doi.org/10.1016/j.enconman.2016.11.046.

[3] Subodh Kharel and Bahman Shabani. "Hydrogen as a Long-Term Large-Scale Energy Storage Solution to Support Renewables". In: *Energies* 11.10 (2018). DOI: 10.3390/en11102825.

[4] K A Kavadias, D Apostolou, and J K Kaldellis. "Modelling and optimisation of a hydrogen-based energy storage system in an autonomous electrical network". In: *Applied Energy* 227 (2018), pp. 574–586. ISSN: 0306-2619. DOI: https://doi.org/10.1016/j.apenergy.2017.08.050.

[5] Zen Clean Energy Solutions. *Hydrogen Strategy for Canada.* Natural Resources Canada, Dec. 2020. ISBN: 978-0-660-36760-6. URL: https://www.nrcan.gc.ca/climate-change/the-hydrogen-strategy/23080.

[6] Jonathan Wilkinson. *Canadian Net-Zero Emissions Accountability Act.* Nov. 2020. URL: https://www.canada.ca/en/services/environment/weather/climatechange/climate-plan/net-zero-emissions-2050/canadian-net-zero-emissions-accountability-act.html (visited on 04/02/2021).

[7] Government of Saskatchewan. *SaskPower.* URL: https://www.saskpower.com/ (visited on 08/23/2021).

[8] Government of Manitoba. *Manitoba Hydro.* URL: https://www.hydro.mb.ca/ (visited on 08/23/2021).

[9] Alberta Electric System Operator. *Guide to understanding Alberta's electricity market.* URL: https://www.aeso.ca/aeso/training/guide-to-understanding-albertas-electricity-market/ (visited on 08/13/2021).

[10] Alberta Electric System Operator. *ISO Rules Section 201.5 - Block Allocation.* URL: https://www.aeso.ca/rules-standards-and-tariff/iso-rules/section-201-5-block-allocation/ (visited on 08/23/2021).

[11] Alberta Electric System Operator. *ISO Rules Section 203.1 - Offers and Bids for Energy*. URL: https://www.aeso.ca/rules-standards-and-tariff/iso-rules/section-203-1-offers-and-bids-for-energy/ (visited on 08/23/2021).

[12] Canada Energy Regulator. *Provincial and Territorial Energy Profiles - Canada*. 2020. URL: https://www.cer-rec.gc.ca/nrg/ntgrtd/mrkt/nrgsstmprfls/cda-eng.html (visited on 06/22/2020).

[13] Government of Canada. *Coal phase-out: the Powering Past Coal Alliance*. 2020. URL: https://www.canada.ca/en/services/environment/weather/climatechange/canada-international-action/coal-phase-out.html (visited on 08/12/2020).

[14] Environment and Climate Change Canada. *The federal carbon pollution pricing benchmark*. Aug. 2021. URL: https://www.canada.ca/en/environment-climate-change/services/climate-change/pricing-pollution-how-it-will-work/carbon-pollution-pricing-federal-benchmark-information.html (visited on 08/06/2021).

[15] Alberta Electric System Operator. *2020 Annual Market Statistics*. Mar. 2021. URL: https://www.aeso.ca/assets/Uploads/2020-Annual-Market-Stats-Final.pdf (visited on 03/23/2021).

[16] Alberta Electric System Operator (@theAESO). *A new summer peak of 11,721 MW was recorded on June 29, 2021*. Twitter Post. URL: https://twitter.com/theAESO/status/1410255280873480199 (visited on 08/28/2021).

[17] Adam Cuthbertson. "Power Price Cannibalisation - How is it affecting your renewables projects?" In: *BDO Global* (June 2020). URL: https://www.bdo.global/en-gb/blogs/valuations-blog/june-en/power-price-cannibalisation-%E2%80%93-how-is-it-affecting-your-renewables-projects (visited on 03/23/2021).

[18] Canada Energy Regulator. *Market Snapshot: Alberta wind farms generate more power at night when demand is low and receive lower prices*. Feb. 2020. URL: https://www.cer-rec.gc.ca/nrg/ntgrtd/mrkt/snpsht/2016/07-04ABwndprcs2016-eng.html?=undefined&wbdisable=true (visited on 06/25/2020).

[19] Lion Hirth. "The market value of variable renewables: The effect of solar wind power variability on their relative price". In: *Energy Economics* 38 (2013), pp. 218–236. ISSN: 0140-9883. DOI: https://doi.org/10.1016/j.eneco.2013.02.004.

[20] Gloria Durán. "Backcasting solar impacts in the Alberta electricity market". unpublished.

[21] California Independent System Operator. *Fast Facts: What the duck curve tells us about managing a green grid*. URL: https://www.caiso.com/documents/flexibleresourceshelprenewables_fastfacts.pdf (visited on 03/16/2021).

[22]   Alberta Electricity System Operator. *Current Supply Demand Report.* URL: http://ets.aeso.ca/ets_web/ip/Market/Reports/CSDReportServlet (visited on 03/16/2021).

[23]   Dharik S. Mallapragada, Nestor A. Sepulveda, and Jesse D. Jenkins. "Long-run system value of battery energy storage in future grids with increasing wind and solar generation". In: *Applied Energy* 275 (2020), pp. 1–13. DOI: 10.1016/j.apenergy.2020.115390.

[24]   Kelly Pickerel. "PG&E plans to bring online 423 MW of lithium-ion energy storage by 2021". In: *Solar Power World* (May 2020). See: Blythe Energy Storage 110. URL: https://www.solarpowerworldonline.com/2020/05/pge-plans-to-bring-online-423-mw-of-lithium-ion-energy-storage-by-2021/.

[25]   Government of Canada. *Canadian Wind Turbine Database.* 2020. URL: https://open.canada.ca/data/en/dataset/79fdad93-9025-49ad-ba16-c26d718cc070 (visited on 06/24/2020).

[26]   Peter J. Donalek. "Pumped Storage Hydro Then and Now". In: *IEEE power & energy magazine* (July 2020), pp. 49–57. DOI: 10.1109/MPE.2020.3001418.

[27]   National Technology & Engineering Sciences of Sandia and U.S. Department of Energy. *Global Energy Storage Database.* Nov. 2020. URL: https://www.sandia.gov/ess-ssl/global-energy-storage-database-home/ (visited on 03/17/2021).

[28]   H Ibrahim, A Ilinca, and J Perron. "Energy storage systems—Characteristics and comparisons". In: *Renewable and Sustainable Energy Reviews* 12.5 (2008), pp. 1221–1250. ISSN: 1364-0321. DOI: https://doi.org/10.1016/j.rser.2007.01.023.

[29]   Xing Luo et al. "Overview of current development in electrical energy storage technologies and the application potential in power system operation". In: *Applied Energy* 137 (2015), pp. 511–536. ISSN: 0306-2619. DOI: https://doi.org/10.1016/j.apenergy.2014.09.081.

[30]   International Energy Agency. *IEA Sankey Diagram: Canada Balance.* 2018. URL: https://www.iea.org/sankey/#?c=Canada&s=Balance (visited on 03/16/2021).

[31]   Canada Energy Regulator. *Provincial and Territorial Energy Profiles – Canda.* June 2020. URL: https://www.cer-rec.gc.ca/en/data-analysis/energy-markets/provincial-territorial-energy-profiles/provincial-territorial-energy-profiles-canada.html (visited on 03/16/2021).

[32]   Oliver Schmidt et al. "Projecting the Future Levelized Cost of Electricity Storage Technologies". In: *Joule* 3.1 (2019), pp. 81–100. ISSN: 2542-4351. DOI: https://doi.org/10.1016/j.joule.2018.12.008.

[33]   Jason Deign. "Did Tesla's Big Australian Battery Kill the Business Case for More?" In: *Green Tech Media* (May 2018). URL: https://www.greentechmedia.com/articles/read/has-teslas-big-australian-battery-killed-the-business-case-for-more (visited on 09/08/2021).

[34] Bloomberg New Energy Finance. *New Energy Outlook 2019*. 2019. URL: https://about.bnef.com/new-energy-outlook/.

[35] Nestor A Sepulveda et al. "The Role of Firm Low-Carbon Electricity Resources in Deep Decarbonization of Power Generation". In: *Joule* 2.11 (2018), pp. 2403–2420. ISSN: 2542-4351. DOI: https://doi.org/10.1016/j.joule.2018.08.006.

[36] Nestor A. Sepulveda et al. "The design space for long-duration energy storage in decarbonized power systems". In: *Nature Energy* 6.5 (2021), pp. 506–516. DOI: 10.1038/s41560-021-00796-8.

[37] Seyed Ehsan Hosseini and Mazlan Abdul Wahid. "Hydrogen production from renewable and sustainable energy resources: Promising green energy carrier for clean development". In: *Renewable and Sustainable Energy Reviews* 57 (2016), pp. 850–866. ISSN: 1364-0321. DOI: https://doi.org/10.1016/j.rser.2015.12.112.

[38] Babatunde Olateju, Amit Kumar, and Marc Secanell. "A techno-economic assessment of large scale wind-hydrogen production with energy storage in Western Canada". In: *International Journal of Hydrogen Energy* 41.21 (2016), pp. 8755–8776. ISSN: 03603199. DOI: 10.1016/j.ijhydene.2016.03.177.

[39] Babatunde Olateju and Amit Kumar. "Hydrogen production from wind energy in Western Canada for upgrading bitumen from oil sands". In: *Energy* 36.11 (2011), pp. 6326–6339. ISSN: 0360-5442. DOI: https://doi.org/10.1016/j.energy.2011.09.045.

[40] Babatunde Olateju, Joshua Monds, and Amit Kumar. "Large scale hydrogen production from wind energy for the upgrading of bitumen from oil sands". In: *Applied Energy* 118 (2014), pp. 48–56. ISSN: 0306-2619. DOI: https://doi.org/10.1016/j.apenergy.2013.12.013.

[41] Sonal Patel. "Hydrogen May Be a Lifeline for Nuclear—But It Won't Be Easy". In: *Power Magazine* (2020). URL: https://www.powermag.com/hydrogen-may-be-a-lifeline-for-nuclear-but-it-wont-be-easy/ (visited on 09/10/2020).

[42] Marc Secanell. *MEC E 643 - Renewable Energy Engineering and Sustainability*. Guest lecture in fuel cells. University of Alberta, Faculty of Engineering, Mechanical Engineering Department, Oct. 2019.

[43] Norazlianie Sazali et al. "New Perspectives on Fuel Cell Technology: A Brief Review". In: *Membranes* 10.5 (2020). DOI: 10.3390/membranes10050099.

[44] James Larminie and Andrew Dicks. *Fuel Cell Systems Explained*. 2nd Edition. Wiley, 2003. DOI: 10.1002/9781118878330.

[45] David B. Layzell et al. "The Future of Freight Part C: Implications for Alberta of Alternatives To Diesel". In: *Cesar Scenarios* 5.1 (2020), pp. 1–58. URL: https://www.cesarnet.ca/sites/%20default/files/pdf/cesar-scenarios/CESAR-Scenarios-Future%7B%5C_%7Dof%7B%5C_%7DFreight%7B%5C_%7DC.pdf.

[46]   Haisheng Chen et al. "Progress in electrical energy storage system: A critical review". In: *Progress in Natural Science* 19.3 (2009), pp. 291–312. ISSN: 1002-0071. DOI: https://doi.org/10.1016/j.pnsc.2008.07.014.

[47]   Paul Denholm and Maureen Hand. "Grid flexibility and storage required to achieve very high penetration of variable renewable electricity". In: *Energy Policy* 39.3 (2011), pp. 1817–1830. ISSN: 0301-4215. DOI: https://doi.org/10.1016/j.enpol.2011.01.019.

[48]   D Pudjianto et al. "Whole-Systems Assessment of the Value of Energy Storage in Low-Carbon Electricity Systems". In: *IEEE Transactions on Smart Grid* 5.2 (2014), pp. 1098–1109. DOI: 10.1109/TSG.2013.2282039.

[49]   Fernando J de Sisternes, Jesse D Jenkins, and Audun Botterud. "The value of energy storage in decarbonizing the electricity sector". In: *Applied Energy* 175 (2016), pp. 368–379. ISSN: 0306-2619. DOI: https://doi.org/10.1016/j.apenergy.2016.05.014.

[50]   Felix Cebulla et al. "How much electrical energy storage do we need? A synthesis for the U.S., Europe, and Germany". In: *Journal of Cleaner Production* 181 (2018), pp. 449–459. ISSN: 0959-6526. DOI: https://doi.org/10.1016/j.jclepro.2018.01.144.

[51]   Vikas Khare, Savita Nema, and Prashant Baredar. "Optimization of hydrogen based hybrid renewable energy system using HOMER, BB-BC and GAMBIT". In: *International Journal of Hydrogen Energy* 41.38 (2016), pp. 16743–16751. DOI: https://doi.org/10.1016/j.ijhydene.2016.06.228.

[52]   Himadry Shekhar Das et al. "Feasibility analysis of hybrid photovoltaic/battery/fuel cell energy system for an indigenous residence in East Malaysia". In: *Renewable and Sustainable Energy Reviews* 76 (2017), pp. 1332–1347. DOI: https://doi.org/10.1016/j.rser.2017.01.174.

[53]   S Karellas and N Tzouganatos. "Comparison of the performance of compressed-air and hydrogen energy storage systems: Karpathos island case study". In: *Renewable and Sustainable Energy Reviews* 29 (2014), pp. 865–882. DOI: https://doi.org/10.1016/j.rser.2013.07.019.

[54]   O H Mohammed et al. "Optimal design of a PV/fuel cell hybrid power system for the city of Brest in France". In: *2014 First International Conference on Green Energy ICGE 2014*. 2014, pp. 119–123. DOI: 10.1109/ICGE.2014.6835408.

[55]   A González, E McKeogh, and B Ó Gallachóir. "The role of hydrogen in high wind energy penetration electricity systems: The Irish case". In: *Renewable Energy* 29.4 (2004), pp. 471–489. ISSN: 0960-1481. DOI: https://doi.org/10.1016/j.renene.2003.07.006.

[56]   Underwriters Laboratories. *HOMER Pro*. Version 3.14.4. 2020. URL: https://www.homerenergy.com/products/pro/index.html.

[57] Tesla. *Power pack - Utility and Business Energy Storage*. URL: https://www. tesla.com/en_CA/powerpack (visited on 08/27/2021).

[58] Underwriters Laboratories. *HOMER Grid*. Version 1.8.7. 2021. URL: https: //www.homerenergy.com/products/grid/index.html.

[59] M. R. Shaner et al. "Geophysical constraints on the reliability of solar and wind power in the Unites States". In: *Energy and Environmental Science* 11 (2018), pp. 914–925.

[60] H Safaei and D. W Keith. "How much bulk energy storage is needed to decarbonize electricity?" In: *Energy and Environmental Science* 8 (2015), pp. 3409–3417.

[61] Micah S. Ziegler et al. "Storage Requirements and Costs of Shaping Renewable Energy Toward Grid Decarbonization". In: *Joule* 3.9 (2019), pp. 2134–2153. DOI: https://doi.org/10.1016/j.joule.2019.06.012.

[62] P. Albertus, J. S. Manser, and S. Litzelman. "Long-duration electricity storage applications, economics, and technologies". In: *Joule* 4 (2020), pp. 21–32.

[63] J. Jenkins and N. Sepulveda. *Enhanced Decision Support for a Changing Electricity Landscape: the GenX Configurable Electricity Resource Capacity Expansion Model*. MIT Energy Initiative Working Paper. 2017.

[64] Clara F Heuberger et al. "A systems approach to quantifying the value of power generation and energy storage technologies in future electricity networks". In: *Computers & Chemical Engineering* 107 (2017), pp. 247–256. ISSN: 0098-1354. DOI: https://doi.org/10.1016/j.compchemeng.2017.05.012.

[65] Terence Conlon, Michael Waite, and Vijay Modi. "Assessing new transmission and energy storage in achieving increasing renewable generation targets in a regional grid". In: *Applied Energy* 250 (2019), pp. 1085–1098. ISSN: 0306-2619. DOI: https://doi.org/10.1016/j.apenergy.2019.05.066.

[66] Jennie Jorgenson, Paul Denholm, and Trieu Mai. "Analyzing storage for wind integration in a transmission-constrained power system". In: *Applied Energy* 228 (2018), pp. 122–129. ISSN: 0306-2619. DOI: https://doi.org/10.1016/j. apenergy.2018.06.046.

[67] Max Tuttman and Scott Litzelman. "Why Long-Duration Energy Storage Matters". In: *Advanced Research Projects Agency–Energy* (Apr. 2020). URL: https://arpa-e.energy.gov/news-and-media/blog-posts/why-long-duration-energy-storage-matters (visited on 08/25/2021).

[68] Maddy Ewing et al. "Hydrogen on the path to net-zero emissions Costs and climate benefits". In: *Pembina Institute* (2020). URL: https://www.pembina. org/pub/hydrogen-primer.

[69] Ho Lung Yip et al. "A Review of Hydrogen Direct Injection for Internal Combustion Engines: Towards Carbon-Free Combustion". In: *Applied Sciences* 9 (2019), pp. 4842–4872. DOI: 10.3390/app9224842.

[70] College of the Desert. *Hydrogen Fuel Cell Engines and Related Technologies Course Manual - Module 1: Hydrogen Properties*. Tech. rep. Revision 0. Dec. 2000, pp. 15–16. URL: https://www.energy.gov/eere/fuelcells/downloads/hydrogen-fuel-cell-engines-and-related-technologies-course-manual (visited on 03/18/2021).

[71] David B Layzell et al. "David B. Layzell, PhD, FRSC." In: *Webinar for the Independent Power Producers Society of Alberta*. Calgary, 2020, pp. 1–15.

[72] Ben Packham. "Brown coal: the hydrogen economy stepping stone". In: *Environmental Clean Technologies Limited* (Apr. 2018). URL: http://ectltd.com.au/brown-coal-the-hydrogen-economy-stepping-stone/.

[73] Stanisław Porada et al. "Kinetics of steam gasification of bituminous coals in terms of their use for underground coal gasification". In: *Fuel Processing Technology* 130 (2015), pp. 282–291. ISSN: 0378-3820. DOI: https://doi.org/10.1016/j.fuproc.2014.10.015.

[74] Jessica Lof et al. "The Future of Freight Part B : Assessing Zero Emission Diesel Fuel Alternatives for Freight Transportation in Alberta". In: 4.2 (2019). URL: https://www.cesarnet.ca/sites/default/files/pdf/cesar-scenarios/CESAR-Scenarios-Future%7B%5C_%7Dof%7B%5C_%7DFreight%7B%5C_%7DB.pdf.

[75] Jessica Lof and David B. Layzell. "The Future of Freight Part A: Trends and Disruptive Forces Impacting Goods Movement in Alberta and Canada". In: *Cesar Scenarios* 4.1 (2019), pp. 1–60. URL: https://www.cesarnet.ca/sites/default/files/pdf/cesar-scenarios/CESAR-Scenarios-Future%7B%5C_%7Dof%7B%5C_%7DFreight%7B%5C_%7DA.pdf.

[76] Zen Clean Energy Solutions. *BC Hydrogen Study - Appendix C*. 2019. URL: https://news.gov.bc.ca/files/ZEN-BCBN-Hydrogen-Study-Appendices.pdf (visited on 08/13/2020).

[77] International Energy Agency. *The Future of Hydrogen*. Tech. rep. 2019. URL: https://www.iea.org/reports/the-future-of-hydrogen.

[78] Statistics Canada. *Table 25-10-0060-01 Household energy consumption, Canada and provinces*. 2017. DOI: https://doi.org/10.25318/2510006001-eng.

[79] David Fickling. "The Hydrogen Economy's Time is Approaching". In: *Bloomberg Opinion* (2020). URL: https://www.bloomberg.com/opinion/articles/2020-05-09/hydrogen-merits-stimulus-support-in-post-coronavirus-economy (visited on 09/10/2020).

[80] Amar Mehta. "Joe Biden reveals first budget - a $6trn spending plan with $800bn for fighting climate change". In: *Sky News* (May 2021). URL: https://news.sky.com/story/joe-biden-reveals-first-budget-a-6trn-spending-plan-with-800bn-for-fighting-climate-change-12319823 (visited on 08/24/2021).

[81]   The White House. *FACT SHEET: The American Jobs Plan*. URL: https://www.whitehouse.gov/briefing-room/statements-releases/2021/03/31/fact-sheet-the-american-jobs-plan/ (visited on 08/24/2021).

[82]   Alex Ivaneko. "What Is The Role Of Hydrogen In Biden's Infrastructure Plan?" In: *Forbes* (Aug. 2021). URL: https://www.forbes.com/sites/forbestechcouncil/2021/08/05/what-is-the-role-of-hydrogen-in-bidens-infrastructure-plan/?sh=48041fb772bd (visited on 08/24/2021).

[83]   P. Friedlingstein et al. "Global Carbon Budget 2019". In: *Earth System Science Data* 11.4 (2019), pp. 1783–1838. DOI: 10.5194/essd-11-1783-2019. URL: https://essd.copernicus.org/articles/11/1783/2019/.

[84]   Gregorio Marbán and Teresa Valdés-Solís. "Towards the hydrogen economy?" In: *International Journal of Hydrogen Energy* 32.12 (2007), pp. 1625–1637. ISSN: 0360-3199. DOI: https://doi.org/10.1016/j.ijhydene.2006.12.017.

[85]   James Temple. "How falling solar costs have renewed clean hydrogen hopes". In: *MIT Technology Reviews* (2020). URL: https://www.technologyreview.com/2020/08/07/1006126/green-hydrogen-affordable-solar-wind-renewables/ (visited on 09/10/2020).

[86]   Gunther Glenk and Stefan Reichelstein. "Economics of converting renewable power to hydrogen". In: *Nature Energy* 4.3 (2019), pp. 216–222. DOI: 10.1038/s41560-019-0326-1.

[87]   Emiliano Bellini. "Solar-powered hydrogen under $2/kg by 2030". In: *PV Magazine* (2020). URL: https://www.pv-magazine.com/2020/08/25/solar-powered-hydrogen-under-2-kg-by-2030/ (visited on 09/10/2020).

[88]   Government of Alberta. "Interprovincial Exports". In: *Economic Comentary* (), p. 5. URL: https://open.alberta.ca/dataset/073fcf5e-c98f-40ab-aad9-56d240929874/resource/578924ee-37c9-497c-b055-af5c6f37afaa/download/sp-commentary-03-16-18.pdf (visited on 09/11/2020).

[89]   Canada Energy Regulator. *Provincial and Territorial Energy Profiles – Alberta*. June 2020. URL: https://www.cer-rec.gc.ca/nrg/ntgrtd/mrkt/nrgsstmprfls/ab-eng.html (visited on 09/16/2020).

[90]   National Renewable Energy Laboratory. *Ten Years of Analyzing the Duck Chart: How an NREL Discovery in 2008 Is Helping Enable More Solar on the Grid Today*. Feb. 2018. URL: https://www.nrel.gov/news/program/2018/10-years-duck-curve.html (visited on 09/21/2020).

[91]   David B. Layzell et al. "Supplemental Material for The Future of Freight Part C: Implications for Alberta of Alternatives To Diesel". In: *Cesar Scenarios* 5.1 (2020), pp. 1–58. URL: https://www.cesarnet.ca/sites/%20default/files/pdf/cesar-scenarios/CESAR-Scenarios-Future%7B%5C_%7Dof%7B%5C_%7DFreight%7B%5C_%7DC.pdf.

[92]   GE Energy Consulting. "Pan-Canadian Wind Integration Study (PCWIS) Final Report Prepared for: Canadian Wind Energy Association (CanWEA)". In: Revision 3 (2016), p. 367. URL: https://canwea.ca/wp-content/uploads/2016/07/pcwis-fullreport.pdf.

[93]   P. Denholm et al. Tech. rep. National Renewable Energy Lab, Aug. 2009, pp. 1–47. DOI: 10.2172/964608. URL: https://www.osti.gov/biblio/964608-LaTU8c/ (visited on 09/18/2020).

[94]   General Electric. *Cypress 4-5 MW Onshore Wind Turbine Platform*. URL: https://www.ge.com/%20renewableenergy/wind-energy/onshore-wind/4-5-mw-platform-cypress (visited on 09/18/2020).

[95]   Natural Resources Canada. *Photovoltaic and Solar Resource Maps*. 2020. URL: https://www.nrcan.gc.ca/18366 (visited on 09/21/2020).

[96]   V Utgikar and T Thiesen. "Life cycle assessment of high temperature electrolysis for hydrogen production via nuclear energy". In: *International Journal of Hydrogen Energy* 31.7 (2006), pp. 939–944. ISSN: 0360-3199. DOI: https://doi.org/10.1016/j.ijhydene.2005.07.001.

[97]   C Koroneos et al. "Life cycle assessment of hydrogen fuel production processes". In: *International Journal of Hydrogen Energy* 29.14 (2004), pp. 1443–1450. ISSN: 0360-3199. DOI: https://doi.org/10.1016/j.ijhydene.2004.01.016.

[98]   Kevork Hacatoglu, Marc A. Rosen, and Ibrahim Dincer. "Comparative life cycle assessment of hydrogen and other selected fuels". In: *International Journal of Hydrogen Energy* 37.13 (2012), pp. 9933–9940. ISSN: 0360-3199. DOI: https://doi.org/10.1016/j.ijhydene.2012.04.020.

[99]   Carl-Jochen Winter. "Hydrogen energy — Abundant, efficient, clean: A debate over the energy-system-of-change". In: *International Journal of Hydrogen Energy* 34.14, Supplement 1 (2009), S1–S52. ISSN: 0360-3199. DOI: https://doi.org/10.1016/j.ijhydene.2009.05.063.

[100] M. Beccali et al. "Method for size optimisation of large wind–hydrogen systems with high penetration on power grids". In: *Applied Energy* 102 (2013), pp. 534–544. ISSN: 0306-2619. DOI: https://doi.org/10.1016/j.apenergy.2012.08.037.

[101] Rodolfo Dufo-López, José L Bernal-Agustín, and José A Domínguez-Navarro. "Generation management using batteries in wind farms: Economical and technical analysis for Spain". In: *Energy Policy* 37.1 (2009), pp. 126–139. ISSN: 0301-4215. DOI: https://doi.org/10.1016/j.enpol.2008.08.012.

[102] Daniel Kroniger and Reinhard Madlener. "Hydrogen storage for wind parks: A real options evaluation for an optimal investment in more flexibility". In: *Applied Energy* 136 (2014), pp. 931–946. ISSN: 0306-2619. DOI: https://doi.org/10.1016/j.apenergy.2014.04.041.

[103]   Dennis Anderson and Matthew Leach. "Harvesting and redistributing renewable energy: on the role of gas and electricity grids to overcome intermittency through the generation and storage of hydrogen". In: *Energy Policy* 32.14 (2004), pp. 1603–1614. ISSN: 0301-4215. DOI: https://doi.org/10.1016/S0301-4215(03)00131-9.

[104]   Guotao Zhang and Xinhua Wan. "A wind-hydrogen energy storage system model for massive wind energy curtailment". In: *International Journal of Hydrogen Energy* 39.3 (2014), pp. 1243–1252. DOI: https://doi.org/10.1016/j.ijhydene.2013.11.003.

[105]   S. Sherif, F. Barbir, and T. Veziroglu. "Wind energy and the hydrogen economy - review of the technology". In: *Solar Energy* 78.5 (2005), pp. 647–660. DOI: https://doi.org/10.1016/j.solener.2005.01.002.

[106]   David B. Layzell et al. "Building a Transition Pathway to a Vibrant Hydrogen Economy in the Alberta Industrial Heartland". In: *Transition Accelerator* 2.5 (2020), pp. 1–59. URL: https://www.cesarnet.ca/sites/%20default/files/pdf/cesar-scenarios/CESAR-Scenarios-Future%7B%5C_%7Dof%7B%5C_%7DFreight%7B%5C_%7DC.pdf.

[107]   Jacob Lawrence Thompson. "Atlantic Canada's Distributed Generation Future: Renewables, Transportation, and Energy Storage". MA thesis. Halifax, Nova Scotia: Saint Mary's University, Aug. 2016.

[108]   American Wind Energy Association. *The U.S. Wind Turbine Database.* 2019. URL: https://eerscmap.usgs.gov/uswtdb/ (visited on 12/09/2019).

[109]   The Highland Council. *Wind Turbine Map.* 2019. URL: https://www.highland.gov.uk/info/198/planning_-_long_term_and_area_policies/152/renewable_energy/4 (visited on 12/09/2019).

[110]   *Wind Turbines in Denmark.* 2018. URL: http://miljoegis.mim.dk/cbkort?profile=miljoegis%5C%20-vindmoeller (visited on 12/09/2019).

[111]   Danish Energy Agency. *Master Data Register of Wind Turbines.* 2019. URL: https://ens.dk/en/our-services/statistics-data-key-figures-and-energy-maps/overview-energy-sector (visited on 12/09/2019).

[112]   *Ontario Wind Turbines.* 2019. URL: http://ontario-wind-turbines.org/ (visited on 12/09/2019).

[113]   Tanya Christidis and Jane Law. "Mapping Ontario's Wind Turbines: Challenges and Limitations". In: *International Journal of Geo-Information* 2 (2013), pp. 1092–1105. DOI: 10.3390/ijgi2041092.

[114]   Michelle Froese. "Global wind-turbine mapping project surpasses 100,000 count". In: *Windpower Engineering & Development* (Apr. 8, 2019). URL: https://www.windpowerengineering.com/global-wind-turbine-mapping-project-surpasses-100000-count/ (visited on 12/09/2019).

[115]   IntelStor. *Asset Geo-location Data.* 2019. URL: http://www.intelstor.com/countries (visited on 12/10/2019).

[116] Canadian Wind Energy Association. *Wind Markets - Installed Capacity*. 2020. URL: https://canwea.ca/wind-energy/installed-capacity/ (visited on 06/22/2020).

[117] Lazard. *Levelized Cost of Energy and Levelized Cost of Storage 2019*. Nov. 2019. URL: https://www.lazard.com/perspective/lcoe2019/ (visited on 12/10/2019).

[118] Canadian Wind Energy Association. *Wind Facts - Affordable Power*. 2019. URL: https://canwea.ca/wind-facts/affordable-power/ (visited on 12/10/2019).

[119] Loren Knopper and Christopher Ollson. "Health effects and wind turbines: a review of the literature". In: *Environmental Health* 10.1 (2011), p. 78. DOI: https://doi.org/10.1186/1476-069X-10-78.

[120] Paul Breeze. "Wind Power Grid Integration and Environmental Issues". In: *Wind Power Generation* (2016), pp. 85–91. DOI: 10.1016/b978-0-12-804038-6.00010-4.

[121] U.S. Department of the Interior Bureau of Land Management. "Wind Energy Final Programmatic Environmental Impact Statement - Volume 1: Main Text". In: 2005. Chap. 4, pp. 4-1–4-64.

[122] Alastair Sharp. "White Pines demolition mourned as Ford dismantles green energy in Ontario". In: *Canada's National Observer* (Oct. 29, 2019). URL: https://www.nationalobserver.com/2019/10/29/news/white-pines-demolition-mourned-ford-dismantles-green-energy-ontario (visited on 12/11/2019).

[123] Kelly Egan. "Ontario cancels nearly-built $200M wind farm over threat to bat populations". In: *Ottawa Citizen* (Dec. 10, 2019). URL: https://ottawacitizen.com/news/local-news/ontario-cancels-nearly-built-200m-wind-farm-over-threat-to-bat-populations (visited on 12/11/2019).

[124] Peter Enevoldsen and Benjamin Sovacool. "Examining the social acceptance of wind energy: Practical guidelines for onshore wind project development in France". In: *Renewable and Sustainable Energy Reviews* 53 (2016), pp. 178–184. DOI: https://doi.org/10.1016/j.rser.2015.08.041.

[125] Eja Pedersen. "Health aspects associated with wind turbine noise-results from three field studies". In: *Noise Control Engineering* 59.1 (2010), pp. 47–53. DOI: 10.3397/1.3533898.

[126] Jesper Hvass Schmidt and Mads Klokker. "Health Effects Related to Wind Turbine Noise Exposure: A Systematic Review". In: *PLoS ONE* 9.12 (2014), e114183. DOI: https://doi.org/10.1371/journal.pone.0114183.

[127] Anna M. Calvart et al. "A Synthesis of Human-related Avian Mortality in Canada". In: *Avian Conservation and Ecology* 8.2 (2013). DOI: 10.5751/ACE-00581-080211.

[128] Robert M.R. Barclay, E.F. Baerwald, and J.C. Gruver. "Variation in bat and bird fatalities at wind energy facilities: Assessing the effects of rotor size and tower height". In: *Canadian Journal of Zoology* 85.3 (2007), pp. 381–387. DOI: 10.1139/Z07-011.

[129] R. May et al. "Mitigating wind-turbine induced avian mortality: sensory, aero-dynamic and cognitive constraints and options". In: *Renewable and Sustainable Energy Reviews* 42 (2015), pp. 170–181. DOI: 10.1016/j.rser.2014.10.002.

[130] Filipa Peste et al. "How to mitigate impacts of wind farms on bats? A review of potential conservation measures in the European context". In: *Environmental Impact Assessment Review* 51 (2015), pp. 10–22. DOI: 10.1016/j.eiar.2014.11.001.

[131] Government of Canada. *Provincial and territorial utility commissions and boards.* 2020. URL: https://ic.gc.ca/eic/site/oca-bc.nsf/eng/ca03012.html (visited on 06/23/2020).

[132] The Wind Power - Wind Energy Market Intelligence. *Online Access: Wind farms.* 2019. URL: https://www.thewindpower.net/windfarms_list_en.php (visited on 12/13/2019).

[133] Phillip Mckay et al. "Advances in Wind Power". In: 2012. Chap. 3, pp. 65–84. DOI: http://dx.doi.org/10.5772/57353.

[134] Peter Enevoldsen et al. "How much wind power potential does europe have? Examining european wind power potential with an enhanced socio-technical atlas". In: *Energy Policy* 132 (2019), pp. 1092–1100. DOI: https://doi.org/10.1016/j.enpol.2019.06.064.

[135] National Renewable Energy Laboratory. *Table 1-1 Classes of wind power density at 10 m and 50 m.* URL: https://rredc.nrel.gov/wind/pubs/atlas/tables/1-1T.html (visited on 05/25/2020).

[136] Department of Wind Energy: Technical University of Denmark. *Global Wind Atlas.* URL: https://globalwindatlas.info/area/Canada (visited on 07/17/2020).

[137] Jake Badger and Hans Ejsing Jørgensen. "A high resolution global wind atlas - improving estimation of world wind resources". In: *Energy Systems and Technologies for the coming Century.* Denmark. Forskningscenter Risoe. Risoe-R 1776(EN). Risø International Energy Conference 2011 ; Conference date: 10-05-2011 Through 12-05-2011. Danmarks Tekniske Universitet, Risø National-laboratoriet for Bæredygtig Energi, 2011, pp. 215–225. ISBN: 978-87-550-3903-2.

[138] TransAlta. *Cowley Ridge.* 2018. URL: https://www.transalta.com/facilities/plants-operation/cowley-ridge/ (visited on 07/15/2020).

[139] Natural Resources Canada. *Evaluation Report: Renewable Energy Deployment Sub-program (RED).* 2015. URL: https://www.nrcan.gc.ca/evaluation/reports/2015/17933 (visited on 07/15/2020).

[140] Natural Resources Canada. *ecoENERGY for Renewable Power.* 2016. URL: https://www.nrcan.gc.ca/ecoaction/14163 (visited on 07/15/2020).

[141] Ministère des Ressources naturelles et de la Faune. "Québec Energy Strategy". In: (2006). URL: https://mern.gouv.qc.ca/english/publications/energy/strategy/energy-strategy-2006-2015.pdf (visited on 07/15/2020).

[142] Ontario Ministry of Energy, Northern Development and Mines. *4.0 Feed-in Tariff Program.* 2019. URL: https://www.ontario.ca/document/renewable-energy-development-ontario-guide-municipalities/40-feed-tariff-program (visited on 06/11/2020).

[143] Alberta Electric System Operator. *Renewable Electricity Program Results.* 2016. URL: https://www.aeso.ca/market/renewable-electricity-program/rep-results/ (visited on 07/15/2020).

[144] Nova Scoatia Department of Energy and Mines. *Community Feed-in Tarrif.* 2019. URL: https://energy.novascotia.ca/renewables/programs-and-projects/comfit (visited on 06/11/2020).

[145] Government of Canada. *Greenhouse Gas Pollution Pricing Act (S.C. 2018, c. 12, s. 186).* 2020. URL: https://laws-lois.justice.gc.ca/eng/acts/G-11.55/ (visited on 07/15/2020).

[146] Government of Alberta. *Natural gas vision and strategy.* Tech. rep. Nov. 2020. URL: https://www.alberta.ca/natural-gas-vision-and-strategy.aspx (visited on 09/07/2021).

[147] Energy Exemplar. *Aurora Forecasting Software.* Version 13.5.1043. 2021. URL: https://energyexemplar.com/solutions/aurora/.

[148] Energy Exemplar. *Simulation-ready Datasets.* URL: https://energyexemplar.com/simulation-datasets/ (visited on 08/30/2021).

[149] TransAlta. "TransAlta Reports Strong First Quarter 2021 Results led by Exceptional Performance at Alberta Hydro". In: *PR Newswire* (May 2021). URL: https://www.prnewswire.com/news-releases/transalta-reports-strong-first-quarter-2021-results-led-by-exceptional-performance-at-alberta-hydro-301290676.html (visited on 08/30/2021).

[150] Milner Power Inc. *HR Milner Generating Station.* URL: https://www.milnerpower.com/ (visited on 08/30/2021).

[151] Heartland Generation. *Our Facilities.* URL: https://www.heartlandgeneration.com/#facilities (visited on 08/30/2021).

[152] National Renewable Energy Laboratory. *National Solar Radiation Database.* URL: https://nsrdb.nrel.gov/ (visited on 08/30/2021).

[153] Natalia Vergara Bonilla et al. "Calibrating the Canadian Wind Atlas Data to Historic Wind Energy Performance in Alberta". unpublished.

[154] William David Lubitz. "Power law extrapolation of wind measurements for predicting wind energy production". In: *Wind Engineering* 33.3 (2009), pp. 259–271. DOI: 10.1260/0309-524X.33.3.259.

[155] A. Ulazia et al. "The consequences of air density variations over northeastern Scotland for offshore wind energy potential". In: *Energies* 12.13 (2019).

[156] National Renewable Energy Laboratory. *System Advisor Model.* Version 2020.2.29. 2020. URL: https://sam.nrel.gov/.

[157] Alberta Electric System Operator. *Connection project reporting*. URL: https://www.aeso.ca/grid/projects/connection-project-reporting/ (visited on 08/31/2021).

[158] Alberta Electric System Operator. *ATC and Intertie Capability Public Reports*. URL: https://itc.aeso.ca/itc/public/atc/ (visited on 08/31/2021).

[159] Alberta Electric System Operator. *Alberta - British Columbia Intertie Restoration*. URL: https://www.aeso.ca/grid/projects/intertie-restoration/ (visited on 08/31/2021).

[160] U.S. Energy Information System Administration. *Capital Cost and Performance Characteristic Estimates for Utility Scale Electric Power Generating Technologies*. Tech. rep. Feb. 2020. URL: https://www.eia.gov/analysis/studies/powerplants/capitalcost/ (visited on 09/01/2021).

[161] U.S. Energy Information System Administration. *Electricity Market Module - NEMS Documentation*. Tech. rep. July 2020. URL: https://www.eia.gov/analysis/pdfpages/m068index.php (visited on 09/01/2021).

[162] Ortech. *Canadian Wind Market Case Study*. July 2007. URL: http://www.ortech.ca/pdf/power/presentations/CanadianWindMarketCaseStudy.pdf (visited on 09/01/2021).

[163] Wind Power Monthly. *Merchant plant ready to run – Southern Alberta lead*. Jan. 2001. URL: https://www.windpowermonthly.com/article/958928/merchant-plant-ready-run-southern-alberta-lead (visited on 09/01/2021).

[164] Merrimack Energy Group. *The Competitive Cost of Wind Power*. Tech. rep. July 2008. URL: http://www.regie-energie.qc.ca/audiences/3676-08/Requete_3676-08/B-1_HQD_Annexe4_3676_29juil08.pdf (visited on 09/01/2021).

[165] Renewable Energy World. *Taber Wind Farm Opens in Alberta*. URL: https://www.renewableenergyworld.com/wind-power/taber-wind-farm-opens-in-alberta-50384/#gref (visited on 09/01/2021).

[166] TransAlta. *TransAlta announces Blue Trail wind power project in southern Alberta*. URL: https://transalta.com/newsroom/news-releases/transalta-announces-blue-trail-wind-power-project-in-southern-alberta/ (visited on 09/01/2021).

[167] TransAlta. *Ardenville*. URL: https://transalta.com/plants-operation/ardenville/ (visited on 09/01/2021).

[168] Advocate Staff. "Wind farm sprouts up in Trochu". In: (Nov. 2010). URL: https://www.reddeeradvocate.com/local-news/wind-farm-sprouts-up-in-trochu/ (visited on 09/01/2021).

[169] TransAlta. *TransAlta adds another 66 MW to Alberta power grid with Summerview wind farm expansion*. URL: https://transalta.com/newsroom/news-releases/transalta-adds-another-66-mw-to-alberta-power-grid-with-summerview-wind-farm-expansion/ (visited on 09/01/2021).

[170] Suncor. *Suncor Energy officially opens Wintering Hills Wind Power Project.* URL: https://www.suncor.com/en-ca/newsroom/community-news/4925 (visited on 09/01/2021).

[171] Richard Gilbert. "Wind farm contract awarded". In: *Wind Watch* (Feb. 2012). URL: https://www.wind-watch.org/news/2012/02/01/wind-farm-contract-awarded/ (visited on 09/01/2021).

[172] Power Technology. *Blackspring Ridge Wind Project, Alberta.* URL: https://www.power-technology.com/projects/blackspring-ridge-wind-project-alberta/ (visited on 09/01/2021).

[173] Alberta Wind Energy Corporation. *Construction Commences in Pincher Creek.* URL: https://www.albertawindenergy.com/construction-commences-on-oldman-2-wind-farm/ (visited on 09/01/2021).

[174] Barry Cassell. "BluEarth lines up financing for 29-MW Bull Creek Wind project in Alberta". In: *Transmission Hub* (2015). URL: https://www.transmissionhub.com/articles/2015/06/bluearth-lines-up-financing-for-29-mw-bull-creek-wind-project-in-alberta.html (visited on 09/01/2021).

[175] Capital Power. *Whitla Wind 1.* URL: https://www.capitalpower.com/operations/whitla-wind/ (visited on 09/01/2021).

[176] Government of Alberta. *Castle Rock Wind Farm - Phase 2.* URL: https://majorprojects.alberta.ca/details/Castle-Rock-Wind-Farm-Phase-2/4131 (visited on 09/01/2021).

[177] Government of Alberta. *Riverview Wind Farm.* URL: https://majorprojects.alberta.ca/details/Riverview-Wind-Farm (visited on 09/01/2021).

[178] Government of Alberta. *Brooks Solar Project Phase 2.* URL: https://majorprojects.alberta.ca/details/Brooks-1-Solar-Power-Plant/652 (visited on 09/01/2021).

[179] Government of Alberta. *Innisfail Solar Project.* URL: https://majorprojects.alberta.ca/details/Innisfail-Solar-Project/4279 (visited on 09/01/2021).

[180] Government of Alberta. *Claresholm Solar Project.* URL: https://majorprojects.alberta.ca/details/Claresholm-Solar-Project/4272 (visited on 09/01/2021).

[181] Government of Alberta. *Burdett Solar Project.* URL: https://majorprojects.alberta.ca/details/Burdett-Solar-Project/4173 (visited on 09/01/2021).

[182] Government of Alberta. *Alberta Solar One Project.* URL: https://majorprojects.alberta.ca/details/Alberta-Solar-One-Project/4420 (visited on 09/01/2021).

[183] Government of Alberta. *Yellow Lake Solar Project.* URL: https://majorprojects.alberta.ca/details/Yellow-Lake-Solar-Project/4172 (visited on 09/01/2021).

[184] Government of Alberta. *Prairie Sunlight Solar Project Phase 2.* URL: https://majorprojects.alberta.ca/details/Prairie-Sunlight-Solar-Project-Phase-2/4178 (visited on 09/01/2021).

[185] Government of Alberta. *Prairie Sunlight Solar Project Phase 2*. URL: https://majorprojects.alberta.ca/details/Prairie-Sunlight-Solar-Project-Phase-3/4179 (visited on 09/01/2021).

[186] Three Nations Energy. *Project Funders*. URL: https://www.3ne.ca/3ne-solar-farm/project-funders/ (visited on 09/01/2021).

[187] Alberta Electric System Operator. *Forecasting*. URL: https://www.aeso.ca/grid/forecasting/ (visited on 08/31/2021).

[188] Government of Alberta. *Technology Innovation and Emissions Reduction Regulation*. URL: https://www.alberta.ca/technology-innovation-and-emissions-reduction-regulation.aspx (visited on 08/31/2020).

[189] Benjamin Thibault, Tim Weis, and Andrew Leach. "Alberta's quiet but resilient electricity transition". Manuscript, Spring 2021.

[190] Alberta Electric System Operator. *Long-term adequacy metrics*. URL: https://www.aeso.ca/market/market-and-system-reporting/long-term-adequacy-metrics/ (visited on 09/01/2021).

[191] Minister of Energy, Government of Alberta. "Ministerial Order 141/2019 [Energy] - Interim targets established". In: *Open Alberta* (2019). URL: https://open.alberta.ca/publications/energy_141_2019#summary (visited on 09/01/2021).

[192] Bank of Canada. *Inflation Calculator*. URL: https://www.bankofcanada.ca/rates/related/inflation-calculator/ (visited on 07/01/2020).

[193] Bank of Canada. *Annual Exchange Rates*. URL: https://www.bankofcanada.ca/rates/exchange/annual-average-exchange-rates/ (visited on 07/01/2021).

[194] T. Ramsden, B. Kroposki, and J. Levene. *Opportunities for Hydrogen-Based Energy Storage for Electric Utilities*. Tech. rep. National Renewable Energy Laboratory, 2008, pp. 1–17. URL: nha.confex.com/nha/2008/recordingredirect.cgi/id/352.

[195] Oliver Schmidt et al. *The future cost of electrical energy storage based on experience curves: dataset*. 2017. URL: http://dx.doi.org/10.6084/m9.figshare.5048062 (visited on 04/28/2021).

[196] Behnam Zakeri and Sanna Syri. "Electrical energy storage systems: A comparative life cycle cost analysis". In: *Renewable and Sustainable Energy Reviews* 42 (2015), pp. 569–596. DOI: https://doi.org/10.1016/j.rser.2014.10.011.

[197] D. Steward et al. *Lifecycle cost analysis of hydrogen versus other technologies for electrical energy storage*. Tech. rep. Nov. 2009. URL: https://www.nrel.gov/docs/fy10osti/46719.pdf (visited on 07/31/2021).

[198] Ballard. *FCgen-HPS Spec Sheet*. URL: https://www.ballard.com/about-ballard/publication_library/product-specification-sheets/fcgen-hps-spec-sheet (visited on 08/11/2021).

[199]   Bjørnar Kruse, Sondre Grinna, and Cato Buch. *Hydrogen Status og muligheter.* Tech. rep. Nov. 2002. URL: https://network.bellona.org/content/uploads/sites/3/Hydrogen_6-2002.pdf (visited on 09/25/2021).

[200]   Jenner Wind Limited Partnership. *Jenner Wind Power Projects.* 2017. URL: jennerwind.com (visited on 08/09/2021).

[201]   Environment and Climate Change Canada. *Historical Climate Data.* URL: %7Bhttps://climate.weather.gc.ca/%7D (visited on 08/11/2021).

[202]   MathWorks. *MATLAB linprog function.* Version R2021a. 2021. URL: https://www.mathworks.com/help/optim/ug/linprog.html.

[203]   MathWorks. *MATLAB Optimization Toolbox.* Version R2021a. 2021. URL: https://www.mathworks.com/help/optim/.

[204]   Wayne L. Winston. *Operations Research. Applications and Algorithms.* Fourth Edition. Indiana: Thompson, 2004.

[205]   MathWorks. *MATLAB Linear Programming Algorithms.* 2021. URL: https://www.mathworks.com/help/optim/ug/linear-programming-algorithms.html (visited on 08/21/2021).

[206]   J. Nocedal and S. J. Wright. *Numerical Optimization. Springer Series in Operations Research.* Second Edition. Springer-Verlag, 2006.

[207]   David Peterson, James Vickers, and Dan DeSantis. *Hydrogen Production Cost From PEM Electrolysis - 2019.* Tech. rep. Feb. 2020. URL: https://www.hydrogen.energy.gov/pdfs/19009_h2_production_cost_pem_electrolysis_2019.pdf (visited on 09/26/2021).

Appendix A: Alberta Operational Wind Farm Information

Wind Farm Name	AESO Asset ID
Ardenville Wind	ARD1
Bull Creek 1	BUL1
Bull Creek 2	BUL2
Blackspring Ridge	BSR1
Blue Trail Wind	BTR1
Castle River 1	CR1
Castle Rock Ridge 2	CRR2
Castle Rock Wind Farm	CRR1
Cowley Ridge	CRE3
Enmax Taber	TAB1
Ghost Pine	NEP1
Halkirk Wind Power Facility	HAL1
Kettles Hill	KHW1
McBride Lake Windfarm	AKE1
Oldman 2 Wind Farm 1	OWF1
Riverview	RIV1
Soderglen Wind	GWW1
Summerview 1	IEW1
Summerview 2	IEW2
Suncor Chin Chute	SCR3
Suncor Magrath	SCR2
Whitla	WHT1
Wintering Hills	SCR4

Table A.1: Alberta electric system operator (AESO) asset ID's for wind farms, used in Figure 1.2

Appendix B: Overnight Capital Costs of Select Alberta Electricity Projects

Plant Name	Overnight Capital Cost ($CAD/kW)	Source
Onshore Wind		
EIA NEMS Region 21	1,824[*]	[160, 161]
Castle River	1,539	[162]
Cowley North	2,000	[163]
McBride Lake	2,726	[162]
Magrath	1,600	[162]
Summerview 1	1,439	[162]
Chin Chute	2,000	[162]
Soderglen	993	[162]
Kettles Hill	2,587	[164]
Taber	1,728	[165]
Blue Trail	1,742	[166]
Ardenville	1,985	[167]
Ghost Pine	1,890	[168]
Summerview 2	1,864	[169]
Wintering Hills	2,273	[170]
Halkirk	2,380	[171]
Blackspring Ridge	2,000	[172]
Oldman 2	1,957	[173]
Bull Creek	2,448	[174]
Whitla 1	1,584	[175]
Castle Rock Ridge 2	1,235	[176]
Riverview	1,276	[177]

Fixed Tilt Solar Photovoltaic (PV)

EIA NEMS Region 21	1,399[*]	[160, 161]
Brooks	1,982	[178]
Innisfail	960	[179]
Claresholm	1,504	[180]
Burdett	1,795	[181]
Alberta Solar 1	1,905	[182]
Yellow Lake	1,795	[183]
Tracking Solar Photovoltaic (PV)		
EIA NEMS Region 21	1,493[*]	[160, 161]
Prairie Sunlight 2	1,633	[184]
Prairie Sunlight 3	1,682	[185]
Three Nations Energy	3,527	[186]

[*]EIA capital costs given in 2017 $USD/kW

Table B.1: Overnight capital costs, not accounting for inflation, of select Alberta renewable projects given relative to EIA estimates

Appendix C: Canadian Wind Turbine Database: Wind Turbine Map
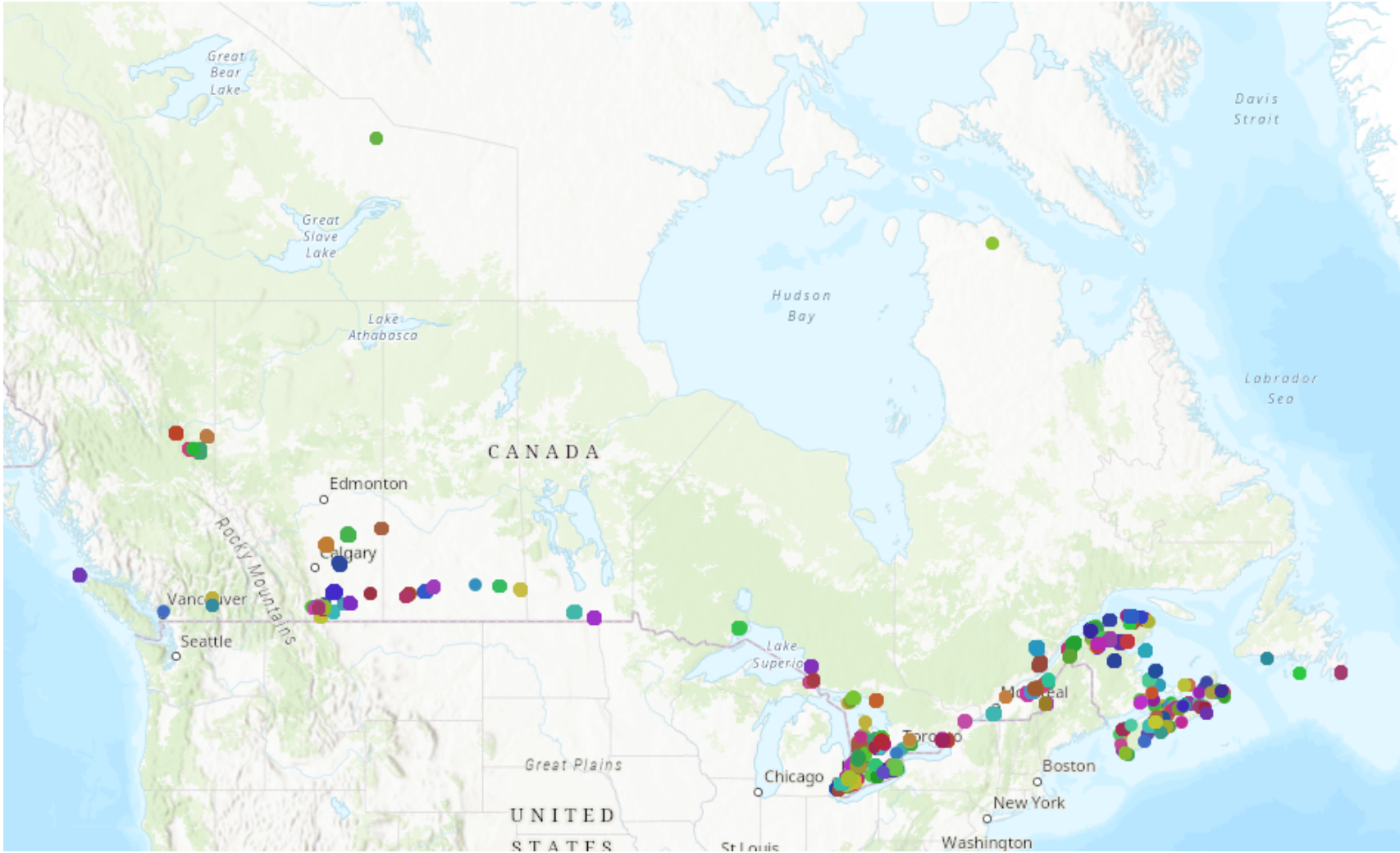
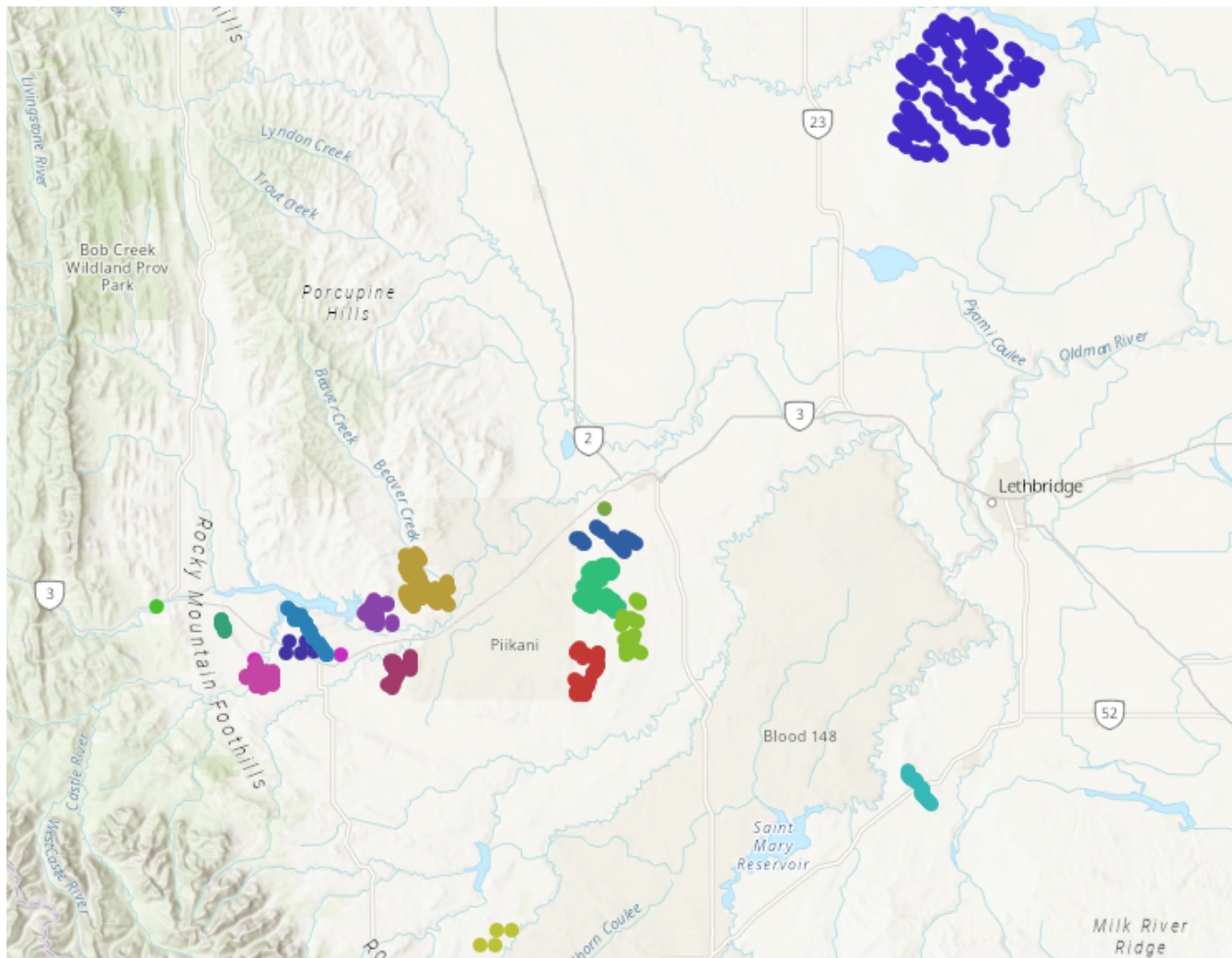Figure C.1: Map of Operational Wind Turbines in Canada

Figure C.2: Map of Operational Wind Turbines in Southern Alberta

Appendix D: Ballard FCGen-hps Fuel Cell Spefications

FCgen®

BALLARD®

Power to change the world®

High Performance Fuel Cell Stack

Introducing FCgen®-HPS
Ballard's high performance proton exchange membrane (PEM) liquid cooled fuel cell stack.

FCgen®-HPS incorporates our latest technology, design and materials to meet the requirements of the most demanding mobility applications delivering one of the highest fuel cell stack power densities in the industry.

The FCgen®-HPS stack uses Ballard's latest generation of proprietary membrane electrode assemblies (MEA) and thin carbon plates to deliver performance and durability.

The FCgen®-HPS stack provides up to 140kW of stable electrical power over a wide range of operating and environmental conditions. The FCgen®-HPS stack can be configured to different power outputs to meet customer requirements.

Designed for motive applications, the FCgen®-HPS features fast, dynamic response and robust and reliable operation. The FCgen®-HPS establishes a new industry standard for power density, performance and product reliability.

Key attributes:
- High power density[1] fuel cell stack
  - o ~ 4.3kW/L
  - o ~ 4.7kW/kg
- Designed to automotive standards
- Freeze start capability
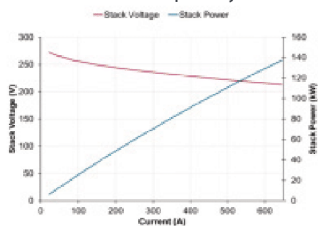
PRODUCT SPECIFICATIONS

PEM (Proton Exchange Membrane) fuel cell stack	
Rated Power	up to 140 kW
Cell Count	309
Rated Current	645 A
Rated Voltage	202 V
Mass (dry)	55 kg
Length	484 mm
Width	555 mm
Height	195 mm
Fuel Standard	ISO 14687-2
Oxidant	Air up to 2.5 bara
Coolant	DI water or Fuel Cell Grade Glycol
Max Coolant Temp.	95°C
Min. Start Temp.	-28°C
Storage Temp. (<12 hrs)	-40°C to 95°C
Storage Temp. (long term)	2°C to 40°C

(1) excludes end plate hardware

Figure D.1: Product Specifications for the Ballard FCgen High Performance Fuel Cell Stack